

THE ROLE OF *PAK1* IN THE CELLULAR AND  
MOLECULAR COMPONENTS OF PLEXIFORM  
NEUROFIBROMAS

Andrew S. McDaniel

Submitted to the faculty of the University Graduate School  
in partial fulfillment of the requirements  
for the degree  
Doctor of Philosophy  
in the Department of Microbiology and Immunology,  
Indiana University

September 2008

Accepted by the Faculty of Indiana University, in partial fulfillment of the requirements for the degree of Doctor of Philosophy.

---

D. Wade Clapp, M.D., Chair

---

Hal E. Broxmeyer, Ph.D.

Doctoral Committee

---

David A. Ingram, M.D.

July 3, 2008

---

Edward F. Srour, Ph.D.

## ACKNOWLEDGMENTS

I would like to thank each of the members of my thesis committee, who have provided me with excellent advice, direction, and support for four years. It has been so appreciated that scientists of such international stature have made my education a priority.

I would like to thank the faculty and staff of the Department of Microbiology and Immunology, for their time and resources that allowed me the opportunity to pursue this degree. I would also like to thank the advisors, staff, and fellow students of the M.D./Ph.D. program, with whom I have forged lifelong relationships.

I would like to thank the many members of the Clapp laboratory, past and present. There are too many to list but each one has provided me with assistance, insight, camaraderie, and support.

I would especially like to thank Dr. Wade Clapp for his mentorship. Working with Wade has been an experience that has shaped me in ways far more profound than my ability to formulate testable hypothesis and generate publishable data. I am privileged to consider him a friend and anticipate eagerly our scientific and personal interactions for many years to come.

I would like to thank my family for providing me with all the love and guidance any person could desire. The love and admiration I have for my parents, Robert and Anna, and brothers, Matthew and Patrick, is beyond my capabilities for description.

Finally, I would like to thank my wife Sarah. She is my best friend and most ardent supporter, and an exceptional scientific mind. Life without her love and companionship is simply unimaginable.

## ABSTRACT

Andrew S. McDaniel

### THE ROLE OF *PAK1* IN THE CELLULAR AND MOLECULAR COMPONENTS OF PLEXIFORM NEUROFIBROMAS

Neurofibromatosis type I (NF1) is a common genetic disease that affects over 200,000 patients in North America, Europe, and Japan. Individuals with NF1 display a wide variety of pathologies; importantly, 15-40% of NF1 patients are affected by plexiform neurofibromas. Neurofibromas are complex tumors consisting of tumorigenic Schwann cells surrounded by endothelial cells, fibroblasts, and inflammatory mast cells. These peripheral nerve sheath tumors contribute significantly to the morbidity and mortality associated with NF1. Currently, no medical therapies exist for treating neurofibromas. Recent evidence indicates that the hematopoietic tumor microenvironment carries out a crucial function in the formation of plexiform neurofibromas. Neurofibromatosis is the result of mutations at the NF1 locus, which encodes the GTPase activating protein neurofibromin. Neurofibromin is a negative regulator of the proto-oncogene Ras. Ras hyperactivation is the molecular basis of NF1 associated phenotypes, and it has been demonstrated that restoration of Ras signaling to wild type levels can correct NF1 associated phenotypes in vitro and in vivo. In keeping with the long term goal of detecting potential molecular targets for medical therapies to treat human plexiform neurofibromas, we have identified the kinase Pak1 as a possible downstream intermediary of Ras signaling in NF1 deficient cells. Studies described here

utilized murine genetic models to study the effects of genetic inactivation of *Pak1* on molecular signaling and cellular functions related to neurofibromas. We demonstrate that inactivation of *Pak1* leads to correction of SCF mediated gain-in-function phenotypes seen in *Nf1* haploinsufficient mast cells, *in vivo* and *in vitro*. However, by using a conditional *Nf1* knockout mouse that is a reliable model of plexiform neurofibroma formation, we shown that loss of *Pak1* alone in the hematopoeitic compartement is not sufficient to prevent neurofibroma formation. Additionally, we describe a key role for *Pak1* in regulating PDGF and TGF- $\beta$  mediated fibroblast functions, *in vitro* and *in vivo*. These studies provide insight into the causes of debilitating tumors related to a common genetic disease, and this research could potentially lead to the development of medical therapies for these tumors, increasing the quality of life for tens of thousands of affected individuals each year.

D. Wade Clapp, M.D., Chair

## TABLE OF CONTENTS

<b>ABBREVIATIONS</b> .....	x
<b>INTRODUCTION</b> .....	1
Disease manifestations of neurofibromatosis type 1 .....	1
Genetic basis of neurofibromatosis type 1 .....	3
Murine models of neurofibromatosis type 1 .....	4
Role of mast cells in neurofibroma formation .....	6
Fibroblasts contribute to neurofibroma pathology .....	9
Ras hyperactivation: the molecular basis of NF1 .....	10
Signaling pathways disrupted in the absence of neurofibromin .....	11
p21 activated kinases: downstream effectors of Rho GTPases .....	12
Pak1 is a multifunctional signal transducer .....	18
Cancer and Pak1 .....	20
Thesis overview .....	21
<b>MATERIALS AND METHODS</b> .....	25
Animals .....	25
Bone marrow mast cell culture .....	25
Mast cell progenitor assay .....	26
Mast cell maturation .....	26
Mast cell immunoblotting .....	27
Mast cell proliferation assay .....	27
Mast cell haptotaxis assay .....	28
F-actin quantitation .....	29

Confocal microscopy .....	29
Mast cell degranulation assay .....	30
Mast cell survival assay .....	30
<i>In vivo</i> mast cell accumulation assay .....	31
<i>Nfl</i> conditional knockout adoptive transfer .....	32
Generation of <i>Krox20Cre;Nflflox<sup>-/-</sup>;Pak1<sup>-/-</sup></i> animals .....	32
Dorsal root ganglion dissection and measurement .....	32
Histological analysis of dorsal root ganglia .....	33
Generation and culture of primary fibroblasts .....	33
Fibroblast proliferation assay .....	34
Fibroblast wound healing assay .....	34
Fibroblast collagen production assay .....	35
Fibroblast apoptosis assay .....	35
Confocal analysis of fibroblast actin cytoskeleton .....	36
Fibroblast immunoblotting .....	36
<i>In vivo</i> fibroblast invasion assays .....	37
Bleomycin induced pulmonary fibrosis model .....	37
<b>RESULTS</b> .....	39
<b>Role of Pak1 in regulating stem cell factor dependent functions in <i>Nfl</i> haploinsufficient mast cells</b> .....	39
Generation of a Pak1 knockout mouse .....	39
Intercross of <i>Nfl<sup>+/-</sup></i> and <i>Pak1<sup>-/-</sup></i> mice .....	42
Loss of <i>Pak1</i> reduces number of mast cell colonies .....	42
Loss of <i>Pak1</i> does not affect expression of mast cell maturation	

markers.....	47
Hyperproliferation of <i>Nf1</i> <sup>+/-</sup> bone marrow derived mast cells is dependent on a Pak1/MAPK pathway .....	47
Loss of <i>Pak1</i> corrects MAPK hyperactivation in <i>Nf1</i> haploinsufficient BMDCs.....	50
A Pak1/p38 pathway regulates increased migration of <i>Nf1</i> <sup>+/-</sup> mast cells.....	60
<i>Pak1</i> is required for the increase in p38 phosphorylation seen in <i>Nf1</i> haploinsufficient mast cells.....	61
<i>Pak1</i> regulates F-actin content and organization in a p38-dependent manner.....	66
Disruption of <i>Pak1</i> reduces granule release from <i>Nf1</i> <sup>+/-</sup> mast cells.....	67
Loss of <i>Pak1</i> does not significantly affect mast cell survival.....	71
Cutaneous expansion and degranulation in <i>Nf1</i> <sup>+/-</sup> mice in response to SCF is <i>Pak1</i> dependent .....	76
<b>Role of <i>Pak1</i> in plexiform neurofibroma formation .....</b>	<b>84</b>
Adoptive transfer of <i>Nf1</i> <sup>+/-</sup> ; <i>Pak1</i> <sup>-/-</sup> bone marrow into Schwann cell nullizygous recipients .....	84
<i>Krox20Cre:Nf1</i> <sup>fllox/fllox</sup> mice reconstituted with <i>Nf1</i> <sup>+/-</sup> ; <i>Pak1</i> <sup>-/-</sup> bone marrow develop neurofibromas .....	87
<i>Krox20Cre:Nf1</i> <sup>fllox/-</sup> mice reconstituted with <i>Nf1</i> <sup>+/-</sup> ; <i>Pak1</i> <sup>-/-</sup> bone marrow develop neurofibromas .....	97
Genetic disruption of <i>Pak1</i> in <i>Krox20Cre:Nf1</i> <sup>fllox/-</sup> mice does not prevent neurofibroma formation.....	98
<b>Role of <i>Pak1</i> in mediating PDGF-BB and TGF-β dependent functions in fibroblasts .....</b>	<b>118</b>
PDGF-BB mediated fibroblast proliferation is <i>Pak1</i> dependent .....	118
Loss of <i>Pak1</i> does not affect TGF-β induced fibroblast proliferation.....	125
<i>Pak1</i> deficient fibroblasts have reduced migration following	



PDGF-BB stimulation.....	125
Disruptions of PDGF-BB mediated activation of the actin cytoskeleton and associated signaling networks are found in <i>Pak1</i> <sup>-/-</sup> fibroblasts .....	128
Loss of <i>Pak1</i> decreases TGF- $\beta$ dependent fibroblast migration.....	137
TGF- $\beta$ stimulated fibroblasts have decreased activation of filamin A and disrupted actin cytoskeletal networks .....	137
<i>Pak1</i> <sup>-/-</sup> fibroblasts have reduced collagen synthesis in response to TGF- $\beta$ .....	138
Reduced survival of <i>Pak1</i> null fibroblasts in response to TGF- $\beta$ and PDGF-BB.....	149
Loss of <i>Pak1</i> inhibits fibroblast recruitment <i>in vivo</i> .....	149
Genetic disruption of <i>Pak1</i> reduces the severity of bleomycin induced lung fibrosis.....	152
<b>DISCUSSION</b> .....	164
Role of <i>Pak1</i> in regulating c-kit mediated <i>Nfl</i> <sup>+/-</sup> mast cell function .....	165
<i>Pak1</i> and plexiform neurofibroma formation .....	168
The role of <i>Pak1</i> in PDGF-BB and TGF- $\beta$ mediated signaling in fibroblasts.....	173
Conclusions and future directions.....	176
<b>REFERENCES</b> .....	179
<b>CURRICULUM VITAE</b>	

## ABBREVIATIONS

$\beta$	Beta
BMMC	Bone Marrow Derived Mast Cell
BSA	Bovine serum albumin
CFU-Mast	Colony forming unit, mast cell
DAPI	4',6-diamidino-2-phenylindole
DMEM	Dulbecco's modified Eagle medium
DMSO	Dimethyl sulfoxide
DNP	Dinitrophenol
DRG	Dorsal root ganglion
ECL	Enhanced chemiluminescence
EDTA	Ethylene diamine tetraacetic acid
ERK	Extracellular regulated kinase
F-actin	Filamentous actin
FBS	Fetal bovine serum
Fc $\epsilon$ RI	High affinity IgE receptor
FGF	Fibroblast growth factor
FITC	Flouroscein isothiocyanate
FACS	Fluorescence activated cell sorting
GRD	GAP related domain
GM-CSF	Granulocyte-macrophage colony stimulating factor
GAP	GTPase activating protein
GDP	Guanine diphosphate
GEF	Guanine nucleotide exchange factor
GRD	GAP-related domain
GTP	Guanine triphosphate
H&E	Hematoxylin and eosin
HEPES	4-(2-hydroxyethyl)-1-piperazineethanesulfonic acid
HSA	Human serum albumin
IgE-DNP	Immunoglobulin E-dinitrophenyl
IL-3	Interleukin-3
IPF	Idiopathic pulmonary fibrosis
IS	Inhibitory switch domain
JMML	Juvenile myelomonocytic leukemia
K-ras	Kirsten-ras
KO	Knockout
LDMNC	Low density mononuclear cells
LOH	Loss of heterozygosity
mAB	Monoclonal antibody
MAPK	Mitogen activated protein kinase
M-CSF	Macrophage-colony stimulating factor
MEK	MAPK/ERK Kinase
MPD	Myeloproliferative disorder
MPNST	Malignant peripheral nerve sheath tumor
NAG	N-acetylglucosamine

NGF	Nerve growth factor
N-ras	Neuroblastoma-ras
NF1	Neurofibromatosis type 1
Nf1	Locus that encodes neurofibromin
PDGF-BB	Platelet derived growth factor-BB isoform
PAK	p21 activated kinase
PBD	p21 binding domain
PBS	Phosphate buffered saline
PCR	Polymerase chain reaction
PE	Phycoerythrin
PI	Propidium iodide
PI3-K	Phosphatidylinositol triphosphate kinase
PMSF	Phenylmethanesulphonylfluoride
Ras	Rat sarcoma viral gene
RPMI	Roswell Park Memorial Institute
SCF	Stem cell factor
SH3	Src homology 3 domain
TGF- $\beta$	Transforming growth factor beta
VEGF	Vascular endothelial growth factor
WT	Wild type

## INTRODUCTION

In 1882, Fredrich von Recklinghausen reported on a 47-year-old male with “innumerable tumors” in the outer skin layer. In this report, he remarked that these tumors were outgrowths of the “externally palpable peripheral nerve trunks”, and in doing so, described the characteristic lesion of the genetic cancer syndrome neurofibromatosis type 1 (NF1) <sup>1</sup>. Although reports of probable neurofibromatosis cases date back to the sixteenth century, and despite an initial review of the disease by Robert W. Smith in 1849 <sup>2</sup>; it was von Recklinghausen’s seminal observation that the tumors afflicting the skin of patients with this disease are derived from neural tissue that instigated significant clinical interest and linked his name to this disease. Today, more than 250,000 people in the United States, Europe and Japan alone are living with NF1; greater than the number of cystic fibrosis, hereditary muscular dystrophy, Huntington’s disease, and Tay-Sach’s disease patients combined.

### Disease manifestations of Neurofibromatosis type 1

NF1 is the most common autosomal dominant genetic disease in humans, with an overall incidence of about 1 in 3500 <sup>3</sup>. Together with Neurofibromatosis type 2, Von-Hippel Lindau syndrome, tuberous sclerosis, and Sturge-Weber syndrome, NF1 is historically classified as a phakomatosis (neurocutaneous syndrome), due to the presence of both dermatologic and neurologic sequelae. Individuals affected with NF1 have a propensity to develop an array of non-malignant and malignant clinical complications <sup>4</sup>.

Skeletal abnormalities, café-au-lait macules, learning disabilities, and other non-malignant complications of NF1 have significant morbidity for affected patients. In addition, children with NF1 are at an increased risk to develop myeloid disorders, especially juvenile myelomonocytic leukemia (JMML) after NF1 loss of heterozygosity in hematopoietic stem and progenitor cells<sup>5,6</sup>.

While the development of other neoplasms such as malignant peripheral nerve sheath tumors (MPNSTs), pheochromocytomas and optic gliomas are also well described in NF1 patients; the most commonly found NF1 related tumor is the neurofibroma (>95% of all patients)<sup>7</sup>. These are complex tumors of the central and peripheral nervous system characterized by aggregations of Schwann cells, fibroblasts, and large deposits of extracellular matrix<sup>4</sup>. Additionally, these lesions are highly vascular with increased concentrations of pro-angiogenic factors such as vascular endothelial growth factor (VEGF) and fibroblast growth factor (FGF)<sup>8</sup>. Furthermore, neurofibromas have a >50 fold higher concentration of mast cells compared to adjacent non-affected areas of skin<sup>9</sup>.

Neurofibromas can be classified into two basic groups: dermal/subcutaneous or plexiform<sup>10</sup>. Dermal/subcutaneous neurofibromas are associated with morbidities such as pain, cosmetic problems, and pruritus (that is unresponsive to antihistamine therapy)<sup>11</sup>. The number of dermal/subcutaneous neurofibromas varies (from <20 to >2000 per individual) from patient to patient as well as between families<sup>12,13</sup>. Dermal/subcutaneous neurofibromas often appear during the onset of puberty and are known to increase in number and size with age and/or pregnancy<sup>14</sup>. However, plexiform neurofibromas, which affect 15-40% of NF1 patients, are generally congenital<sup>15</sup>. These tumors have significant impact in the quality of life of NF1 patients, and plexiform neurofibromas

have the potential to inflict severe morbidity upon NF1 patients, including severe disfigurement, life-threatening organ dysfunction, and premature death<sup>12</sup>. While dermal/subcutaneous neurofibromas are usually benign, plexiform neurofibromas are capable of malignant transformation to MPNSTs. Plexiform neurofibromas carry up to a 10% lifetime risk of malignant transformation, usually accompanied by widespread metastasis<sup>16,17</sup>.

At present, therapies for neurofibromas are lacking at best. For dermal/subcutaneous neurofibromas surgery is the only treatment option, and this is often impractical or impossible due to the sheer number or complexity of the tumors. Furthermore, surgical resection of dermal/subcutaneous neurofibromas is often followed by regrowth of the tumor and/or hypertrophic scarring<sup>11</sup>. Plexiform neurofibromas, due to their location, mass, and diffuse morphology, create significant challenges for effective treatment. Many plexiform neurofibromas are not candidates for surgical resection due to the risk of hemorrhage owing to the highly vascular nature of these tumors (especially facial plexiforms) as well as encroachment into neighboring structures. Radiotherapy of benign plexiform neurofibromas is contraindicated due to the risk of instigating malignant change<sup>11</sup>. Furthermore, no effective medical therapies for neurofibromas exist. Considering the significant clinical complications caused by neurofibromas in patients, the need to identify molecular targets for pharmacologic therapies is pressing.

## Genetic basis of neurofibromatosis type 1

Work using linkage analysis identified the gene responsible for NF1 to reside on chromosome 17<sup>18</sup>. Positional cloning led to the discovery of the *NFI* locus at 17q11.2<sup>19-21</sup>. The *NFI* locus is composed of 60 exons that span over 300kb of genomic DNA and encodes a protein, neurofibromin, which contains 2818 amino acids<sup>22-24</sup>. Neurofibromin is ubiquitously expressed in all tissues; however, neurons, Schwann cells, astrocytes, oligodendrocytes, and leukocytes are noted for their exceptionally high expression of *NFI*<sup>19,25</sup>. Approximately 50% of NF1 diagnoses are the result of new mutations<sup>26</sup>; therefore it is not surprising that a variety of *NFI* mutations have been described, including missense replacements and truncations along the length of the entire gene<sup>27</sup>. It is interesting to note that to date, no correlation between specific mutations and clinical presentation or severity has been reported<sup>27</sup>.

## Murine models of Neurofibromatosis type 1

Initial attempts to model neurofibromatosis in mice used homologous recombination techniques to target *Nfi*, the murine homolog of *NFI*, for disruption<sup>28</sup>. Attempts to generate *Nfi*<sup>-/-</sup> mice were not successful, as these embryos died between days 12 and 14 post-coitus due to abnormalities of cardiac development, specifically located in the outlet vessels of the right ventricle<sup>28</sup>. Furthermore, while *Nfi*<sup>+/-</sup> mice were generated without cardiac malformations, a proportion of *Nfi*<sup>+/-</sup> mice (~10%) did develop a myeloproliferative disorder reminiscent of JMML during the second year of life,

complete with leukemic cells that display loss of heterozygosity at the intact *Nf1* allele<sup>28</sup> and *in vitro* hypersensitivity to GM-CSF<sup>29</sup>, similar to human JMML samples. Importantly, *Nf1*<sup>+/-</sup> mice do not develop either dermal/subcutaneous or plexiform neurofibromas. However, since NF1 patients are obligate heterozygotes, these animals have proven useful for studying the basic cellular biology of cells found in and near neurofibromas.

A second generation of murine neurofibromatosis type 1 models was initiated with the development of a conditionally deleted *Nf1* mouse, using a Cre-Lox system<sup>30</sup>. By breeding the *Nf1*<sup>fllox/fllox</sup> mice with mice that expressed Cre driven by various lineage selective promoters, adult mice could be generated with specific organ systems that totally lacked neurofibromin. Creating a conditional knockout of *Nf1* that caused deletions in Schwann cells (by means of the *Krox20* promoter driving Cre expression) yielded interesting results. Although tumor samples from patients have demonstrated that Schwann cells harbor the somatic *NF1* mutation<sup>31</sup>, mice that contained *Nf1* null Schwann cells (*Krox20Cre;Nf1*<sup>fllox/fllox</sup>) did not develop neurofibromas<sup>30</sup>. However, despite the fact that *Krox20Cre;Nf1*<sup>fllox/fllox</sup> mice are functionally wild type, *Krox20Cre;Nf1*<sup>fllox/fllox</sup> mice that were backcrossed with *Nf1*<sup>+/-</sup> mice to generate one conditionally deleted allele and one traditionally disrupted allele (*Krox20Cre;Nf1*<sup>fllox/-</sup>) developed multiple neurofibromas<sup>30</sup>.

These experiments demonstrated that nullizyosity of *Nf1* in tumorigenic Schwann cells is necessary, but not sufficient for plexiform neurofibroma formation. Critically, haploinsufficiency of *Nf1* in at least a subset of lineages within the tumor microenvironment is required to promote neurofibroma development. The results generated from the *Krox20Cre* NF1 murine model have laid a foundation for the



development of rationally designed therapeutics that target the cells of the microenvironment rather than the tumorigenic cells alone.

### Role of mast cells in neurofibroma formation

Virchow first hypothesized that cancer was the result of an overactive inflammatory response in 1863; indeed, recent studies in multiple murine models have supported this hypothesis and implicated that inflammatory cells are essential for the progression to malignancy<sup>32</sup>. Chronic inflammation is well known to contribute directly to the formation of breast<sup>33</sup>, hepatic<sup>34</sup>, dermal<sup>35</sup>, ovarian<sup>36</sup>, prostate<sup>37</sup>, and many other carcinomas. Patients with chronic inflammatory diseases such as Crohn's disease and ulcerative colitis have increased risks for developing colorectal carcinoma<sup>38</sup>. Further evidence underscoring the importance of inflammation on colon cancer development were studies demonstrating patients who were treated long term with non steroidal anti inflammatory drugs (NSAIDs) had nearly a 50% reduction in their overall risk of developing large bowel adenocarcinoma<sup>39</sup>.

Besides mediating innate immune responses and allergic hypersensitivity, there is an emerging understanding that inflammatory mast cells in the tumor microenvironment have relevance in the promotion of neoplastic development as well. Described relationships between mast cells and tumors date back over 100 years<sup>40</sup>; Mast cells in particular are critical for the transformation to malignancy in a squamous epithelial cancer murine model, by releasing matrix metalloproteinases such as tryptase and activating progelatinase B to activate the angiogenic switch<sup>41</sup>. Since mast cells are the

predominant inflammatory cell found in the neurofibroma microenvironment and are found at such high density at these sites<sup>9</sup>, we have been particularly interested in understanding the potential role these cells play in neurofibroma pathophysiology.

One notable observation drawn from the *Krox20Cre;Nfl<sup>fllox/-</sup>* mouse model is the appearance of mast cells in peripheral nerves well in advance of tumor development<sup>30</sup>. Our laboratory has generated data identifying potential mechanisms that regulate the unique association of mast cells with neurofibromas, centered on the c-Kit/stem cell factor (SCF) signaling axis. SCF, a glycoprotein also known as Steel factor, mast cell growth factor or Kit ligand, is the ligand of the receptor tyrosine kinase (RTK) c-kit<sup>42,43</sup>. SCF exists in both soluble and membrane-bound forms<sup>44</sup>. SCF is a cytokine that induces pleiotropic effects; resulting in the growth and development of hematopoietic stem cells<sup>45</sup>, germ cells<sup>46</sup>, and melanocytes<sup>47</sup>. Importantly, SCF is a potent mitogenic factor for mast cells<sup>48-50</sup>. SCF also stimulates mast cell chemotaxis<sup>51,52</sup> and survival<sup>53,54</sup>. Upon stimulation with SCF or cross-linking of IgE molecules on the cell surface, mast cells release numerous inflammatory byproducts<sup>55,56</sup>. These include VEGF, which stimulates angiogenesis and Schwann cell proliferation<sup>57</sup>, transforming growth factor beta (TGF- $\beta$ )<sup>58</sup>, which is a known growth factor for fibroblasts, as well as many reactive oxygen species and proteases. Therefore, mast cells have the ability to stimulate the growth of cells that compose the neurofibroma as well as remodel the extracellular matrix.

We have demonstrated that *Nfl* haploinsufficient mast cells have increased proliferation, survival, migration, and degranulation *in vitro* and *in vivo*<sup>59-61</sup>. These findings identify that loss of one copy of *Nfl* has functional consequences in mast cells.

We have shown that *Nf1*<sup>+/-</sup> mast cells preferentially migrate toward SCF released from *Nf1*<sup>-/-</sup> Schwann cells compared to wild type mast cells<sup>62</sup>. This Schwann cell/mast cell interaction resulting from the hypersecretion of SCF is thought to be an inciting factor in the early development of neurofibromas<sup>63</sup>.

Studies by Dr. Feng-Chun Yang have revealed the importance of contributions from bone marrow derived cells to neurofibroma development *in vivo*. *Nf1*<sup>+/-</sup> bone marrow was transplanted into *Krox20Cre;Nf1*<sup>fllox/fllox</sup> mice (which normally do not develop tumors). By one year post-transplant, 100% of the *Krox20Cre;Nf1*<sup>fllox/fllox</sup> mice reconstituted with *Nf1*<sup>+/-</sup> marrow had neurofibromas<sup>64</sup>. As a complementary experiment, wild type marrow was transferred into *Krox20Cre;Nf1*<sup>fllox/-</sup> mice (which spontaneously develop tumors). Interestingly, by one year post transplant, these *Krox20Cre;Nf1*<sup>fllox/-</sup> mice did not generate neurofibromas<sup>64</sup>. These experiments show that *Nf1* haploinsufficiency in the hematopoietic portion of the tumor microenvironment is required to induce Schwann cells into forming neurofibromas.

Additional experiments utilized *Krox20Cre;Nf1*<sup>fllox/fllox</sup> mice transplanted with *Nf1*<sup>+/-</sup>; *W<sup>41</sup>W<sup>41</sup>* marrow. The *W<sup>41</sup>* mutation in the c-kit receptor kinase domain leads to mice with a mottled coat color, normal bone marrow cellularity, mild but persistent anemia, and markedly decreased numbers of mast cells and their progenitors<sup>65</sup>. *Krox20Cre;Nf1*<sup>fllox/fllox</sup> mice that were recipients of *Nf1*<sup>+/-</sup>; *W<sup>41</sup>W<sup>41</sup>* marrow did not develop plexiform neurofibromas<sup>64</sup>, implying that the identity of the active component of the tumor-promoting hematopoietic compartment to be a c-Kit dependent cell type, such as mast cells. Given the results from *in vitro* studies on mast cell activity and our data using

the *Krox20Cre* conditional knockout of *Nf1*, we hypothesize that haploinsufficiency at *Nf1* in mast cells specifically is required for the evolution to neoplasia *in vivo*.

### Fibroblasts contribute to neurofibroma pathology

Fibrosis often develops in chronic inflammatory conditions that involve large-scale mast cell activation. In pathologically fibrotic conditions such as scleroderma, post-operative peritoneal adhesions, and radiation induced lung fibrosis, high densities of mast cells are observed<sup>66</sup>. Mast cells can provide growth factors that stimulate this fibroblast growth and invasion, such as TGF- $\beta$  and PDGF<sup>38,58</sup>.

Fibroblasts are also an important component of neurofibromas, and are known to secrete large amounts of extracellular matrix (ECM) at the tumor site<sup>67</sup>. Indeed, up to 50% of the dry weight of neurofibromas is composed of ECM, mainly collagen<sup>68</sup>. The invasion, proliferation, and the extracellular matrix released by fibroblasts in developing tumors, besides adding bulk and mass to neurofibromas, are critical for providing an cellular and protein foundation for angiogenesis and Schwann cell invasion<sup>69</sup>.

Additionally, fibroblasts that are disrupted at *Nf1* have a reduced capability to form perineurial sheaths around Schwann cells, allowing increased access for mast cells and serum growth factors to Schwann cells<sup>70</sup>.

Furthermore, we have recently demonstrated that *Nf1*<sup>+/-</sup> mast cells secrete increased amounts of TGF- $\beta$ , and that this leads to Ras dependent gains of function in proliferation, migration, and ECM secretion by *Nf1*<sup>+/-</sup> fibroblasts<sup>71</sup>. This data provides a potential mechanism for the profound fibrosis seen histologically in neurofibroma

samples and again implicates the mast cell as an inducer, via paracrine factors, of cellular events important for neurofibroma formation.

### Ras hyperactivation: the molecular basis of NF1

As a tumor suppressor, neurofibromin functions as a member of a molecular switchboard involved in transducing extracellular signals to the nucleus via Ras<sup>3</sup>. Neurofibromin acts as an important negative regulator of this signaling network by acting as a GTPase activating protein (GAP) via its binding to active Ras and increasing GTP hydrolysis<sup>72</sup>. In hematopoietic cells, p120 GAP is also expressed, although the gene encoding this protein is not associated with cancer development<sup>73</sup>. The Ras-GAP related domain (GRD) responsible for GTPase inactivation is located between amino acids 1125-1537 in *NF1*<sup>20</sup>. *NF1* GRD is highly homologous with p120 GAP catalytic domain<sup>72</sup>; however, reconstitution of *Nf1* deficient cells with *Nf1* GRD, but not p120 GRD, is sufficient to correct gain-in-function phenotypes, both *in vitro* and *in vivo*<sup>62,74,75</sup>. Although neurofibromin has been described to regulate cAMP levels<sup>76</sup> and associate with microtubules<sup>77</sup>; to date, Ras-GRD is the only domain within neurofibromin with an associated biological function that has an impact on disease<sup>10</sup>.

Ras coordinates the growth, differentiation, and survival of many cell types and its activation status is tightly regulated<sup>78</sup>. Upon ligand binding, numerous growth factor receptors (including c-Kit) recruit Ras to the plasma membrane and initiate the formation of an activation complex that includes the Grb2 adapter and guanine nucleotide exchange factor Sos, which loads GTP onto Ras. Signal transduction from the Ras network

proceeds until GAP proteins are able to bind Ras and facilitate the hydrolysis of GTP to GDP. Therefore loss or inactivation of *Nf1* leads to a shift towards increased Ras-GTP vis-à-vis Ras-GDP, leading to hyperactivation of downstream signaling molecules <sup>79</sup>. Hyperactivation of Ras at the molecular level is believed to be responsible for NF1 related pathologies ranging from JMML <sup>80</sup>, pilocytic astrocytomas <sup>81</sup>, optic glioma <sup>82</sup>, learning disabilities <sup>83</sup>, and neurofibromas <sup>84</sup>.

### Signaling pathways disrupted in the absence of neurofibromin

Ras activation by in response to growth factor stimulation leads to the recruitment and activity of Raf-1 serine/threonine kinase <sup>85</sup>. Raf-1, in turn activates the MAPKK Mek1/2 <sup>86</sup> and subsequently p42/p44 MAPK (Erks) <sup>87,88</sup>. This classical Ras/Raf/Mek/Erk cascade is well described as essential to numerous cells type for the proliferation and survival signals sent by growth factors such as interleukin-3 (IL-3), granulocyte-macrophage colony stimulating factor (GM-CSF), stem cell factor (SCF), and many others <sup>89-91</sup>. Many groups have found hyperactivation of the Ras/Raf/Mek/Erk pathway following growth factor stimulation in the context of neurofibromin deficiency, particularly in cellular lineages relevant to neurofibromas, including: Schwann cells <sup>92</sup>, fibroblasts <sup>71</sup>, endothelial cells <sup>93</sup>, vascular smooth muscle cells <sup>94</sup>, and mast cells <sup>59</sup>.

Additionally, Ras has been demonstrated to bind to the p110 catalytic subunit of Class I phosphatidylinositol 3-kinases (PI3-K), leading to increased lipid kinase activity <sup>95</sup>. Similar to Ras, PI3-K itself transduces signals through a number of networks to regulate multiple cellular functions <sup>95</sup>. Some downstream effectors of PI3-K have been

shown to be hyperactivated in neurofibroma-associated cells without neurofibromin; including Akt<sup>60,96</sup>, mTOR<sup>97</sup>, p70S6 kinase<sup>97</sup>, and the small GTPase Rac1/2<sup>60</sup>.

While the critical contribution of the Ras/Raf/Mek/Erk pathway to NF1 associated phenotypes is well known, the prolonged activation of this pathway is dependent on other signals, including PI3-K<sup>98</sup>. Work from our laboratory has established that pharmacologic inhibition or genetic disruption of PI3-K in *Nf1*<sup>+/-</sup> mast cells will reduce the SCF mediated hyperactivation of Raf-1, Mek1/2 and Erk1/2 kinase activity *in vitro*<sup>60</sup>, implying the existence of cross talk between the PI3-K and MAPK pathways. Further efforts showed that genetic loss of *Rac2*, and important downstream target of PI3-K will correct the hyperactivation of Erk, as well as the gains in proliferation in *Nf1*<sup>+/-</sup> mast cells<sup>60</sup>. However, identification of the mediators downstream of Rac that are responsible for the inter-pathway signaling in *Nf1*<sup>+/-</sup> mast cell activity is incomplete. Elucidation of the specific molecules involved in the hyperactive gain-in-function phenotypes associated with *Nf1* haploinsufficiency is critical for understanding the biochemical mechanisms underlying tumor pathophysiology in NF1.

#### p21 activated kinases: downstream effectors of Rho GTPases

The Ras related-Rho family of GTPases (including Rac, Rho, cdc42, among others) are molecular switches that regulate a wide variety of cellular activities that are important in normal as well as pathological states<sup>99</sup>. The Rho GTPase family has roles in cellular functions as diverse as cytoskeletal activation and regulation, vesicle transport, gene expression, cell cycle transitioning, and oxidant generation<sup>100</sup>. Considerable effort

has been put forth in identifying the signaling networks downstream of these GTPases and their related functions<sup>101</sup>. The first kinase proteins known to be regulated by the Rho family of GTPases were identified in 1994 in a gel overlay assay for Rac1 binding partners, and were termed p21 activated kinases, or Paks<sup>102</sup>. The binding partners found at 68, 65, and 62 kd were later termed Pak1 (or  $\alpha$ -Pak), Pak3 (or  $\beta$ -Pak), and Pak2 (or  $\gamma$ -Pak), respectively. Pak1 was found to share 77% identity with Pak2 and 81% identity with Pak3<sup>103</sup>. Pak proteins interacted only with active (GTP), not inactive (GDP) bound Rac or cdc42<sup>102</sup>. Furthermore, the intrinsic phosphotransferase activity of Paks on myelin basic protein was dramatically increased after interacting with GTP bound Rac or cdc42<sup>104</sup>.

Sequence analysis of the Pak proteins showed high homology with the yeast Ste20 serine/threonine kinase<sup>105,106</sup>. Phylogenetic investigations have revealed that all eukaryotic kinomes contain multiple members of the Ste20 family<sup>106</sup>. Paks and Ste20 have a highly conserved catalytic domain located near the C-terminus (amino acid residues (aa) 255–529 in PAK 1). Outside of this catalytic domain, Paks and Ste20 diverge in sequence, save for a short regulatory region close to the N-terminus. This regulatory region, called the p21 binding domain or PBD (aa 67-113 in Pak1), is very highly conserved among all Ste20 proteins and allows for binding with activated Rac or cdc42<sup>105</sup>. Overlapping with, but not congruent to, the PBD is an autoinhibitory segment known as the inhibitory switch (aa 83-149 in Pak1) that regulates basal kinase activity<sup>107</sup>. Other sequence commonalities between Paks1-3 include two N-terminal canonical PXXP SH3-binding domains, the first has been shown to interact with the adapter protein Nck<sup>108</sup>, the second binds to Grb2<sup>109</sup>; as well as a non-classical PXP SH3-binding domain,



known to interact with PIX (also known as Rac/cdc42 GEF6)<sup>110</sup>. Furthermore, Pak1 contains two additional PXXP SH3-binding domains in its N-terminal region that are not found in Pak2.

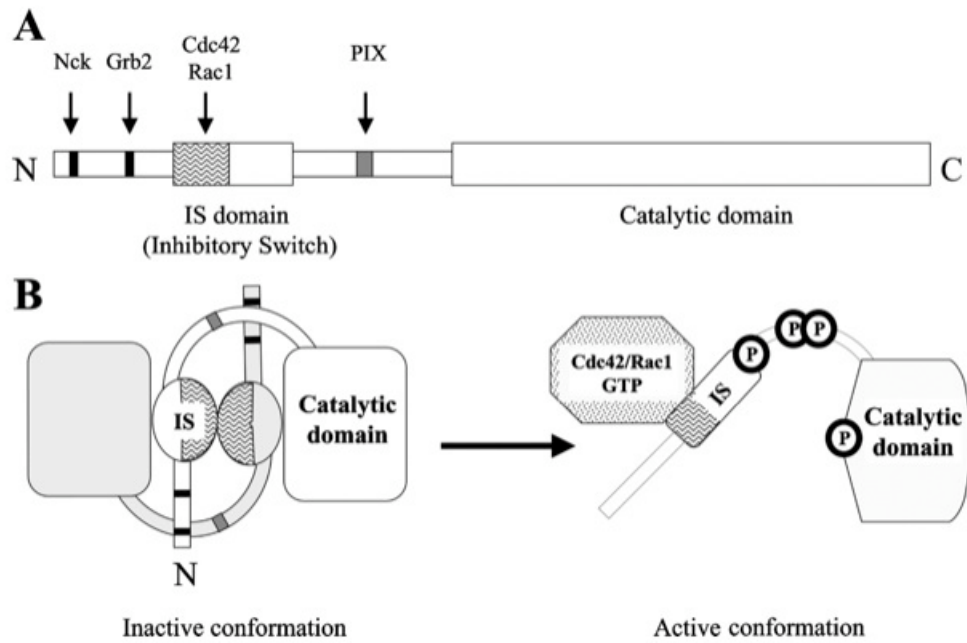
Crystal structure of Pak1 revealed it exists as an inactivated homodimer *in vivo*, arranged in a trans-inhibited conformation: the N-terminal autoinhibitory segment of one of the dimer partners binds and inactivates the C-terminal catalytic domain of the other<sup>111</sup>. Binding of GTP-bound Rac to the PBD of one of the dimer partners disrupts dimerization, causing conformational changes that destabilize the inhibitory switch and disassociate it from its partner's catalytic domain<sup>101</sup>. Once freed from the dimerized state, the kinase domain is capable for catalytic function<sup>107</sup>. However, full catalytic efficiency and sustained alleviation from reforming autoinhibitory dimers requires phosphorylation in the activation loop of the catalytic domain (Thr423 in Pak1)<sup>112-114</sup>. In addition to phosphorylation at Thr423, Pak1 kinase activity is also upregulated by phosphorylation at Ser144, which is located in the inhibitory switch domain<sup>115</sup>. Both of these residues are known autophosphorylation sites; however, maximal Pak1 kinase activity is dependent upon PDK1 phosphorylation of Thr423 after Rac/cdc42 binding<sup>113,116</sup>.

Although Pak proteins are primarily thought of and initially discovered as downstream effectors of Rac and cdc42, GTPase independent activation has also been described. The SH3-binding domains in the N-terminal region allow for membrane recruitment by Nck and Grb2, which leads to induction of Pak kinase activity<sup>117-119</sup>. Also, Paks are autophosphorylated and activated following certain protease treatments<sup>120</sup>. For example, Pak2, but not Pak1, is constitutively activated following

cleavage by caspase 3 at Asp212 during apoptosis<sup>121</sup>. Lipids such as sphingosine and sphingosine derived lipids, gangliosides, and phosphatidic acids all are known to activate Pak1 independent of GTPase binding<sup>122</sup>. The understanding of the physiologic importance of lipid activation relative to GTPase activation of Pak1 is incomplete at best.

Despite having high affinity for myelin basic protein and histone H4 in *in vitro* kinase assays, it is unlikely that Pak1 phosphorylates these proteins in physiologic systems<sup>115</sup>. Biochemical studies have indicated that Pak1 is a “basic directed” kinase, with a (K/R)RXS target sequence for phosphorylation<sup>123</sup>. This is a similar phosphorylation sequence to proteins such as PKA and PKC; however, an acidic residue at the -1 position is well tolerated by Pak but not by PKA and PKC<sup>123</sup>. In addition, Pak1 cannot tolerate proline residues at -1 or +1 positions, which are required critical for substrate phosphorylation by proline directed kinases such as MAPKs and cdc2,<sup>123</sup> indicating that Pak1 and proline-directed kinases do not share phosphorylation targets.

**Figure 1**



Biochemical Society Transactions [www.biochemsoctrans.org](http://www.biochemsoctrans.org) Biochem. Soc. Trans. (2005) 33, 646-648

**Figure 1- Structure of Pak1.** **A)** Schematic representation of relevant domains in primary structure of Pak1. The PXXP SH3-binding sites of Pak1 for the adaptors Nck and Grb2, the PXP SH3-binding site for the exchange factor PIX, and the PBD for the GTPases Cdc42 and Rac1 are shown. **B)** Diagram of conformational changes induced upon activation by GTPases. The inactive state is a trans-inhibited dimer. The IS domain overlaps portions of the PBD, regulates the dimerization of Pak1 and inhibits the kinase activity of the other member of the Pak1 homodimer. GTPase binding to the PBD leads to conformational changes of the IS domain, releasing the Pak1 homodimer. The active state is a monomer whose open conformation is stabilized by auto-phosphorylation. This figure was first published in its original form by M.C. Parrini, et al. in *Biochem. Soc. Trans.* 33, 646-648 (2005).

## Pak is a multifunctional signal transducer

Pak1 is well described as a modulator of cytoskeletal dynamics. Immunofluorescence analysis of cells stimulated with agents such as PDGF, insulin, and transformation by v-src revealed subcellular localization of Pak1 into cortical actin structures<sup>124</sup>. This interaction with the cytoskeleton helps regulate motility, as expression of dominant negative Pak1 lead to decreased migration of NIH-3T3 cells, with associated loss of organized actin structures<sup>125</sup>. Conversely, overexpression of constitutively active Pak1 lead to increases in both motility as well as large actin structures at the leading edge<sup>125</sup>. Pak1 has a number of downstream targets that regulate actin organization and polymerization, including filamin A, which leads to crosslinking of filamentous actin into orthogonal networks at the membrane<sup>126</sup>; and LIM kinase, which inactivates the F-actin destabilizing protein cofilin, leading to aggregation of F-actin fibers<sup>127</sup>. Pak can also regulate microtubule dynamics through its inactivation of the microtubule destabilize stathmin<sup>128</sup>. One working model of Pak and its critical role in regulating cell motility describes Pak1 being activated by Rac and cdc42 near the leading edge of the cell after chemotactic stimulation, leading to stabilization of actin structures after activating Filamin A and inhibiting cofilin (via LIM kinase) and maintenance of growing microtubule structures by inhibition of stathmin<sup>101</sup>.

In addition to regulating the cytoskeleton, Pak has an important role in regulating activation of MAPK signaling pathways. This role was initially suggested from the fact that Ste20 is known to act as a MEKK (MAPK/Erk kinase kinase) in yeast pheromone signaling<sup>106</sup>. Pak1 directly activates Raf-1, by phosphorylating serine residue 338<sup>129</sup>.

Phosphorylation of Ser338 is critical for full activation of Raf-1 kinase activity<sup>130</sup>. In addition, Pak1 also directly activates MEK1, phosphorylating serine 298<sup>131</sup>. Serine 298 is important for “priming” MEK1 for activation by increasing Raf-1 kinase activity toward Ser217/221 on MEK, leading to increased Mek kinase activation<sup>132</sup>.

Furthermore, transfection of siRNA to Pak1 greatly reduced Erk activation by PDGF in NIH-3T3 cells, associated with congruent decreases in Raf and Mek activity<sup>133</sup>. The phosphorylation of Pak1 targets on Raf-1 (Ser338) and Mek1 (Ser298) can increase efficiency of Erk activation by facilitating protein-protein interactions and result in increased responses to low-level stimuli<sup>134</sup>.

Besides activating the Erk MAPK, overexpressed Pak1 has also been reported to activate p38 MAPKs<sup>135,136</sup>. Overexpression of constitutively active Pak1 increases p38 kinase activity following phosphorylation at Thr180<sup>136</sup>. p38 activity following growth factor stimulation is linked to the migration of numerous cell types; overexpression of dominant negative Pak1 impedes p38 dependent migration in smooth muscle cells<sup>137</sup> and macrophages<sup>138</sup>. Unlike the well described interactions between Pak1 and the Raf/Mek/Erk pathway, the manner in which Pak1 effects p38 is incompletely understood. p38 is not a direct target of Pak1 kinase activity, and the exact mechanism of how Pak1 leads to increased p38 activity is unclear. Even less understood is the relationship between Pak1 and JNK. Overexpression of Pak1 has produced reports that indicate both enhanced<sup>135,139,140</sup> as well as impaired<sup>141,142</sup> JNK activity. Pak/JNK interactions may be cell type specific, and as with p38, the nature of these inchoate interactions requires further examination<sup>101</sup>.

In multiple cellular systems, Pak1 has been reported to be a member of an anti-apoptotic signaling network via its interactions with Bad<sup>143-146</sup>. Bad is a death promoting Bcl-2 family member that binds to Bcl-2 and Bcl-xL, preventing their anti-apoptotic activities<sup>146</sup>. However, after phosphorylation, Bad is unable to associate with Bcl-2 or Bcl-xL, and instead is sequestered by the 14-3-3 cytosolic adapter protein. Pak1 phosphorylates Bad at Ser112 and Ser136 *in vitro* and *in vivo*, leading to decreased association of Bad with Bcl-2 and Bcl-xL and corresponding decreases in apoptosis following stimulation with survival signals<sup>143</sup>.

### Cancer and Pak1

In recent years, Pak1 activity has been linked to the development of an extremely wide variety of human cancers, including: breast<sup>145,147-149</sup>, melanoma<sup>150</sup>, glioblastoma<sup>151</sup>, bladder<sup>152</sup>, kidney<sup>153</sup>, ovarian<sup>154</sup>, liver<sup>155</sup>, colorectal<sup>156</sup>, and pancreatic<sup>157</sup>. The role of Pak1 in carcinomas of the breast is very well documented. Initial reports described PI3-K/Pak1 dependent reorganization of the actin cytoskeleton following heregulin stimulation, leading to increased migration of breast cancer cells<sup>158</sup>. More recent reports have focused on overexpression of Pak1 in breast cancer cells, particularly in the nucleus, resulting in increased phosphorylation of the estrogen-receptor alpha and subsequent progressive tamoxifen resistance<sup>159</sup>.

In addition, Pak1 activity has been linked to oncogenic processes in cell types relevant to neurofibromas. Pak1 initially drew attention with regards to NF1 due to the fact that Pak1 can induce many cellular functions similar to those caused by activated

Ras. In Rat-1 fibroblasts, kinase dead Pak1 reduced oncogenic transformation mediated by overexpression of K-Ras by over 90% in soft-agar foci assays <sup>160</sup>. This result was linked to the decreased Erk activation found in the Rat-1 cells that co-expressed K-Ras and kinase dead Pak1 <sup>160</sup>. In a similar manner, expression of dominant negative Pak1 in rat Schwann cell lines prevented Ras-mediated transformation <sup>161</sup>. Using a *NF1*<sup>-/-</sup> Schwann cell line taken from a NF1 patient, mouse xenograft experiments revealed that *in vivo* tumorigenicity could be greatly reduced by transfecting the *NF1* null Schwann cells with kinase dead Pak1 prior to implantation <sup>161</sup>. Other groups using FK228, an inhibitor of the histone deacetylase complex that reduces Pak1 kinase activity, have shown that treatment of mice with FK228 causes the complete regression of xenografts resulting from MPNST cells derived from NF1 patients <sup>162</sup>. Importantly, *Nf1*<sup>+/-</sup> mast cells that have been stimulated with SCF have increased Pak1 kinase activity <sup>60</sup>. Given this finding and the critical role ascribed to Rac in regulating *Nf1* haploinsufficient gains-in-function, *Pak1* is an appealing candidate gene for modulating the hyperactive MAPK signaling in cells of the tumor microenvironment that allows neurofibroma progression.

### Thesis overview

Identification of the specific mediators downstream of hyperactive Ras is critical for understanding the biochemical mechanisms underlying the abnormal cell phenotypes that contribute to the pathophysiology of neurofibromas in NF1. Studies described here examine the role of *Pak1* in regulating aberrant Ras signaling in cells that have disruptions in *Nf1*. The aims of this work are threefold, first to evaluate the role of Pak1



as an effector of SCF mediated gain-in-function phenotypes associated with Nf1 haploinsufficiency in mast cells *in vitro* and *in vivo*. Second, we use a conditional *Nf1* knockout animal disease model to determine the significance of Pak1 disruption in the development of *Nf1* deficient neoplasia such as a plexiform neurofibroma. And third, we examine if Pak1 loss has functional consequences in PDGF and TGF- $\beta$  mediated signaling events and cellular functions in fibroblasts. We expect that these studies will provide unique insights into the pathophysiology of NF1 and highlight Pak1 as a possible drug target for the treatment of the disease.

Figure 2

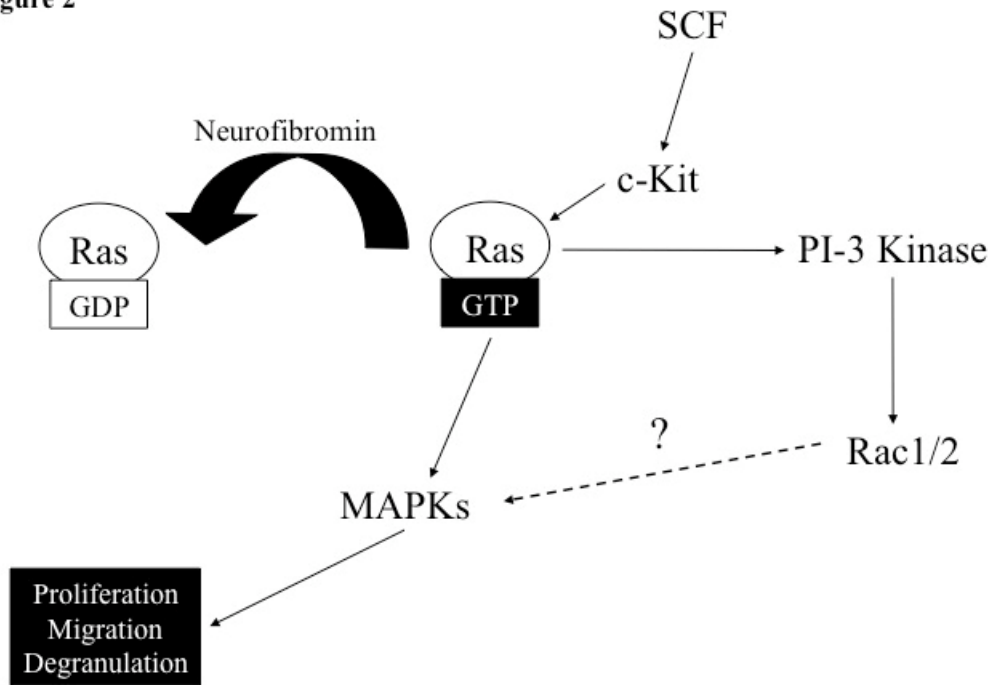


**Figure 2- Schematic representation of signaling events associated with *Nf1***

**haploinsufficiency.** Ras is activated by the binding of SCF to its receptor c-Kit, which activates a number of GEFs that catalyze the conversion of inactive Ras-GDP to active Ras-GTP. Disruptions at *Nf1* prevent the normal conversion of active Ras back to its inactive state, leading to its hyperactivation. Hyperactive Ras in turn recruits and activates the MAPK effector pathway that ultimately increase many cellular functions, including proliferation, migration, and degranulation. These gains-in-function and increases in MAPK signaling are dependent upon Ras activation of PI3-K/Rac. The signaling events downstream of Rac that lead to MAPK hyperactivation are incompletely understood.

## MATERIALS AND METHODS

### ANIMALS

Nf1<sup>+/-</sup> mice were obtained from Tyler Jacks at the Massachusetts Institute of Technology (Cambridge, MA) in a C57BL/6.129 background and backcrossed for 13 generations into the C57BL/6J strain. Pak1<sup>-/-</sup> mice were generated in Dr. Jonathan Chernoff's Laboratory (Temple University) and are backcrossed six generations to be on a C57BL/6J strain. These studies were conducted with a protocol approved by the Indiana University Laboratory Animal Research Center. The Nf1 allele was genotyped as described previously<sup>163</sup>. The Pak1 allele was genotyped by PCR using the following primers: Pak 1 Forward=GCCCTTCACAGGAGCTTAATGA, Pak 1 Reverse: GAAAGGACTGAATCTAATAGCA, neoReverse: CATTTGTCACGTCCTGCACGA set up in two separate reactions (one for WT and one for KO band) PCR program Pak1: 94 2 min, 94 20s (92 for KO reaction), 52 (58 for KO reaction) 20s X 35 cycles, 71 2min, 71 7 min, 4 48 hr. WT Reaction, yields a 240 bp band; KO reaction, yields a 360 bp band. Multiple F0 founders were used to generate the four Nf1 and Pak1 genotypes used in these experiments as outlined. F0: Nf1<sup>+/-</sup>; Pak1<sup>+/+</sup> x Nf1<sup>+/+</sup>; Pak1<sup>-/-</sup>. F1: Nf1<sup>+/-</sup>; Pak1<sup>+/-</sup> x Nf1<sup>+/+</sup>; Pak1<sup>+/-</sup>. F2: Nf1<sup>+/-</sup>; Pak1<sup>-/-</sup>, Nf1<sup>+/+</sup>; Pak1<sup>-/-</sup>, Nf1<sup>+/-</sup>; Pak1<sup>+/+</sup>, Nf1<sup>+/+</sup>; Pak1<sup>+/+</sup>.

### BONE MARROW MAST CELL CULTURE

□ BMMCs were cultured in RPMI (Gibco BRL) supplemented with 10% fetal calf serum (HiClone), 1% glutamine (BioWhittaker), 1.5% HEPES (BioWhittaker), 2%

penicillin/streptomycin (BioWhittaker) and 5 ng/mL IL-3 (Peprotech). Cells were cultured in a 37°C, 5% CO<sub>2</sub>, humidified incubator. All proliferation, migration, and biochemical assays utilized BMMCs that had been in culture between four to eight weeks. All experiments were conducted using at least three independent lines from each genotype.

#### MAST CELL PROGENITOR ASSAY

Using an established methylcellulose culture based method<sup>164,165</sup>, we determined the *in vitro* mast cell colony forming ability of *Pak1*<sup>-/-</sup> and *Nfl*<sup>+/-</sup>;*Pak1*<sup>-/-</sup> bone marrow. Briefly, whole marrow from both femurs and tibias were collected from animals and pooled. LDMNC were isolated using Histopaque 1119 (Sigma Aldrich) and counted using a hemocytometer. 2x10<sup>4</sup> cells were then plated in 1mL methylcellulose containing 20% fetal calf serum (HiClone), 1% glutamine (BioWhittaker), 1.5% HEPES (BioWhittaker), 2% penicillin/streptomycin (BioWhittaker), 2.5ng/mL IL-3 (Peprotech), and 10ng/mL SCF (Peprotech). After 21 days growth in a 37°C, 5% CO<sub>2</sub>, humidified incubator, the surviving mast cell colonies were counted and are expressed as number of mast cell colonies per animal. Assays were performed in triplicate.

#### MAST CELL MATURATION

Maturation of cultured bone marrow mast cells was assayed by the expression levels of c-Kit and FcεRI using fluorescence cytometry as described in other reports<sup>164</sup>. 4-week-old mast cell cultures were blocked with unconjugated anti-FcγRII/III (BD Pharmingen) and washed. This was followed by incubation with anti-DNP monoclonal antibody IgE clone SPE-7 (Sigma Chemical Co), anti-mouse CD 117 (c-kit) PE conjugated antibody (BD

Pharmingen), and FITC conjugated anti-mouse IgE (BD Pharmingen) secondary antibody. Cells were then washed to remove unbound antibodies and resuspended in 0.5% BSA PBS Buffer. Aliquots of mast cells were also stained with FITC and PE conjugated rat IgG2b,K isotype antibodies to serve as negative controls. Cells were analyzed by FACS<sup>TM</sup>. Cells that were double positive for both c-kit and FcεRI were considered to be mature and suitable for use in *in vitro* experiments.

#### MAST CELL IMMUNOBLOTTING

Whole cell protein extracts were obtained from SCF stimulated BMBC in lysis buffer (50mM Tris pH 7.4, 150mM NaCl, 2mM EDTA pH 8.0, 1% Triton X-100, 1mM PMSF, 1mM NaF, 1mM Na<sub>3</sub>VO<sub>4</sub>, 10% glycerol and Complete protease inhibitor), and equivalent amounts of protein were electrophoresed on 10% SDS-PAGE gels, transferred to nitrocellulose membranes (Amersham Biosciences), and detected by Western blotting using the ECL Plus system (Amersham Biosciences). Antibodies used were Phospho-p44/42 MAPK (Thr202/Tyr204) (197G2) Rabbit mAb (Cell Signaling Technology), p44/42 MAP Kinase Antibody (Cell Signaling Technology) Phospho-MEK1/2 (Ser217/221) Antibody (Cell Signaling Technology), Anti-MEK1, NT (Upstate), Phospho-MEK1/2 (Ser298) Antibody (Biosource International) Anti-phospho-Raf-1 (Ser338) (Upstate), Monoclonal β-actin antibody (clone AC-15) (Sigma-Aldrich).

#### MAST CELL PROLIFERATION ASSAY

Proliferation assays were performed as described previously<sup>59</sup>. Briefly, BMBCs from each genotype were deprived of growth factors for 24 h, and treated with 10μM

Mek1 inhibitor PD98059 (Biosource International), 10 $\mu$ M p38 MAPK inhibitor SB203580 (Biosource International) or DMSO for 2h prior to stimulation. 3 x 10<sup>5</sup> cells were plated in 24-well dishes in 1 ml RPMI containing 10% fetal calf serum, 1% glutamine (BioWhittaker), 1.5% HEPES (BioWhittaker), 2% penicillin/streptomycin (BioWhittaker), and 50 ng/ml SCF (PeproTech) or no growth factors as indicated in a 37°C, 5% CO<sub>2</sub>, humidified incubator. After 72 h, cells were counted using a hemocytometer. Cell viability was determined by a trypan blue exclusion assay. Assays were performed in triplicate.

#### MAST CELL HAPTOTAXIS ASSAY

To evaluate mast cell migration, a transwell haptotaxis assay was used as previously described<sup>164,166</sup>. 2.5x10<sup>5</sup> cells were resuspended in 100  $\mu$ l RPMI with 10 $\mu$ M Mek1 inhibitor PD98095 (Biosource International), 10 $\mu$ M p38 MAPK inhibitor SB203580 (Biosource International) or DMSO for 2h prior to stimulation. These cells were loaded onto transwell filters (8mm pore filter Transwell, 24 well cluster; Costar) that were coated with recombinant fibronectin fragment (Retronectin CH296, Takara), which then were placed in wells containing 600  $\mu$ l of serum free RPMI supplemented with 25ng/mL SCF. After four hours of incubation at 37°C in 5% CO<sub>2</sub>, non-migratory cells on the upper membrane surface were removed with a cotton swab, and migrated cells attached to the bottom surface of the membrane were stained with 0.1% crystal violet in 0.1 M borate, pH 9.0, 2% ethanol for 10 minutes at room temperature. The average number of migrated cells per higher-power field was counted with an inverted microscope using the 20x objective lens. Assays were performed in triplicate.

## F-ACTIN QUANTITATION

To evaluate F-actin content, BMMCs were pre treated with inhibitors and stimulated as described above for migration assays. After 30 minutes of incubation at 37°C in 5% CO<sub>2</sub> cells were removed from the upper chamber of the transwell and placed into 3.7% formaldehyde solution for fixation. Fixed cells were treated with 0.01% Triton X-100 (Sigma-Aldrich) in PBS for 5 minutes at 25°C, washed, and then incubated with 160nM Alexa Fluor® 488 Phalloidin (Invitrogen) for 20 minutes at 25°C prior to FACS analysis by fluorescence cytometry. A minimum of 10,000 mast cell events were recorded, and the results are reported as the fold increase in mean channel fluorescence from unstimulated cells. Assays were performed in triplicate.

## CONFOCAL MICROSCOPY

To evaluate F-actin organization, BMMCs were pre treated with inhibitors and stimulated as described above for migration assays. After 30 minutes of incubation at 37°C in 5% CO<sub>2</sub> cells were removed from the upper chamber of the transwell and were placed into cytopsin chambers for centrifugation onto microscope slides. The slides were placed into 3.7% formaldehyde solution for fixation. Fixed cells were treated with 0.01% Triton X-100 (Sigma-Aldrich) in PBS for 5 minutes at 25°C, washed, and then incubated with 160nM Alexa Fluor® 488 Phalloidin (Invitrogen) for 20 minutes at 25°C prior to mounting with DAPI. Cells were then analyzed via confocal microscope with the Zeiss UV LSM-510 system. Quantization of the fluorescent intensity of the confocal image was analyzed using NIH ImageJ software.



## MAST CELL DEGRANULATION ASSAY

Measurements of *in vitro* degranulation of mast cells are proposed using a  $\beta$ -hexosaminidase release assay as previously described<sup>167,168</sup>. Four to six weeks after initiation of culture, BMDCs were washed and sensitized for 2 hours at  $2 \times 10^6$  cell/ml in 0.5% BSA RPMI 1640 containing 1.5  $\mu$ g/ml of anti-DNP IgE monoclonal antibody (clone SPE-7, Sigma Chemical Co). Excess antibody was removed and cells were resuspended at  $2 \times 10^6$  cells/ml in Tyrode's buffer (10 mM HEPES buffer, 130 mM NaCl, 5 mM KCl, 1.4 mM CaCl<sub>2</sub>, 1mM MgCl<sub>2</sub>, 5.6 mM glucose, and 0.05% BSA, pH=7.4). Sensitized BMDCs were then stimulated with 30ng/ml dinitrophenyl conjugated to human serum albumin (DNP-HSA) (Sigma Chemical Co.) and 25ng/ml SCF for 15 minutes at 37°C. The cell pellet was solubilized in Tyrode's buffer, 0.5% Triton X-100.  $\beta$ -hexosaminidase release was measured in both the supernatant and the cell pellet by incubating with 4-Nitrophenyl N-acetyl-beta-D-glucosaminide (p-nitrophenyl-N-acetyl-b-D-glucosamine) prepared in sodium citrate (pH 4.5) for one hour at 37°C. A 0.1 M Sodium carbonate/sodium bicarbonate buffer (pH 10) was used to stop the reaction and the assay was read at 405 nm. Degree of degranulation was reflected as a percent of  $\beta$ -hexosaminidase released = (OD of supernatant)/ (OD of total (supernatant + pellet)) x 100. Assays were performed in triplicate.

## MAST CELL SURVIVAL ASSAY

To examine the effect of *Pak1* loss on the survival of *Nfl* +/- mast cells in response to SCF, mast cells cultured as above were deprived of growth factors for 24 hours, and  $5 \times 10^5$  cells were plated in 24-well dishes with serum free RPMI containing 1% glutamine

(BioWhittaker), 1.5% HEPES (BioWhittaker), and 2% penicillin/streptomycin (BioWhittaker) supplemented with 50ng/ml of SCF. The number of surviving cells was determined by trypan blue exclusion at 48 hours of culture post stimulation in a 37°C, 5% CO<sub>2</sub>, humidified incubator. The number of apoptotic cells was measured by using the Annexin V-FITC Apoptosis detection kit (BD Pharmingen) and FACS™ analysis. Cells that stained double positive for both Annexin V and PI were counted as apoptotic. Assays were performed in triplicate.

#### *IN VIVO* MAST CELL ACCUMULATION ASSAY

Adapting methods described previously<sup>169</sup>, Adult Nf1<sup>+/-</sup>; Pak1<sup>-/-</sup>, Nf1<sup>+/+</sup>; Pak1<sup>-/-</sup>, Nf1<sup>+/-</sup>; Pak1<sup>+/+</sup>, Nf1<sup>+/+</sup>; Pak1<sup>+/+</sup> mice received a continuous infusion of various doses of SCF or vehicle (PBS) from microosmotic pumps (Alzet) placed under the dorsal back skin. Osmotic pumps were surgically placed under light avertin anesthesia. SCF or vehicle was released over 7 d at a rate of 0.5 µl/hour, and osmotic pumps were surgically removed on day 7 after sacrifice by cervical dislocation. To accurately identify cutaneous sections for quantitating changes in mast cell numbers in response to SCF, the dorsal skin was stained with a drop of Davidson Marking System® green tissue dye at the point of exit of SCF from the osmotic pump before removal of the pump. 3-cm sections of skin marked with tissue dye were removed, fixed in buffered formalin, and processed in paraffin-embedded sections. Specimens were stained with hematoxylin and eosin to assess routine histology and with Giemsa to identify mast cells. Cutaneous mast cells were quantitated in a blinded fashion by counting 2-mm<sup>2</sup> sections in proximity to the tissue dye stain. Cells were considered degranulated if there was a change from their

normal compacted and granular appearance resulting in an extensive dispersion of more than 15 extruded vesicles localized near the cell, or when there was an extensive loss of granule staining, giving the cell a “ghostly” or “hollow” look<sup>170</sup>.

#### *Nf1* CONDITIONAL KNOCKOUT ADOPTIVE TRANSFER

*Krox20Cre;Nf1flox/flox* and *Krox20Cre;Nf1flox/-* mice were used as recipients to see if the adoptive transfer of *Nf1*<sup>+/-</sup>;*Pak1*<sup>-/-</sup> hematopoietic system would alter the development or progression of plexiform neurofibromas. Briefly, 5x10<sup>6</sup> whole bone marrow cells from either *Nf1*<sup>+/-</sup> or *Nf1*<sup>+/-</sup>;*Pak1*<sup>-/-</sup> mice were transplanted via tail vein injection into 6-8 week old *Krox20Cre;Nf1flox/flox* and *Krox20Cre;Nf1flox/-* mice after the recipients had been treated with a split dose of 1100 rads of ionizing radiation (700 rads followed by 400 additional rads 5 hours later). These animals were followed for over one year to assess the development of plexiform neurofibromas in the spinal nerve roots.

#### GENERATION OF *Krox20Cre;Nf1flox/-;Pak1*<sup>-/-</sup> ANIMALS

*Krox20Cre;Nf1flox/-* mice on a C57BL/6J strain were intercrossed with *Pak1*<sup>-/-</sup> mice also on a C57BL/6J strain. These animals were followed for over a year to assess to assess the development of plexiform neurofibromas in the spinal nerve roots. These studies were conducted with a protocol approved by the Indiana University Laboratory Animal Research Center.

## DORSAL ROOT GANGLION DISSECTION AND MEASUREMENT

Immediately following sacrifice induced by CO inhalation, whole mice were perfused and fixed in 4% paraformaldehyde. The dorsal root ganglia and peripheral nerves were then dissected out under a dissection microscope. To evaluate the size of the dorsal root ganglion, an anatomic measurement of the dorsal root ganglia from the sciatic nerve was performed using calipers to measure the ganglion's widest and longest dimensions. Using a formula which approximates spheroidal volume ( $0.52 \times (\text{width})^2 \times (\text{length})$ ), the volume of the ganglia was determined.

## HISTOLOGIC ANALYSIS OF DORSAL ROOT GANGLIA

To make detailed observations about the cellular composition and morphology of the dorsal root ganglia, paraffin sections were stained with hematoxylin and eosin (H&E). Given collagen accounts for approximately 60% of the dry weight of human plexiform neurofibromas, the tissue sections were also stained with Masson trichrome to identify collagen deposition. Additionally, to identify the presence of mast cells in the tissue, Alcian blue staining was performed.

## GENERATION AND CULTURE OF PRIMARY FIBROBLASTS

Using an established method<sup>75</sup>, fibroblasts were derived from 13.5 days post coitus embryos of WT and *Pak1*<sup>-/-</sup> mice. Cells were maintained in culture using high glucose DMEM (Gibco BRL) supplemented with 10% fetal calf serum (HiClone), 1% glutamine (BioWhittaker), 1.5% HEPES (BioWhittaker), and 2% penicillin/streptomycin (BioWhittaker). Cells were cultured in a 37°C, 5% CO<sub>2</sub>, humidified incubator. All

assays utilized fibroblasts were from passage two to four. For all cellular and biochemical assays, fibroblasts were stimulated with human recombinant PDGF-BB (PeproTech) or human recombinant TGF- $\beta$  (PeproTech). All experiments were conducted using at least three independent lines from each genotype.

#### FIBROBLAST PROLIFERATION ASSAY

<sup>[3H]</sup>Thymidine incorporation assays were used to examine fibroblast proliferation, in a manner described previously <sup>71</sup>. Briefly, fibroblasts were plated at a concentration of  $2 \times 10^4$  cells in 200 $\mu$ L of media containing 10% fetal calf serum per well in 96 well tissue culture treated plates. After 24 hours, the cells were washed and media was replaced with DMEM without serum containing PBS as a vehicle controls, 50ng/mL PDGF-BB, or 2ng/mL TGF- $\beta$  and incubated at 37°C in a 5% CO<sub>2</sub>, humidified incubator. After 36 hours tritiated thymidine (PerkinElmer Life and Analytical Sciences) was added to each well 6 hours prior to harvest on glass filter fibers (Packard Instrument) and  $\beta$ -emission was measured.

#### FIBROBLAST WOUND HEALING ASSAY

To assess the migration of fibroblasts, we used an established wound healing assay protocol <sup>71</sup>.  $1 \times 10^5$  cells in 1mL of media containing 10% fetal calf serum were plated in a 12 well plate. After 24 hours, the cells were washed and media was replaced with DMEM without serum before incubation at 37°C in a 5% CO<sub>2</sub>, humidified incubator. After 16 hours, the cells were washed and treated with 10 $\mu$ g/mL of Mitomycin C (Sigma-Aldrich) for 1 hour. The cells were then washed, and media was

replaced with DMEM without serum containing PBS as a vehicle control, 50ng/mL PDGF-BB, or 2ng/mL TGF- $\beta$ . A wound was created using a plastic pipette tip across the diameter of the well, and the cells were incubated for 12 hours at 37°C and followed by time-lapse microscopic photography. After incubation, cells were stained with crystal violet solution, and the number of cells that invaded the wound was determined by using ImageJ (NIH) software.

#### FIBROBLAST COLLAGEN PRODUCTION ASSAY

To examine collagen production by fibroblasts after stimulation by PDGF-BB or TGF- $\beta$ , the Sircol<sup>TM</sup> soluble collagen assay was used. Confluent fibroblast cultures on 10cm tissue culture dishes were stimulated for 48 hrs with PBS as a vehicle control, 50ng/mL PDGF-BB, or 2ng/mL TGF- $\beta$ . After stimulation, 200 $\mu$ L of the media were incubated with the Sircol<sup>TM</sup> dye reagent. Dye collagen complexes were resolubilized by addition of alkali reagent and OD readings were made on a microplate reader at a wavelength of 540nm.

#### FIBROBLAST APOPTOSIS ASSAY

To determine the effects of PDGF-BB and TGF- $\beta$  on fibroblast survival, TUNEL staining with the APO-DIRECT<sup>TM</sup> kit (BD Pharmingen) was used.  $1 \times 10^5$  cells in 2mL of media containing 10% fetal calf serum were plated on a 6 well plate. After 24 hours, the cells were washed and media without serum containing PBS as a vehicle control, 50ng/mL PDGF-BB, or 2ng/mL TGF- $\beta$  was added. After 72 hours, the cells were removed from the wells by treatment with 0.1% Trypsin-EDTA (Gibco BRL) and fixed

in a 1% w/v paraformaldehyde in PBS. After fixation, the cells were stained with the APO-DIRECT™ kit components and analyzed by flow cytometry.

#### CONFOCAL ANALYSIS OF FIBROBLAST ACTIN CYTOSKELETON

To evaluate the F-actin cytoskeleton in fibroblasts, cells were prepared and stimulated as described above for wound healing assays, with the fibroblasts on coverslips rather than tissue culture plates. After 4 hours of incubation at 37°C in 5% CO<sub>2</sub>, the fibroblast covered coverslips were placed into 3.7% formaldehyde solution for fixation. Fixed cells were treated with 0.01% Triton X-100 (Sigma-Aldrich in PBS for 5 minutes at 25°C, washed, and then incubated with 160nM Alexa Fluor® 488 Phalloidin (Invitrogen) for 20 minutes at 25°C prior to mounting with DAPI. Cells were then analyzed via confocal microscope with the Zeiss UV LSM-510 system.

#### FIBROBLAST IMMUNOBLOTTING

Whole cell protein extracts were obtained from fibroblasts stimulated with 50ng/mL PDGF-BB, or 2ng/mL TGF-β in lysis buffer (50mM Tris pH 7.4, 150mM NaCl, 2mM EDTA pH 8.0, 1% Triton X-100, 1mM PMSF, 1mM NaF, 1mM Na<sub>3</sub>VO<sub>4</sub>, 10% glycerol and Complete protease inhibitor), and equivalent amounts of protein were electrophoresed on 10% SDS-PAGE gels, transferred to nitrocellulose membranes (Amersham Biosciences), and detected by Western blotting using the ECL Plus system (Amersham Biosciences). Antibodies used were Phospho-p44/42 MAPK (Thr202/Tyr204) (197G2) Rabbit mAb (Cell Signaling Technology), p44/42 MAP Kinase Antibody (Cell Signaling Technology), Phospho-Cofilin (Ser3) polyclonal

antibody (Cell Signaling Technology), Cofilin polyclonal antibody (Cell Signaling Technology), Phospho-Filamin A (Ser2152) polyclonal antibody (Cell Signaling Technology), Filamin A polyclonal antibody (Cell Signaling) Monoclonal  $\beta$ -actin antibody (clone AC-15) (Sigma-Aldrich).

#### *IN VIVO* FIBROBLAST INVASION ASSAYS

Adapting a method described previously<sup>71,171</sup>, we used a Cultrex<sup>TM</sup> plug assay to evaluate the invasion of fibroblasts *in vivo* in response to PDGF-BB or TGF- $\beta$ . The Cultrex<sup>TM</sup> media (R&D Systems) was thawed at 4° for 24h and mixed with PBS as a vehicle control, 200ng/mL PDGF-BB, or 10ng/mL TGF- $\beta$ . 300 $\mu$ L of vehicle containing Cultrex<sup>TM</sup> or 300 $\mu$ L of growth factor containing Cultrex<sup>TM</sup> were injected subcutaneously into the left or right groin of WT or *Pak1*<sup>-/-</sup> mice, respectively. The plug was removed on day 7 and was frozen immediately on dry ice. Tissues were sectioned and stained with H&E to assess histology. The number of invaded cells per high power field was quantitated by using ImageJ software. At least 3 mice per genotype were examined.

#### BLEOMYCIN INDUCED PULMONARY FIBROSIS MODEL

Harrison<sup>172</sup> described a model system where continuous release of bleomycin sulfate would induce a fibrotic reaction in mice that mimicked human pulmonary disease. We implanted microosmotic pumps (Alzet) containing PBS or 125mg/kg/day bleomycin subcutaneously in the dorsum of lightly anesthetized WT and *Pak1*<sup>-/-</sup> mice. 28 days after surgery, mice were sacrificed, bronchoalveolar lavage was performed and the lungs removed. The right lung was minced and used to assess total collagen content using the



Sircol™ collagen assay described above. The left lung was fixed in 1% formalin and sectioned for histological analysis. Both H&E to assess structure and Masson's Trichrome to assess collagen deposition were performed.

## RESULTS

### ROLE OF *Pak1* IN REGULATING STEM CELL FACTOR DEPENDENT FUNCTIONS IN *Nf1* HAPLOINSUFFICIENT MAST CELLS

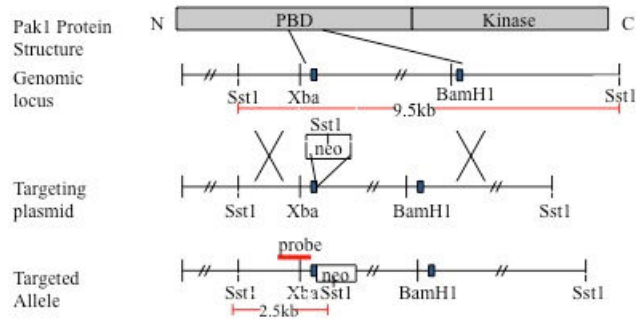
#### Generation of a *Pak1* knockout mouse

In order to study the effects of Pak1 loss in primary cells, a *Pak1*<sup>-/-</sup> mouse was generated by targeted disruption of the *Pak1* allele in embryonic stem (ES) cells (J.D. Allen and D.W. Clapp, submitted for publication). The resultant allele contains a neomycin cassette and is lacking 2 kb of genomic DNA encoding the p21-binding domain (Figure 3a). *Pak1*<sup>-/-</sup> mice are observed at the predicted Mendelian frequency and are viable and fertile. *Pak1*<sup>-/-</sup> mice have a normal lifespan and no noted hematopoietic defects. To verify that *Pak1*<sup>-/-</sup> mice produce no Pak1 protein, cell lysates isolated from WT and *Pak1*<sup>-/-</sup> BMMCs were subjected to Western blot using a Pak1 specific antibody (Figure 3b). To further document the absence of Pak1 protein being expressed at levels below detection of Western blot, RT-PCR was conducted to look for expression of the Pak1 mRNA transcript. As expected, Pak1 mRNA was detected in WT BMMCs, but no Pak1 mRNA was detected in *Pak1*<sup>-/-</sup> BMMCs (Figure 3c).

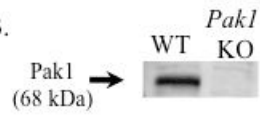
**Figure 3**

A.

Disruption of the *Pak1* gene



B.



C.

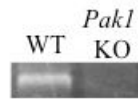


**Figure 3- Targeted disruption of the *Pak1* allele.** **A)** Partial restriction map of the native *Pak1* gene (genomic locus), the targeting vector replacing the coding sequence of a portion of the N-terminus, including the p21-binding domain (PBD) and the inhibitory domain (ID) with the *Neo-resistance* gene in the anti-sense orientation (targeting vector), and the organization of the targeted *Pak1* allele (targeted allele). The 1 kb genomic probe used for screening is indicated along with the expected sizes of the wild type (WT) and targeted *HindIII* fragments. **B)** Western blot analysis. WT and *Pak1*<sup>-/-</sup> bone marrow-derived mast cell (BMMC) lysates were subjected to immunoblotting with anti-Pak1. The 68 kDa Pak1 protein is present in WT BMMCs and absent in the *Pak1*<sup>-/-</sup> cells. **C)** RT-PCR analysis. After reverse transcription of isolated mast cell RNA, *Pak1* cDNA was amplified by PCR from BMMCs to generate a 352 base pair fragment (corresponding to base pairs 306-658) in the WT cells, which is absent in the *Pak1*<sup>-/-</sup> cells. GAPDH mRNA in WT and *Pak1*<sup>-/-</sup> BMMCs is also shown.

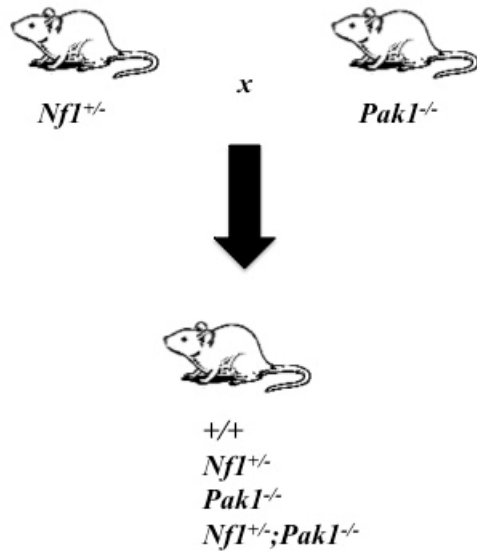
### Intercross of *Nfl*<sup>+/-</sup> and *Pak1*<sup>-/-</sup> mice

To test our hypothesis that Pak1 is an important mediator of hyperactive Ras signaling, we designed a breeding strategy to intercross *Nfl*<sup>+/-</sup> mice with *Pak1*<sup>-/-</sup> mice to generate *Nfl*<sup>+/-</sup>;*Pak1*<sup>-/-</sup> double mutant mice (Figure 4). Initial breedings of multiple C57BL/6 *Nfl*<sup>+/-</sup> and *Pak1*<sup>-/-</sup> founders generated *Nfl*<sup>+/-</sup>;*Pak1*<sup>+/-</sup> and *Pak1*<sup>+/-</sup> progeny. Intercrossing of the *Nfl*<sup>+/-</sup>;*Pak1*<sup>+/-</sup> mice from the F1 generation yielded four F2 genotypes that were used to generate mast cells for cellular and biochemical assays: *Nfl*<sup>+/+</sup>;*Pak1*<sup>+/+</sup> (wild type or +/+), *Nfl*<sup>+/-</sup>, *Pak1*<sup>-/-</sup>, and *Nfl*<sup>+/-</sup>;*Pak1*<sup>-/-</sup>.

### Loss of *Pak1* reduces numbers of mast cell colonies

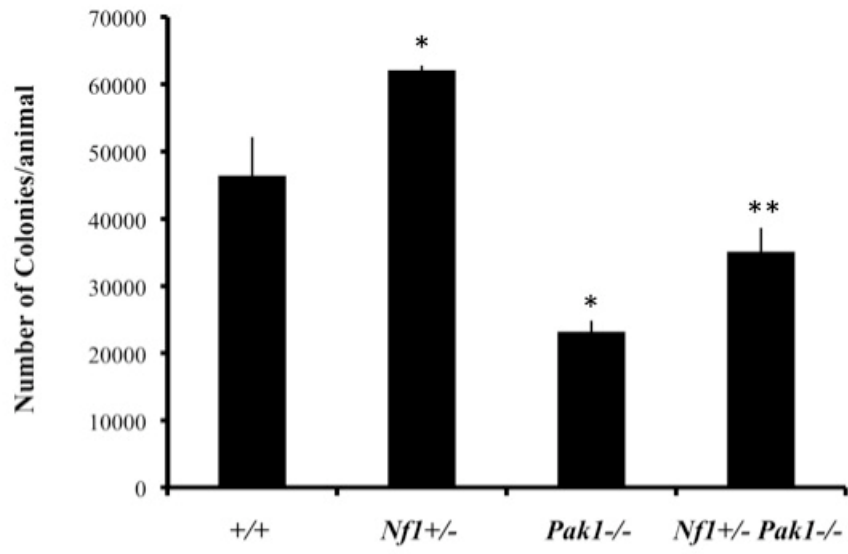
*Nfl* haploinsufficient mice have a characteristic increase in mast cell progenitors compared to wild type controls<sup>59</sup>. While genetic disruption of *Pak1* does not cause any frank disruption of hematopoiesis, we were interested to see if *Pak1* loss would affect the colony forming ability of mast cell progenitors. 2x10<sup>4</sup> low-density mononuclear cells (LDMNC) from bone marrow were cultured in methylcellulose with growth factors for 21 days to generate mast cell colonies and then scored. As expected, more mast cell colonies were found in *Nfl*<sup>+/-</sup> cultures than wild type cultures (Figure 5). Loss of *Pak1* caused a significant decrease in the number of mast cell forming units compared to wild type controls. Additionally, *Nfl*<sup>+/-</sup>;*Pak1*<sup>-/-</sup> LDMNC generated significantly fewer mast cell colonies compared to *Nfl*<sup>+/-</sup> cultures, close to a level seen in wild type controls.

Figure 4



**Figure 4- Genetic intercross of *Nf1*<sup>+/-</sup> and *Pak1*<sup>-/-</sup> mice.** The four F2 genotypes generated (+/+; *Nf1*<sup>+/-</sup>; *Pak1*<sup>-/-</sup>; and *Nf1*<sup>+/-</sup>;*Pak1*<sup>-/-</sup>) were used to generate BMMCs for use in *in vitro* biochemical and cellular assays as well as *in vivo* whole animal studies to investigate the role of *Pak1* in mediating *Nf1* haploinsufficient phenotypes.

**Figure 5**





**Figure 5- Loss of *Pak1* reduces mast cell colony forming unit ability.** Low-density mononuclear cells ( $2 \times 10^4$ ) were plated for the growth of CFU-Mast cell in methylcellulose supplemented with 20% FCS, 2.5ng/mL IL-3, and 10ng/mL of SCF. After 21 days of incubation, CFU-Mast were enumerated using indirect microscopy and normalized to the cellularity of both femurs, tibias, and iliac crests. This total is expressed above as colony number/animal. Each value represents the mean and the error bars represent the standard error of the mean of 3 independent experiments. \* indicates  $p < 0.05$  compared to WT control and \*\* indicates  $p < 0.05$  compared to *Nfl*<sup>+/-</sup> control using Student's unpaired T test.

### Loss of *Pak1* does not affect expression of mast cell maturation markers

To investigate whether genetic disruption of *Pak1* does not influence mast cell development in intercrossed mast cells, low-density mononuclear bone marrow cells in the presence of serum and IL-3 were cultured for 4-5 weeks and expression of the c-kit receptor and FcεRI receptor was examined. Fluorescence cytometry analysis of the F2 progeny demonstrated equivalent expression of both c-kit and FcεRI receptors in all genotypes (Figure 6). Further, the cells had typical cellular morphology and staining of cytoplasmic granules upon Alcian Blue/Saffranin-O staining (data not shown). Collectively, the fluorescence cytometry and histological data indicate that alterations in *Pak1* expression do not influence c-kit expression or mast cell development in cells that are WT or haploinsufficient at the *Nfl* locus.

### Hyperproliferation of *Nfl*<sup>+/-</sup> bone marrow derived mast cells is dependent on a *Pak1*/MAPK pathway

Given previous work demonstrating elevated Pak kinase activity in *Nfl*<sup>+/-</sup> mast cells, as well as a pathological increase in *Nfl*<sup>+/-</sup> mast cell proliferation through Ras-MAPK signals<sup>60</sup>, a combination of genetic and pharmacologic experiments were conducted to test the functional consequences of *Pak1* loss on BMMCs. Proliferation was assessed by Trypan blue exclusion at the time SCF was added (day 0) and after 72 h in culture. As anticipated, *Nfl*<sup>+/-</sup> BMMCs showed greater proliferation in response to SCF compared with wild-type cells (Figure 7, black bars). Genetic disruption of *Pak1*

Figure 6

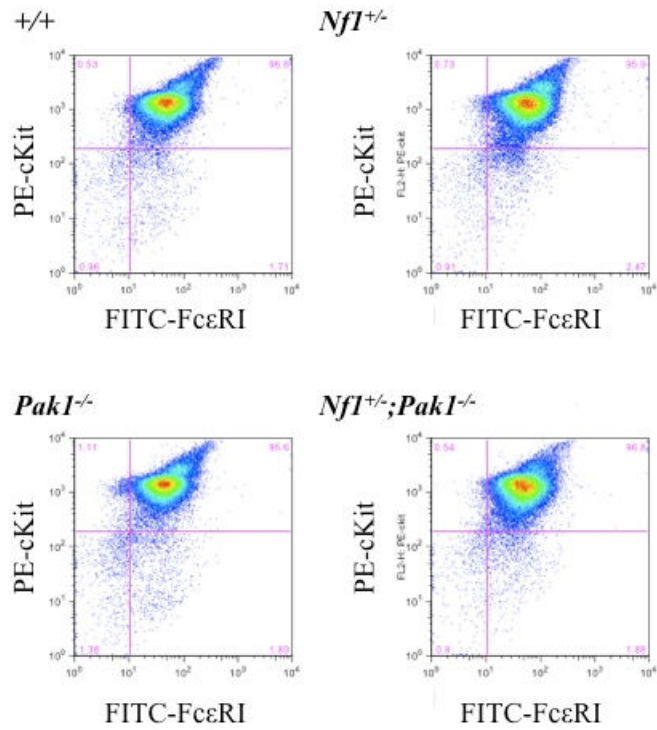


**Figure 6- Loss of *Pak1* does not affect expression of important mast cell maturation markers.** Mast cells were cultured for 4 weeks, and expression of c-kit and FcεRI were measured by incubation with anti-IgE followed by FITC-conjugated anti-mouse IgG, as well as PE-conjugated anti-c-kit antibodies. Double positive cells (upper right quadrant) are mature mast cells, expressing both c-kit and FcεRI. Data shown are representative of 6 independent lines from each genotype.

resulted in a significant decrease in proliferation at 72 hours in *Nf1*<sup>+/-</sup> cells (p<0.005), implicating Pak1 as a critical mediator of *Nf1* haploinsufficient BMMC hyperproliferation. Further, *Pak1*<sup>-/-</sup> BMMCs had reduced proliferation (~60%) at 72 hours compared to wild-type cells (p<0.05), suggesting that Pak1 is important for regulating proliferation in the setting of normal Ras activity as well.

To link this phenotype to a particular MAPK pathway, concomitant proliferation experiments of cultured mast cells were performed in the presence or absence of 10μM PD98059, a selective inhibitor of Mek1 activity (Figure 7, white bars) or 10μM SB203580, a selective inhibitor of p38 MAPK (Figure 7, striped bars). Addition of p38 inhibitor SB203580 did not affect the proliferation of BMMCs of any genotype, indicating that p38 has little control over BMMC growth. Conversely, inhibition of Mek by PD98059 caused significant decreases in mast cell proliferation in the context of normal *Pak1* (~100% and 150% decreases for WT and *Nf1*<sup>+/-</sup> BMMCs, respectively). Importantly, Mek inhibition did not significantly affect proliferation of *Pak1* null cells, regardless of *Nf1* genotype. Collectively, these data imply that Pak1 interacts with the Mek/Erk MAPK pathway in *Nf1*<sup>+/-</sup> mast cells to selectively regulate proliferation.

#### Loss of *Pak1* corrects MAPK hyperactivation in *Nf1* haploinsufficient BMMCs

To establish the role of Pak1 signaling in the activation of the Ras-Raf-Mek-Erk signaling pathway and to identify the specific MAPK residues that are phosphorylated, BMMCs were stimulated with SCF and assayed for activated MAPK pathway members by using phospho-specific antibodies after Western blotting. First, Erk1/2

**Figure 7**

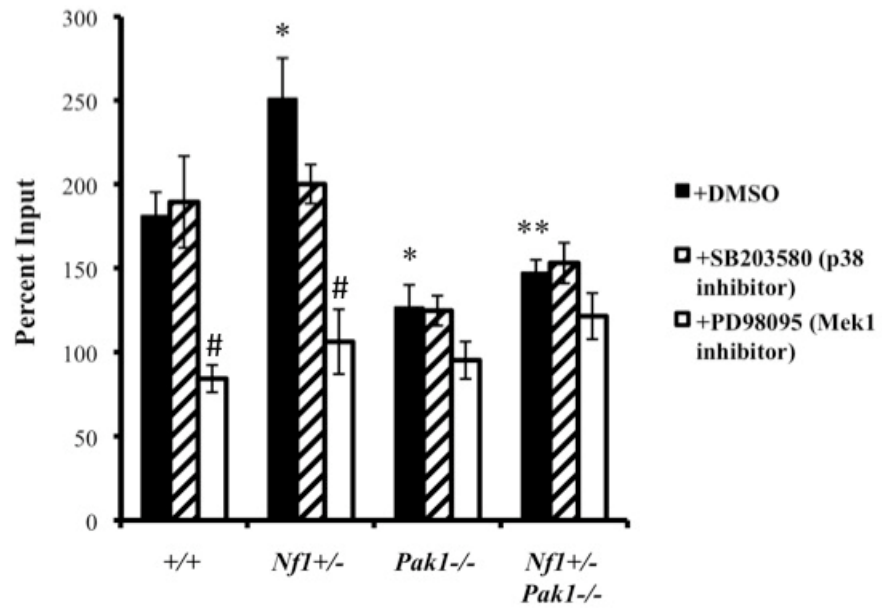


**Figure 7- Pak1 regulates the increased proliferation of *Nf1*<sup>+/-</sup> mast cells in cooperation with Mek/Erk.** Mast cells were starved overnight in RPMI and plated in a 24-well plate at  $3 \times 10^5$  per well in triplicate samples after treatment with DMSO (control; black bars), 10 $\mu$ M of selective p38 inhibitor SB203580 (striped bars), or 10 $\mu$ M of selective Mek1 inhibitor PD98059 (white bars). Cells were then stimulated with 25ng of SCF for 72 hours, and viable cells were measured by trypan blue exclusion. Results are expressed as percent of input number of cells at 72 hours post stimulation. Each value represents the mean and the error bars represent the standard error of the mean of 6 independent experiments. \* indicates  $p < 0.05$  compared to WT control, \*\* indicates  $p < 0.05$  compared to *Nf1*<sup>+/-</sup> control, and # indicates  $p < 0.05$  compared to DMSO treated cells within a genotype using Student's unpaired T test.

phosphorylation was measured. Consistent with previous studies<sup>60</sup>, *Nf1*<sup>+/-</sup> BMMCs have a 2.5-fold increase in phosphorylated (activated) Erk1/2 (Figure 8). *Pak1*<sup>-/-</sup> mast cells had decreased Erk activation, and importantly genetic disruption of *Pak1* fully corrects the hyperphosphorylation of Erk1/2 in *Nf1*<sup>+/-</sup> mast cells to that of wild-type controls, which correlates with the correction in proliferation (Figure 7).

Frost et al. previously established that Pak1 directly activates Mek at serine residue 298 in NIH3T3 cells<sup>131</sup>. Immunoblotting of lysates from SCF stimulated *Nf1*<sup>+/-</sup> BMMCs revealed increased phosphorylation of Mek1 at this established target residue of direct Pak1 kinase activity compared to wild type controls (Figure 9). *Nf1*<sup>+/-</sup>;*Pak1*<sup>-/-</sup> mast cells showed greatly diminished phospho-Ser 298 Mek1 levels compared to *Nf1*<sup>+/-</sup> cells (Figure 9). In a similar manner, in *Nf1*<sup>+/-</sup> BMMCs Mek phosphorylation at Ser 217/222, the site of Raf-1 dependent activation, is increased compared to wild type (Figure 10). In *Nf1*<sup>+/-</sup>;*Pak1*<sup>-/-</sup> mast cells stimulated with SCF, Mek Ser 217/222 activation is reduced compared to *Nf1*<sup>+/-</sup> cells, close to wild type control levels (Figure 10). Raf-1 has been described in multiple systems as a direct substrate of Pak at serine residue 338<sup>129,133,173</sup>. These studies establish that Pak1, a downstream mediator of PI-3 K/Rac signaling, is biochemically linked to the classical Ras/Raf/Mek/Erk pathway in primary cells. Together with the proliferation data displayed in Figure 7, we establish a crucial role for *Pak1* kinase activity in regulating the increased proliferation of *Nf1*<sup>+/-</sup> BMMCs by relaying signals to the Mek/Erk pathway.



**Figure 8**

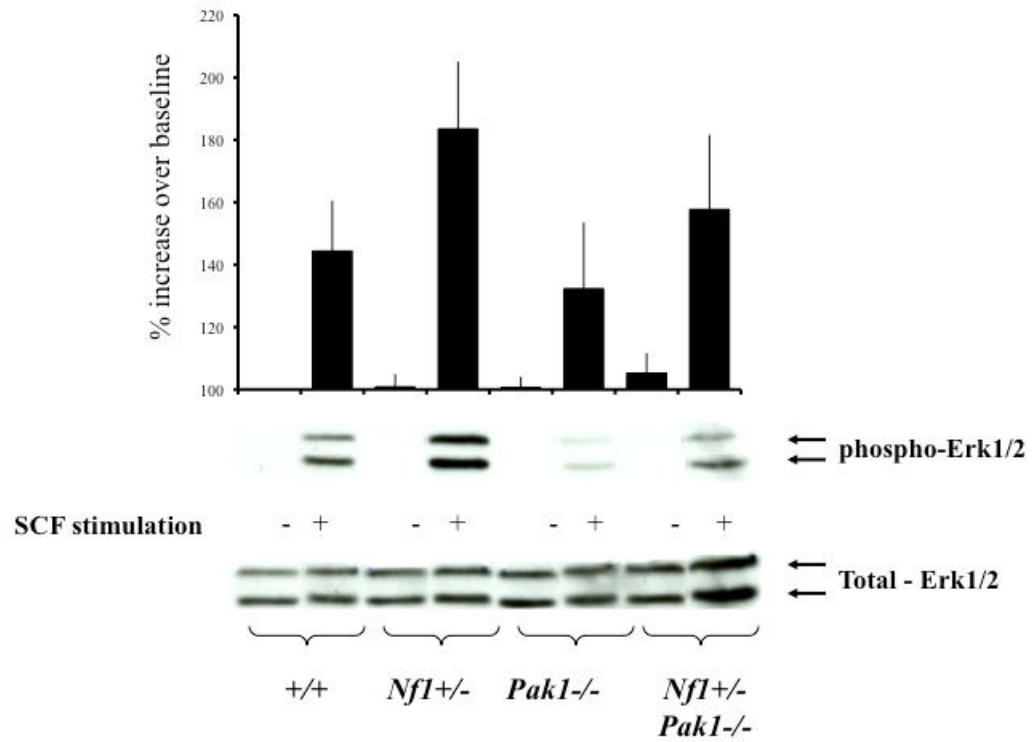


**Figure 8- Erk activation is reduced in cells that lack *Pak1*.** Mast cells were serum starved overnight, stimulated with SCF, and cell lysates isolated at 0 and 2 minutes following stimulation. 100µg of protein were used for each time point. Levels of active Erk1/2 were determined by immunoblotting using phospho-specific antibodies. Levels of total Erk1/2 are shown as loading controls. Western blot of the results is shown and is a representative of three independent experiments. Each value represents the mean and the error bars represent the standard error of the mean of three independent experiments

**Figure 9**

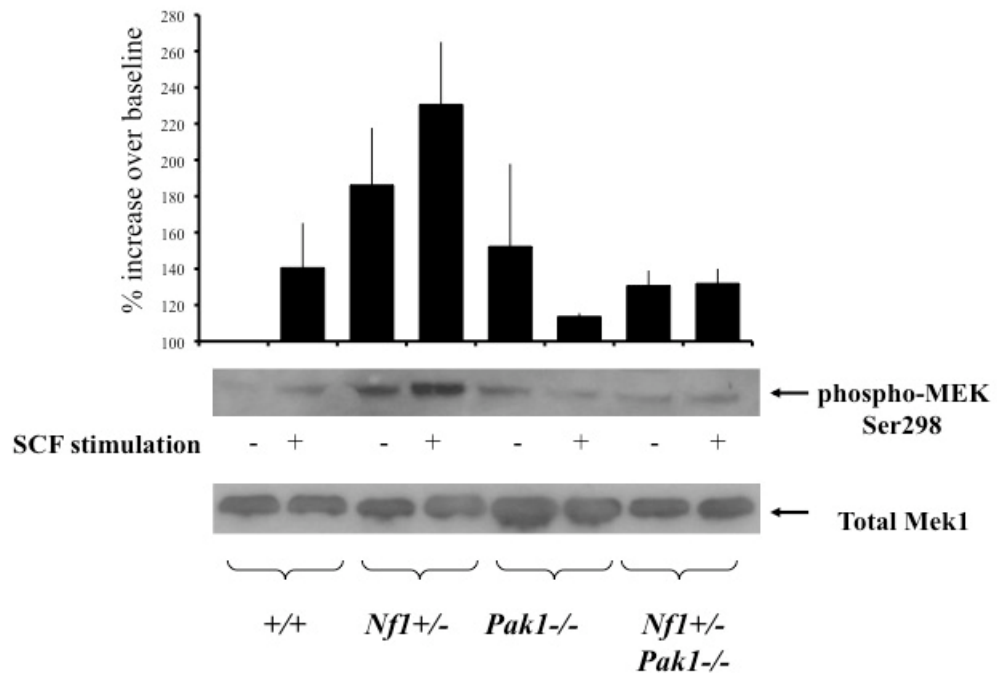


**Figure 9- Phosphorylation of Mek1 at Ser 298 is reduced in *Pak1*<sup>-/-</sup> cells.** Mast cells were serum starved overnight, stimulated with SCF, and cell lysates isolated at 0 and 2 minutes following stimulation. 100µg of protein were used for each time point. Levels of active Mek1 were determined by immunoblotting using phospho-specific antibodies. Levels of total Mek1 are shown as loading controls. Western blot of the results is shown and is a representative of three independent experiments. Each value represents the mean and the error bars represent the standard error of the mean of 3 independent experiments.

**Figure 10**

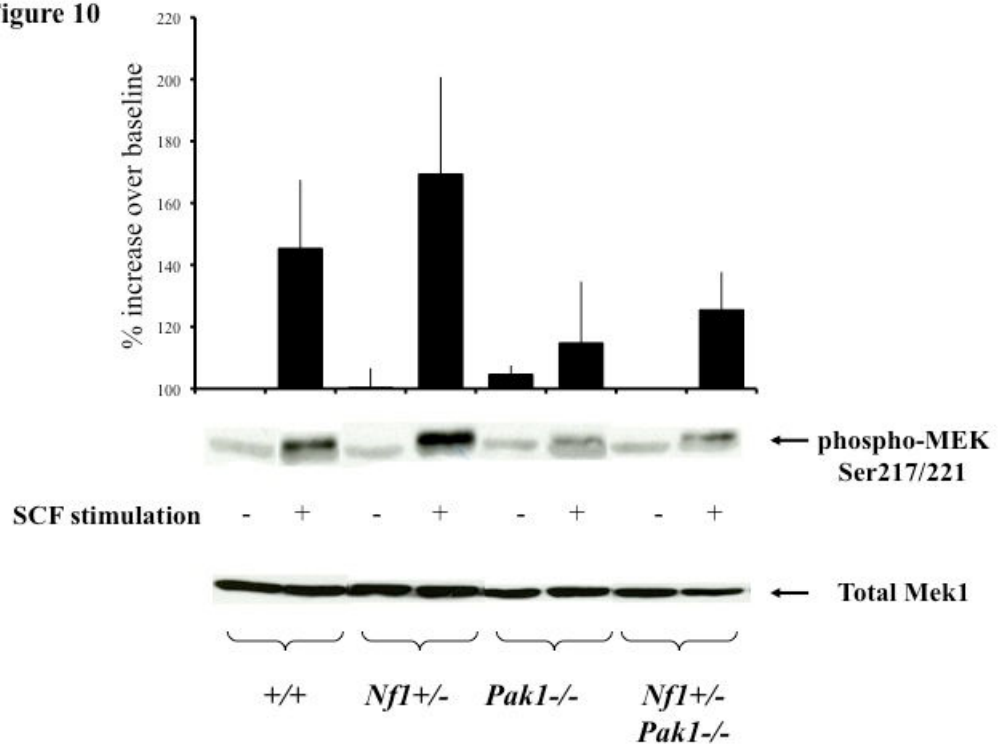


**Figure 10- *Pak1* loss reduces phosphorylation of Ser217/221 on Mek1.** Mast cells were serum starved overnight, stimulated with SCF, and cell lysates isolated at 0 and 2 minutes following stimulation. 100µg of protein were used for each time point. Levels of active Mek1 were determined by immunoblotting using phospho-specific antibodies. Levels of total Mek1 are shown as loading controls. Western blot of the results is shown and is a representative of three independent experiments. Each value represents the mean and the error bars represent the standard error of the mean of three independent experiments.

## A Pak1/p38 pathway regulates increased migration of *Nf1*<sup>+/-</sup> mast cells

The recruitment of mast cells from the peripheral blood to sites of developing tumors is believed to be an early and required process in the formation of plexiform neurofibromas<sup>30,62,174</sup>. *Nf1*<sup>+/-</sup> BMMCs have a PI3K- Rac-dependent gain-in-function in SCF mediated haptotaxis compared to wild type BMMCs<sup>62</sup>. Therefore, we questioned whether loss of *Pak1* would be sufficient to correct the pathological increase in migration of *Nf1*<sup>+/-</sup> BMMCs toward SCF. To explore these questions transwells were coated with recombinant fibronectin fragment CH296 (Takara Biosystems) and migration assays were performed in response to 25ng/mL of SCF. Following 4 hours of incubation in the transwells, the number of mast cells that had migrated to the bottom surface of the fibronectin-coated membrane was counted after staining the cells with crystal violet. BMMCs that were stimulated with media alone showed fewer than 5 cells per high power field had migrated to the lower side of the membrane (data not shown). As expected, increased numbers of *Nf1*<sup>+/-</sup> mast cells migrate toward SCF compared to wild type mast cells (Figure 11, black bars). Also, loss of *Pak1* causes a decrease in migration compared to wild type BMMCs (p<0.05). Notably, *Nf1*<sup>+/-</sup>;*Pak1*<sup>-/-</sup> BMMCs have decreases in the number of migrated mast cells compared to BMMCs haploinsufficient at the *Nf1* locus, indicating that the increased migration in *Nf1*<sup>+/-</sup> mast cells is *Pak1* dependent.

Previous studies have established that mast cells migrate in response to SCF in a p38-dependent manner<sup>175-177</sup>. To test if the gain-in-function phenotype for *Nf1*<sup>+/-</sup> mast cell migration was the result of communication from Pak1 to p38, BMMCs were treated with 10μM of the selective inhibitor of p38 SB203580 (Figure 11, striped bars), 10μM of

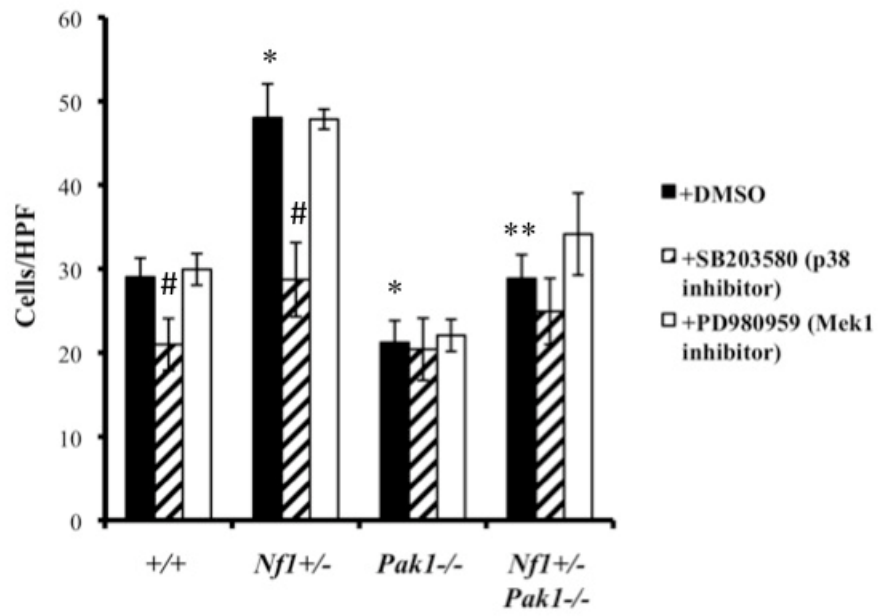
the selective inhibitor of Mek1 PD98059 (Figure 11, white bars), or the vehicle only and stimulated as described above. Interestingly, treatment of BMMCs with p38 inhibitor results in a significant decrease in migration of wild type and *Nfl*<sup>+/-</sup> mast cells (by 28% and 41%, respectively), but does not further reduce migration of *Pak1*<sup>-/-</sup> or *Nfl*<sup>+/-</sup>;*Pak1*<sup>-/-</sup> mast cells, implying that SCF stimulates *Nfl*<sup>+/-</sup> BMMC hyperactive migration through a Pak1/p38 pathway. Treatment with the Mek1 inhibitor PD98059 did not affect the migration of BMMCs to SCF, as reported previously<sup>175</sup>.

*Pak1* is required for the increase in p38 phosphorylation seen in *Nfl* haploinsufficient mast cells

To establish a biochemical correlate to the functional results shown in Figure 9, which implicate a Pak1/p38 axis in mediating the increased migration of *Nfl*<sup>+/-</sup> mast cells, BMMCs were stimulated with SCF and examined for levels of activated phospho-p38 (R180/Y182). Figure 12 shows that *Nfl*<sup>+/-</sup> BMMCs have increased activated p38, consistent with the results of Figure 9. Additionally, loss of *Pak1* greatly diminishes phospho-p38 levels after SCF stimulation, providing biochemical evidence that SCF activates a Pak1/p38 pathway in mast cells. This pathway is hyperactivated in *Nfl*<sup>+/-</sup> mast cells and leads to increased migration. Therefore, molecular targeting of this pathway could potentially inhibit the recruitment of *Nfl*<sup>+/-</sup> mast cells to sites of growing neurofibromas and delay or prevent tumor development.

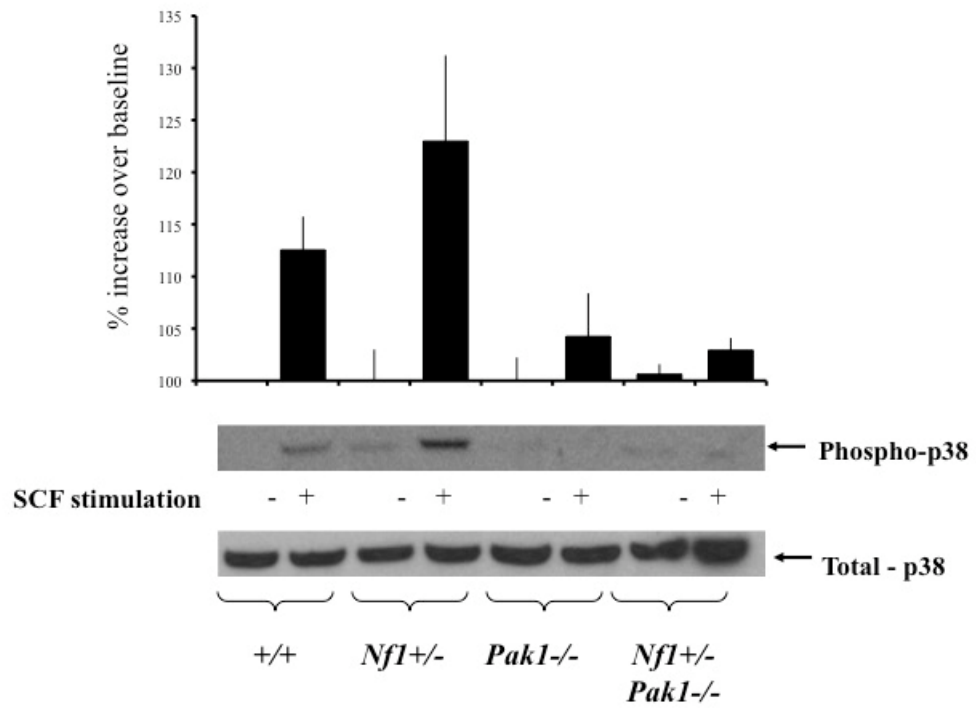


Figure 11



**Figure 11- Increased migration of *Nf1*<sup>+/-</sup> mast cells is mediated through a Pak/p38 pathway.** Mast cells were starved overnight in RPMI without serum and plated in the upper well of a transwell chamber at  $1 \times 10^5$  per well in triplicate samples after treatment with DMSO (control; black bars), 10 $\mu$ M of selective p38 inhibitor SB203580 (striped bars), or 10 $\mu$ M of selective Mek1 inhibitor PD98059 (white bars). Cells were then stimulated with 25ng of SCF in the lower chamber for 4 hours, and mast cells that had migrated to the bottom surface of the CH296-coated membrane in response to SCF were counted after staining the cells with crystal violet. Results are expressed as cells per 20x high power field. Each value represents the mean and the error bars represent the standard error of the mean of 6 independent experiments. \* indicates  $p < 0.05$  compared to WT control, \*\* indicates  $p < 0.05$  compared to *Nf1*<sup>+/-</sup> control, and # indicates  $p < 0.05$  compared to DMSO treated cells within a genotype using Student's unpaired T test.

**Figure 12**



**Figure 12- *Pak1*<sup>-/-</sup> Mast cells have diminished p38 activation.** Mast cells were serum starved overnight, stimulated with SCF, and cell lysates isolated at 0 and 5 minutes following stimulation. 100µg of protein were used for each time point. Levels of active p38 were determined by Western blotting using phospho-specific antibodies. Level of total p38 is shown as a loading control. Western blot of the results is shown and is a representative of three independent experiments. Each value represents the mean and the error bars represent the standard error of the mean of three independent experiments.

*Pak1* regulates F-actin content and organization in a p38-dependent manner

Actin polymerization at the cell front leads to the early extension of plasma membrane, which is necessary for cell migration<sup>178</sup>. c-Kit-mediated mast cell migration is highly dependent on alterations and activation of the actin cytoskeleton by Ras and PI-3K<sup>164,179,180</sup>. Additionally, other groups have used overexpression systems to describe a role for *Pak1* in the regulation of actin dynamics and migration in murine embryonic fibroblasts<sup>181</sup>, murine bone marrow derived macrophages<sup>138</sup>, and others. Mast cells deficient in *Rac2* (a direct activator of Pak1) have diminished actin cytoskeleton dependent functions<sup>164</sup>. Based on the established association of increases in F-actin content with the increases in migration seen in *Nf1*<sup>+/-</sup> BMBCs<sup>62</sup>, we hypothesized that the Pak1-dependent decrease in *Nf1*<sup>+/-</sup> BMBC migration (Figure 11) stemmed from a disruption of the F-actin content and/or organization in these cells.

To determine if *Pak1* loss affects BMBC F-actin content, SCF-stimulated BMBCs were stained with phalloidin and analyzed using fluorescence cytometry and confocal microscopy. Figure 13a-l shows representative confocal images of phalloidin and DAPI co-stained BMBCs. At a single cell level, confocal images reveal that at baseline (Figure 11d) and after SCF stimulation (Figure 13e), *Nf1*<sup>+/-</sup> BMBCs have increased phalloidin staining compared to wild type BMBCs (Figure 13a and 13b), while *Pak1*<sup>-/-</sup> cells (Figure 13h) have decreased F-actin compared to wild type cells (Figure 13b) after SCF stimulation. Consistent with the functional migration data (Figure 11), the *Nf1*<sup>+/-</sup>;*Pak1*<sup>-/-</sup> BMBCs (Figure 13k) have a reduction in F-actin levels compared to *Nf1*<sup>+/-</sup> cells (Figure 13e) after SCF stimulation. Figure 13m details a formal

quantification of the phalloidin intensity from six independent experiments utilizing FACS™ to quantitate F-actin content on SCF stimulated BMMCs.

As shown in Figure 11, inhibition of p38 MAPK leads to decreases in wild type and *Nf1*<sup>+/-</sup> mast cell migration, but does not affect the migration of *Pak1*<sup>-/-</sup> cells. To see if the observed differences in the cytoskeleton after SCF stimulation were linked to p38 activity, we examined the F-actin content and organization of BMMCs that were incubated with 10μM SB203580 for 2h before stimulation. As shown in Figure 13m, the total F-actin content in *Nf1*<sup>+/-</sup> BMMCs was decreased after SB203580 treatment (striped bar). Similar to the migration results in figure 11, inhibition of p38 MAPK did not significantly affect the total F-actin content of *Nf1*<sup>+/-</sup>;*Pak1*<sup>-/-</sup> BMMC after SCF stimulation (Figure 13m); indicating that a hyperactive Pak1/p38 pathway regulates F-actin formation in *Nf1*<sup>+/-</sup> mast cells. Confocal analysis of phalloidin stained BMMCs pretreated with SB203580 shows that the inhibition of p38 in wild type (Figure 13c) and *Nf1*<sup>+/-</sup> mast cells (Figure 13f) disrupts the organization of F-actin to a pattern similar to that seen in BMMCs lacking *Pak1* (Figures 13i and 13l).

#### Disruption of *Pak1* reduces granule release from *Nf1*<sup>+/-</sup> mast cells

The molecular processes that regulate the degranulation of preformed mediators in mast cells have implications in the development of neurofibromas, since *Nf1*<sup>+/-</sup> mast cells have increased release of stored granules *in vitro*<sup>61</sup> as well as in NF1 patient samples<sup>9</sup>.

Figure 13

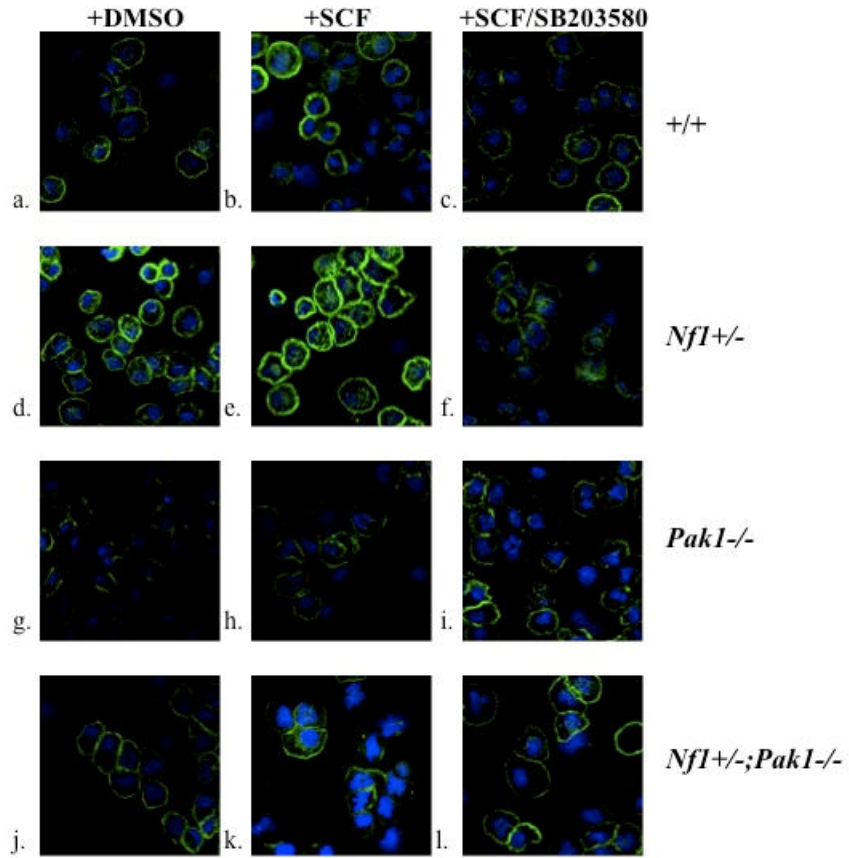
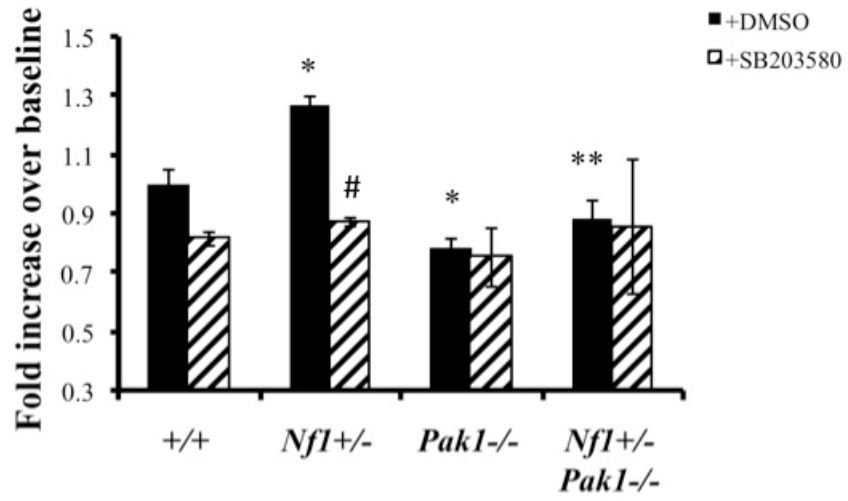


Figure 13m





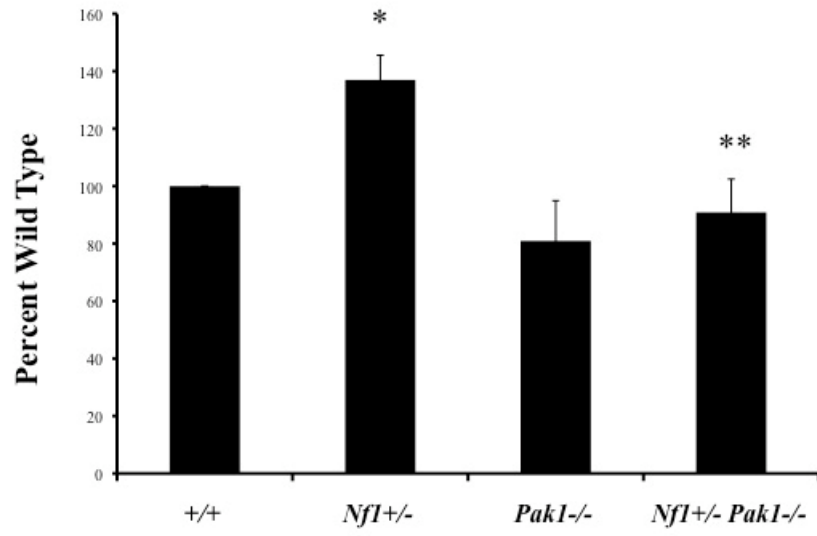
**Figure 13- *Pak1* and *p38* cooperate to regulate activation and organization of the F-actin cytoskeleton.** Mast cells were starved overnight in RPMI and plated in the upper well of a transwell chamber at  $1 \times 10^5$  per well in triplicate samples after treatment with DMSO or 10 $\mu$ M of selective p38 inhibitor SB203580. Cells were then stimulated with 25ng of SCF in the lower chamber for 30 minutes, and mast cells were removed from the upper chamber for phalloidin staining of the F-actin cytoskeleton. **A-L)** Representative micrographs of phalloidin stained mast cells analyzed with the Zeiss UV LSM-510 confocal microscope system. Green=phalloidin stain, blue=DAPI nuclear stain. Original magnification x400. **M)** Fluorescence intensity of phalloidin stained mast cells, determined by fluorescence cytometry. Data are expressed as fold increases over wild type levels, each value represents the mean and the error bars represent the standard error of the mean of 6 independent experiments. \* indicates  $p < 0.05$  compared to WT control, \*\* indicates  $p < 0.05$  compared to *Nf1*<sup>+/-</sup> control, and # indicates  $p < 0.05$  compared to DMSO treated cells within a genotype using Student's unpaired T test.

To establish a role for *Pak1* in regulating the gain-in-function of degranulation in *Nfl*<sup>+/-</sup> mast cells, we evaluated the release of  $\beta$  hexosaminidase in response to SCF and IgE receptor stimulation. Consistent with published reports<sup>61</sup>, *Nfl*<sup>+/-</sup> BMMCs have a significant increase (37%) in  $\beta$  hexosaminidase release over wild type cells (Figure 14). However, *Nfl*<sup>+/-</sup>; *Pak1*<sup>-/-</sup> BMMCs have a reduction in degranulation compared to *Nfl*<sup>+/-</sup> cells, back to the levels of wild type controls. The Mek/Erk MAPK pathway has been implicated in regulating mast cell degranulation<sup>182</sup>; however, treating mast cells with SB203580 to inhibit p38 does not affect mast cell mediator release<sup>183</sup>. In contrast to the proliferation data shown in Figure 7, treatment of *Pak1* null BMMCs with PD98059 did reduce the amount of  $\beta$  hexosaminidase released after IgE stimulation compared to DMSO treated controls (Figure 15), implying that for degranulation, the Pak1 and Mek/Erk pathways operate independently. These findings support a role for *Pak1* in mediating signals that control the hyperactive degranulation phenotype seen in mast cells haploinsufficient at *Nfl*.

#### Loss of *Pak1* does not significantly affect mast cell survival

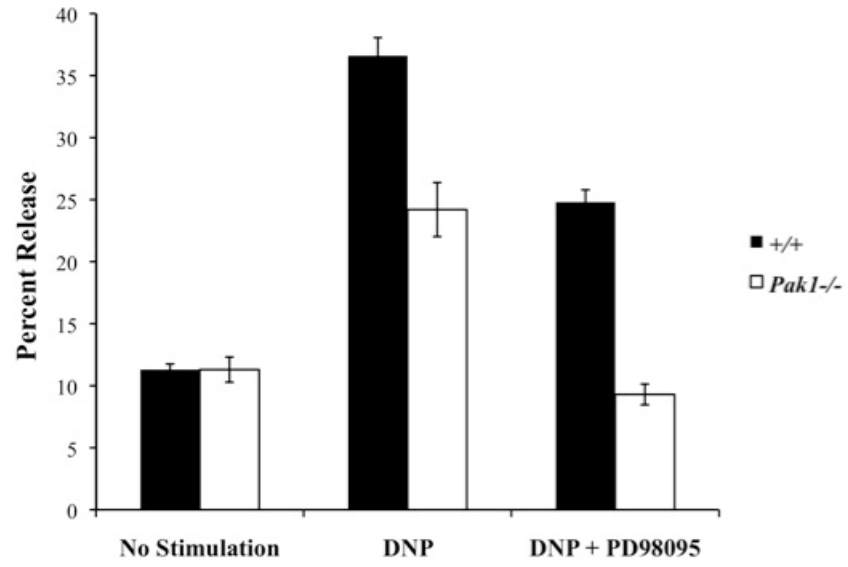
Previous reports have established SCF as a survival factor for mast cells<sup>53</sup>. Given the finding that *Nfl*<sup>+/-</sup> mast cells have increased, PI3-K dependent survival in response to SCF stimulation<sup>75</sup>, and that Pak1 has been described as anti-apoptotic in multiple cellular lineages<sup>143,184,185</sup>, we examined whether loss of *Pak1* would affect the survival of SCF

Figure 14



**Figure 14- Increased degranulation in *Nf1*<sup>+/-</sup> mast cells is corrected by disruption of *Pak1*.** Mast cells were sensitized with anti-DNP IgE monoclonal antibody and assayed for degranulation by measuring the release of  $\beta$  hexosaminidase release following treatment with 25ng/mL of SCF and 30ng/mL of DNP-HSA IgE receptor stimulation. Values express the mean percent difference of the wild type response and the error bars represent the standard error of the mean of 4 independent experiments. \* indicates  $p < .05$  compared to WT control, \*\* indicates  $p < .05$  compared to *Nf1*<sup>+/-</sup> control using Student's unpaired T test.

Figure 15



**Figure 15- Pak1 and Mek1/Erk operate in parallel pathways to regulate mast cell granule release.** Mast cells were sensitized with anti-DNP IgE monoclonal antibody and treated with 10 $\mu$ M of selective Mek1 inhibitor PD98059 for 2h. Cells were assayed for degranulation by measuring the release of  $\beta$  hexosaminidase release following treatment with 30ng/mL of DNP-HSA IgE receptor stimulation. The percent release was calculated using the equation: (OD of supernatant/OD of pellet + OD of supernatant) x 100. Values represent the mean from one representative experiment of three.

stimulated mast cells. As expected, *Nf1*<sup>+/-</sup> mast cells have reduced apoptosis 48 hours after SCF stimulation compared to wild type cells (Figure 16); however, genetic disruption of *Pak1* did not significantly affect the survival of BMMCs, regardless of *Nf1* genotype. These experiments demonstrate that, contrary to other cellular studies, *Pak1* does not regulate the survival responses induced by c-Kit stimulation in mast cells.

#### Cutaneous expansion and degranulation of mast cells in *Nf1*<sup>+/-</sup> mice in response to SCF is Pak1-dependent

*In vivo* mast cell expansion in response to local injection of SCF occurs secondary to local proliferation<sup>169</sup>. In order to determine if our *in vitro* findings are relevant in a more physiologic system, we examined cutaneous mast cell accumulation *in vivo* after local administration of SCF. The progeny generated from the *Nf1*<sup>+/-</sup> and *Pak1*<sup>-/-</sup> genetic intercross were implanted with slow release osmotic pumps to deliver 10 µg/kg/day of SCF or PBS (as a vehicle control) continuously. Overlying skin sections were harvested 7 days later and stained with Giemsa to identify mast cells.

Representative histological sections from animals treated with SCF and stained with Giemsa are shown in Figure 17c-f. Figure 17a shows quantitative results scoring the number of mast cells in the sections per mm<sup>2</sup>. *Pak1* null mice had a significant decrease in cutaneous mast cells compared to wild type mice after SCF delivery (Figure 17a). *Nf1*<sup>+/-</sup> mice had a greater accumulation (>80% increase) of mast cells at the site of SCF infusion compared with wild type control mice (Figure 17a). In keeping with the *in vitro* proliferation data (Figure 7), this excess expansion of cutaneous mast cells in *Nf1*<sup>+/-</sup> mice

Figure 16

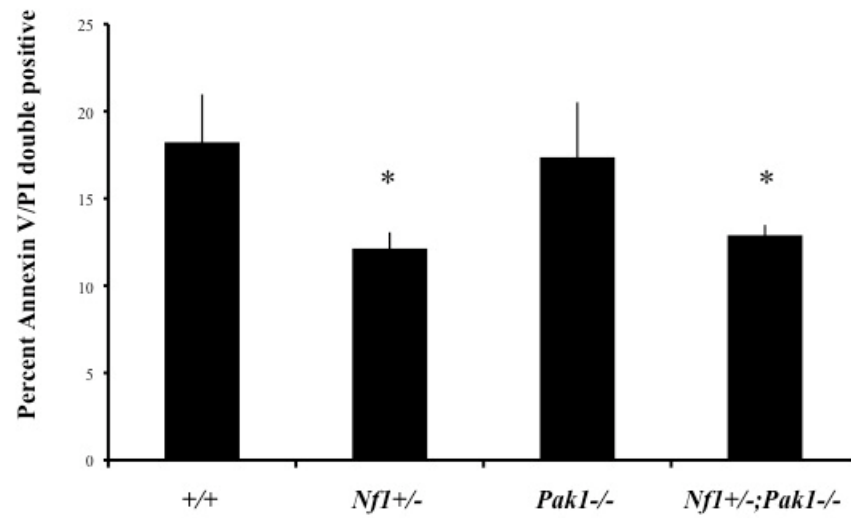




**Figure 16- Loss of *Pak1* does not affect the survival of wild type or *Nfl*<sup>+/-</sup> mast cells.**

Bone marrow-derived mast cells were starved overnight in RPMI, plated in triplicate samples, and then stimulated with 25 ng/mL SCF. Cells were assayed for apoptosis at each indicated time point by Annexin V/PI staining and analyzed by fluorescence cytometry. Cells that were doubly positive for both Annexin V and PI were considered apoptotic. Values represent the mean and the error bars represent the standard error of the mean 1 of 3 independent experiments performed in quadruplicate. \* indicates  $p < 0.05$  compared to WT control using Student's unpaired T test.

was corrected in *Nfl<sup>+/-</sup>;Pak1<sup>-/-</sup>* mice. SCF infusion into *Nfl<sup>+/-</sup>* mice causes increased degranulation of local mast cells compared to wild type mice<sup>61</sup>. We reproduced this result (Figure 17b, and 17d, open arrows) and also found that loss of *Pak1* corrects this phenotype by significantly reducing the percentage of degranulating mast cells in the skin of *Nfl<sup>+/-</sup>;Pak1<sup>-/-</sup>* mice. Our observations suggest that the biochemical mechanisms identified *in vitro* resulting from genetic disruption of *Pak1* in mast cells are biologically operative *in vivo*.

Figure 17a

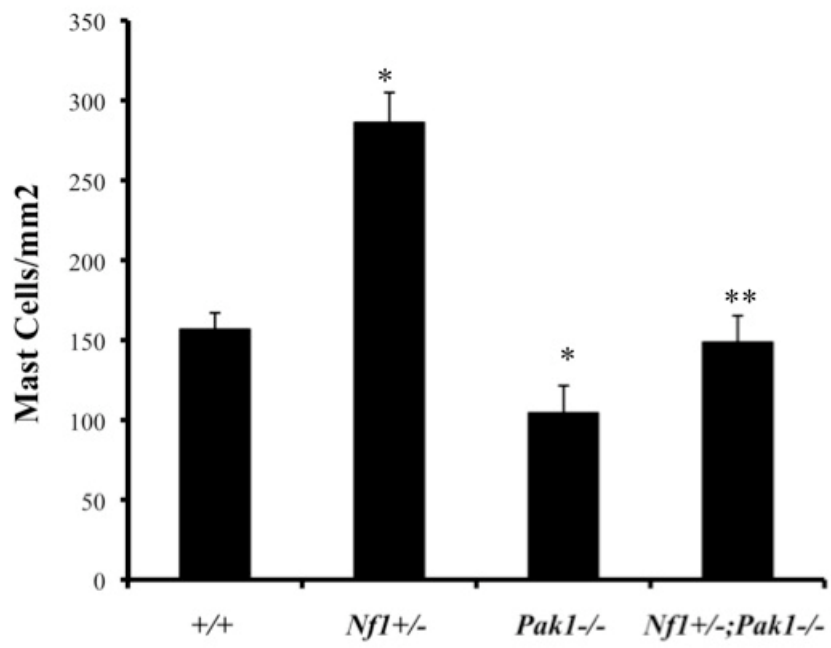
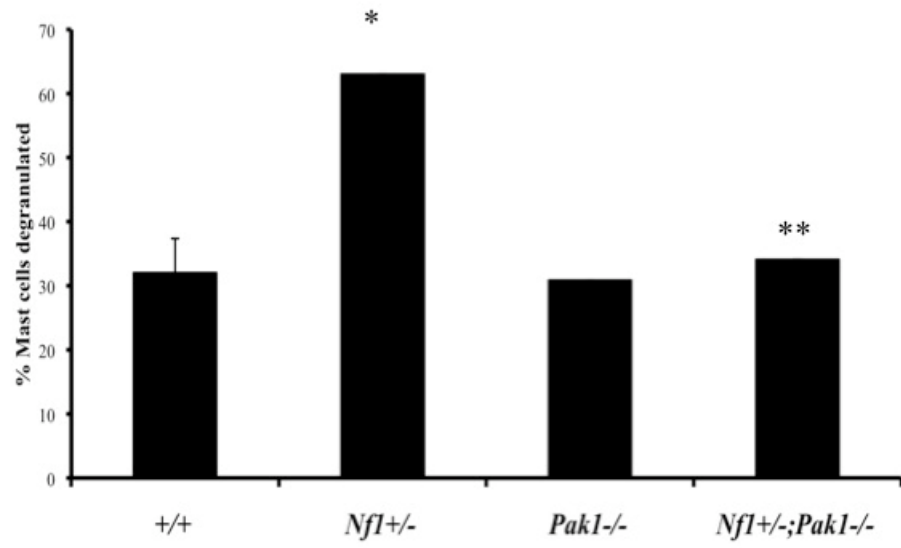
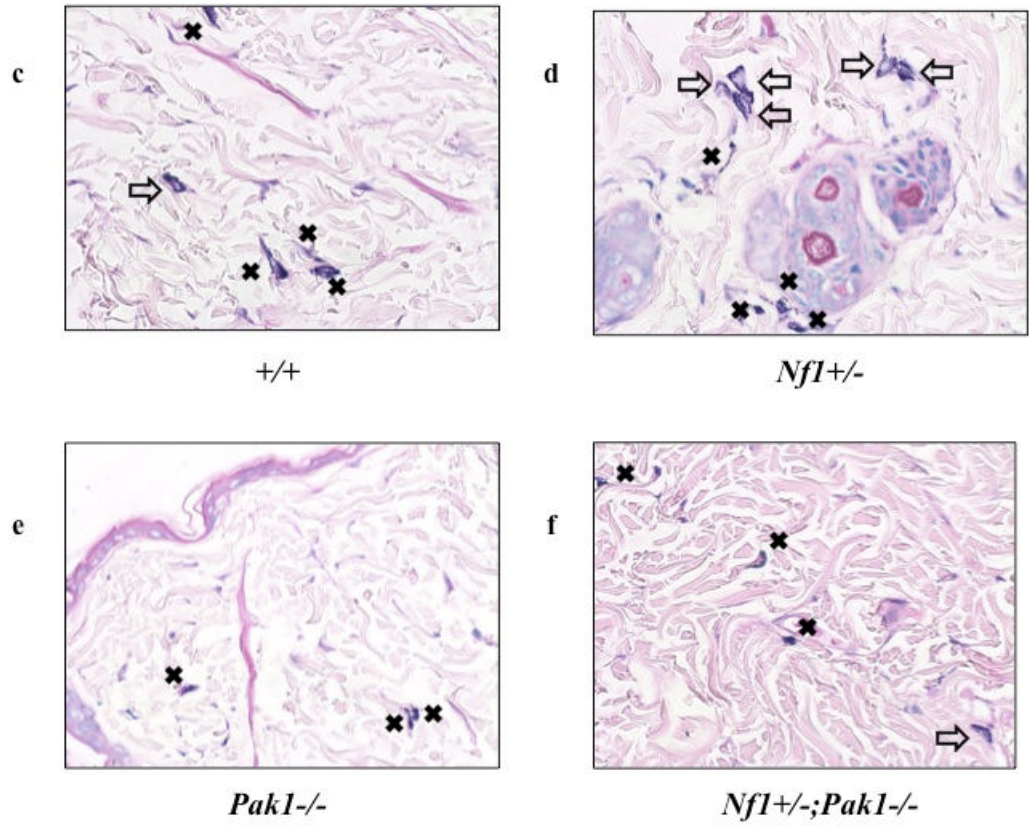


Figure 17b





**Figure 17- Effect of genetic inactivation of *Pak1* on accumulation of cutaneous *Nfl*<sup>+/-</sup> mast cells in response to local administration of SCF *in vivo*.** SCF was delivered *in vivo* via a microosmotic pump on the middorsum at 10ug/kg/day. Skin sections at the site of SCF administration were fixed and stained with hematoxylin and eosin to assess routine histology along with Giemsa to identify mast cells. **A)** Cutaneous mast cells were quantitated in a blinded fashion by counting 2mm<sup>2</sup> sections, and **B)** The percentage of degranulating mast cells present per 2mm<sup>2</sup> section was calculated. Representative sections are displayed in **C-F)**. Resting mast cells in **C-F)** are marked with an ✖, degranulating mast cells in **C-F)** are marked with an open arrow. Values in **A)** and **B)** represent the mean of 3 independent experiments each using 3 mice per genotype and the error bars represent the standard error of the mean. \* indicates p<0.05 compared to WT control and \*\* indicates p<0.05 compared to *Nfl*<sup>+/-</sup> control using Student's unpaired T test.

## ROLE OF *Pak1* IN PLEXIFORM NEUROFIBROMA FORMATION

### Adoptive transfer of *Nf1*<sup>+/-</sup>;*Pak1*<sup>-/-</sup> bone marrow into Schwann cell nullizygous recipients

Based on the results above which identified *Pak1* as a regulator of gains-in-function associated with *Nf1* haploinsufficiency in mast cells, we hypothesized that *Pak1* signaling in the hematopoietic compartment of the neurofibroma microenvironment could contribute to tumor formation *in vivo*. To test this hypothesis, we transferred either *Nf1*<sup>+/-</sup> (as a positive control) or *Nf1*<sup>+/-</sup>;*Pak1*<sup>-/-</sup> bone marrow into mice with conditionally ablated *Nf1* alleles in the Schwann cell lineage. Two experimental groups of recipient mice were used. First, we used *Krox20Cre;Nf1*<sup>flx/flx</sup> mice, which are functionally WT in all non-Schwann cell lineages and do not spontaneously develop neurofibromas. Recent work has shown that transplantation of *Nf1*<sup>+/-</sup> bone marrow into *Krox20Cre;Nf1*<sup>flx/flx</sup> mice is sufficient to stimulate neurofibroma development<sup>64</sup>, therefore we hypothesized that transfer of *Nf1*<sup>+/-</sup>;*Pak1*<sup>-/-</sup> bone marrow would not be permissive to allow tumor formation. Additionally, we used *Krox20Cre;Nf1*<sup>flx/-</sup> as recipients, which contain a germline disruption of one copy of *Nf1* and a floxed allele susceptible to recombination in the Schwann cell lineage. *Krox20Cre;Nf1*<sup>flx/-</sup> consistently develop plexiform neurofibromas around the spinal nerve roots within 8 months of life<sup>30,64</sup>. We predicted that *Krox20Cre;Nf1*<sup>flx/-</sup> mice reconstituted with *Nf1*<sup>+/-</sup>;*Pak1*<sup>-/-</sup> bone marrow would prevent or delay the formation of tumors in these mice. A schematic of the experimental design is outlined in Figure 18.

**Figure 18**

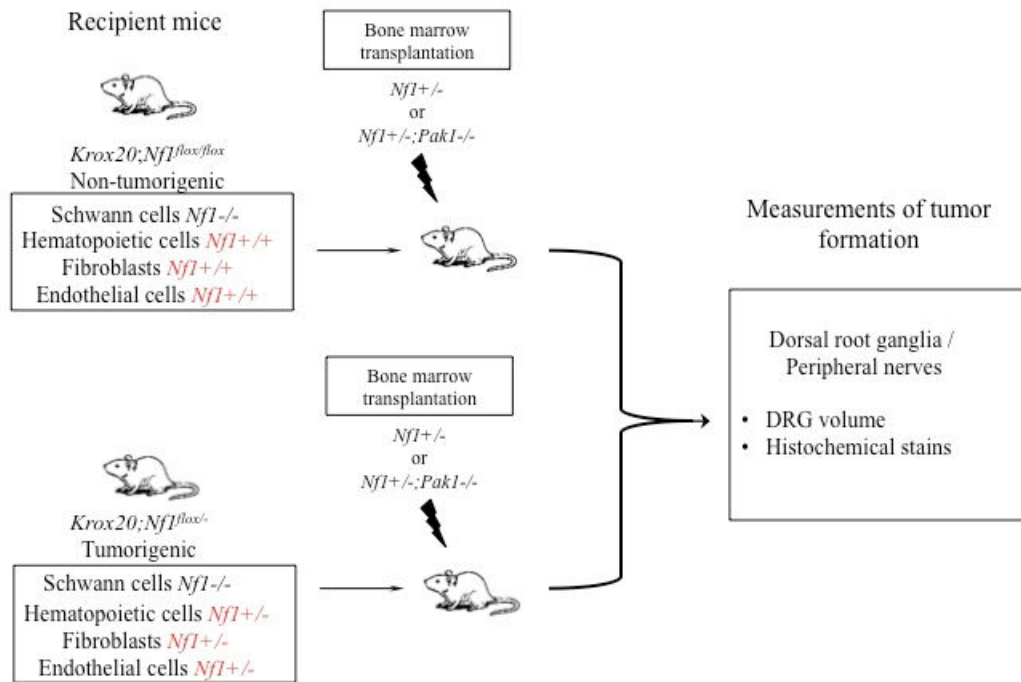




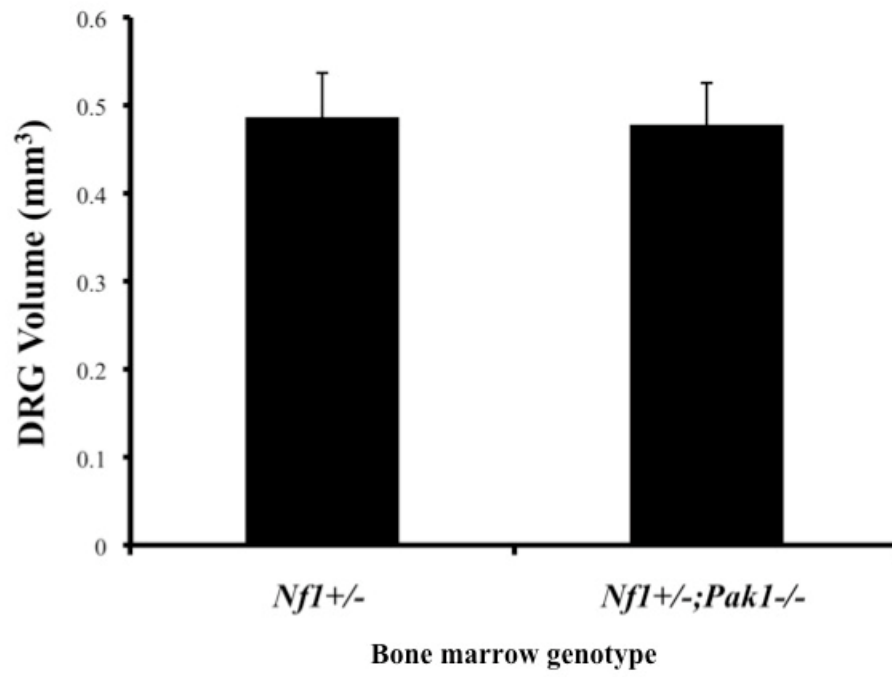
**Figure 18- Neurofibroma formation experimental design.** Schematic showing the genotypes of recipient mice, the genotypes of adoptively transferred cells following ionizing radiation of the recipients, and measurements obtained following transplantation.

*Krox20Cre;Nf1<sup>lox/lox</sup>* mice reconstituted with *Nf1<sup>+/-</sup>;Pak1<sup>-/-</sup>* bone marrow develop plexiform neurofibromas

Following 1100 Rads of ionizing radiation,  $5 \times 10^6$  whole bone marrow cells from *Nf1<sup>+/-</sup>* mice or *Nf1<sup>+/-</sup>;Pak1<sup>-/-</sup>* mice were transplanted into *Krox20Cre;Nf1<sup>lox/lox</sup>* mice. These mice were followed after transplant for 12-15 months before they were sacrificed and investigated for tumor formation along the spinal nerve roots. There was no difference in post-transplant survival between the recipients of *Nf1<sup>+/-</sup>* marrow or *Nf1<sup>+/-</sup>;Pak1<sup>-/-</sup>* marrow (over 85% survival in both groups at 12 months). Necropsy of the spinal nerves showed enlargement of dorsal root ganglia in both recipients of *Nf1<sup>+/-</sup>* marrow as well as recipients of *Nf1<sup>+/-</sup>;Pak1<sup>-/-</sup>* marrow. Volumetric analysis of these dorsal root ganglia showed no significant changes in the volume of the dorsal root ganglia of the sciatic nerve (which is a common location for neurofibromas in *Krox20Cre;Nf1<sup>lox/-</sup>* mice) between recipients of *Nf1<sup>+/-</sup>* marrow versus recipients of *Nf1<sup>+/-</sup>;Pak1<sup>-/-</sup>* marrow (Figure 19).

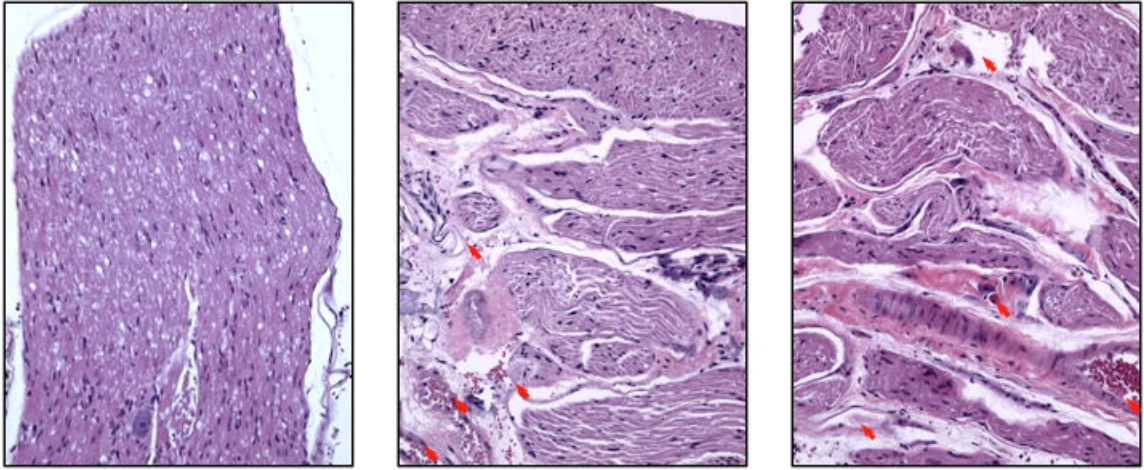
Unexpectedly, histological examination of sections of dorsal root ganglia and proximal peripheral nerves from 100% of recipients of both of *Nf1<sup>+/-</sup>* bone marrow as well as 100% of recipients of *Nf1<sup>+/-</sup>;Pak1<sup>-/-</sup>* bone marrow revealed the presence of classical pathologic features of plexiform neurofibromas. These include disruptions of nerve root architecture and Schwann cells (Figure 20), increased angiogenesis and blood vessel presence in the nerve (Figure 20, red arrows), as well as substantial collagen deposition (Figure 21). Interestingly, while both recipients of both of *Nf1<sup>+/-</sup>* bone marrow and recipients of *Nf1<sup>+/-</sup>;Pak1<sup>-/-</sup>* bone marrow have increases in the number of infiltrating

Figure 19



**Figure 19- *Krox20Cre;NfI<sup>flox/flox</sup>* mice reconstituted with *NfI<sup>+/-</sup>;Pak1<sup>-/-</sup>* mice develop enlarged sciatic nerve dorsal root ganglia.** *Krox20Cre;NfI<sup>flox/flox</sup>* mice were sacrificed 12-15 months after transplantation with *NfI<sup>+/-</sup>* or *NfI<sup>+/-</sup>;Pak1<sup>-/-</sup>* bone marrow and the spinal cord and nerve roots of each animal were dissected. The dorsal root ganglia dimensions were obtained by measurement with calipers and volume was determined by using the formula (0.52 x (width)<sup>2</sup> x (length)) to approximate spheroidal volume. Values represent the mean of 15 recipients of *NfI<sup>+/-</sup>* marrow and 11 recipients of *NfI<sup>+/-</sup>;Pak1<sup>-/-</sup>* marrow, and error bars represent the standard error of the mean. No significant difference between the means of the two genotypes was found using Student's unpaired T test.

**Figure 20**



**Normal**

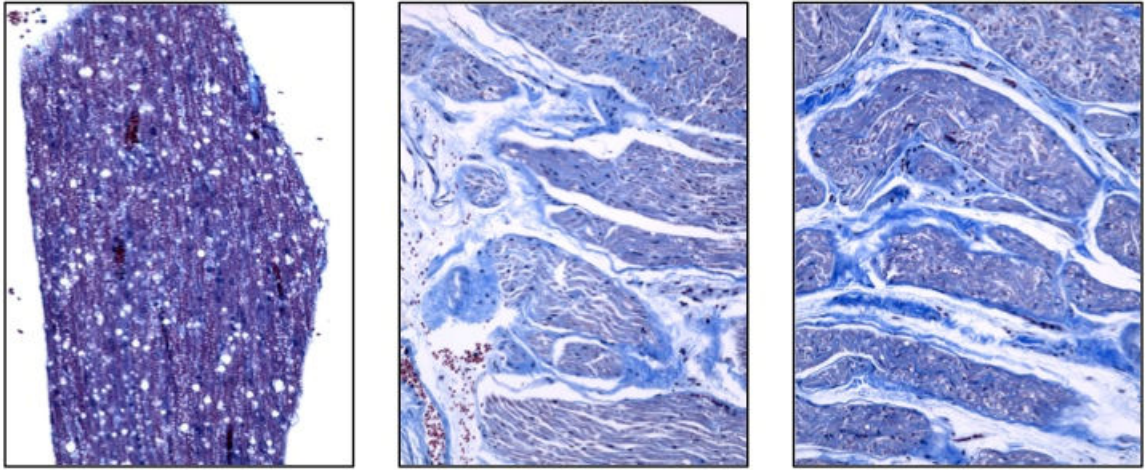
***Nf1*+/-**

***Nf1*+/-;*Pak1*-/-**

**Bone marrow genotype**

**Figure 20- *Krox20Cre;Nf1<sup>flox/flox</sup>* mice reconstituted with *Nf1<sup>+/-</sup>;Pak1<sup>-/-</sup>* bone marrow develop histologically identifiable plexiform neurofibromas.** Representative hematoxylin and eosin (H&E) stained sections of dorsal root ganglia and proximal peripheral nerves from *Krox20Cre;Nf1<sup>flox/flox</sup>* mice transplanted with either *Nf1<sup>+/-</sup>* marrow or *Nf1<sup>+/-</sup>;Pak1<sup>-/-</sup>* marrow. Blood vessels are identified by red arrows. Genotypes of donor bone marrow are indicated, along with a representative section of normal nerve root. Photos were taken with a light microscope under 200x magnification.

**Figure 21**



**Normal**

***Nf1*<sup>+/-</sup>**

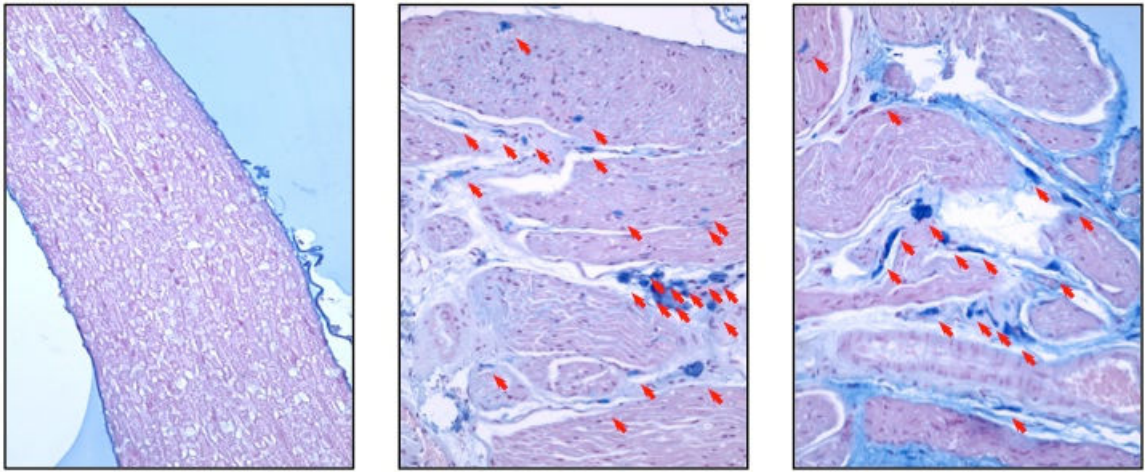
***Nf1*<sup>+/-</sup>;*Pak1*<sup>-/-</sup>**

**Bone marrow genotype**

**Figure 21- *Krox20Cre;Nf1<sup>flx/flx</sup>* mice reconstituted with *Nf1<sup>+/-</sup>;Pak1<sup>-/-</sup>* bone marrow have collagen deposition characteristic of plexiform neurofibromas.** Representative sections of dorsal root ganglia and proximal peripheral nerves from *Krox20Cre;Nf1<sup>flx/flx</sup>* mice transplanted with either *Nf1<sup>+/-</sup>* marrow or *Nf1<sup>+/-</sup>;Pak1<sup>-/-</sup>* marrow were stained with Masson's trichrome to identify collagen content.. Collagen is identified by bright blue staining. Genotypes of donor bone marrow are indicated, along with a representative section of normal nerve root. Photos were taken with a light microscope under 200x magnification.



**Figure 22a**



**Normal**

***Nf1+/-***

***Nf1+/-;Pak1-/-***

**Bone marrow genotype**

Figure 22b

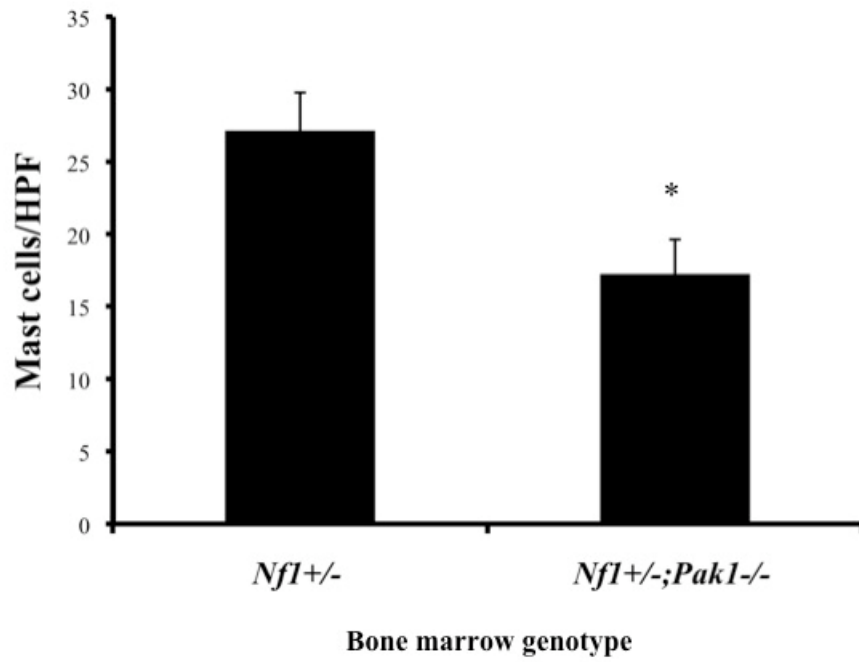


**Figure 22- *Krox20Cre;Nf1<sup>flx/flx</sup>* mice reconstituted with *Nf1<sup>+/-</sup>;Pak1<sup>-/-</sup>* bone marrow have reduced mast cell numbers present in plexiform neurofibromas. A)**

Representative sections of dorsal root ganglia and proximal peripheral nerves from *Krox20Cre;Nf1<sup>flx/flx</sup>* mice transplanted with either *Nf1<sup>+/-</sup>* marrow or *Nf1<sup>+/-</sup>;Pak1<sup>-/-</sup>* marrow were stained with Alcian blue to identify mast cell numbers. Mast cells are identified by red arrows. Genotypes of donor bone marrow are indicated, along with a representative section of normal nerve root. Photos were taken with a light microscope under 200x magnification. **B)** Number of mast cells present in Alcian blue sections from 8 animals per genotype were quantitated by counting mast cells per high power field. Values represent the mean and the error bars represent the standard error of the mean. \* indicates  $p < 0.05$  compared to *Nf1<sup>+/-</sup>* recipients using Student's unpaired T test.

mast cells to the dorsal root ganglia (Figure 22a, red arrows), recipients of *Nf1*<sup>+/-</sup>;*Pak1*<sup>-/-</sup> bone marrow have a significant decrease (~38%) in the number of mast cells compared to recipients of *Nf1*<sup>+/-</sup> bone marrow (Figure 22b). Despite this decrease in mast cell number, reconstitution of *Krox20Cre;Nf1*<sup>fllox/fllox</sup> mice with *Nf1*<sup>+/-</sup>;*Pak1*<sup>-/-</sup> bone marrow lead to similar outcomes in terms of neurofibroma development and structure as *Krox20Cre;Nf1*<sup>fllox/fllox</sup> mice with *Nf1*<sup>+/-</sup> bone marrow, indicating that loss of *Pak1* in the tumor microenvironment still permitted the hematopoietic compartment to induce neurofibroma formation.

*Krox20Cre;Nf1*<sup>fllox/-</sup> mice reconstituted with *Nf1*<sup>+/-</sup>;*Pak1*<sup>-/-</sup> bone marrow develop plexiform neurofibromas

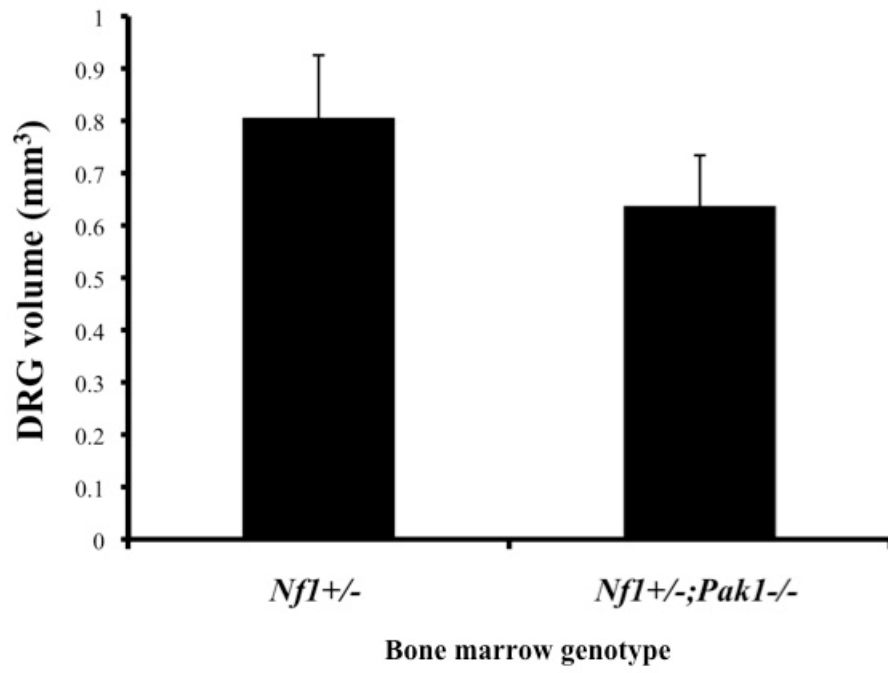
In a similar manner, irradiated *Krox20Cre;Nf1*<sup>fllox/-</sup> mice received bone marrow from *Nf1*<sup>+/-</sup> mice or *Nf1*<sup>+/-</sup>;*Pak1*<sup>-/-</sup> mice and were followed after transplant for 12-15 months before they were sacrificed and investigated for tumor formation along the spinal nerve roots. As with *Krox20Cre;Nf1*<sup>fllox/fllox</sup> recipients, *Krox20Cre;Nf1*<sup>fllox/-</sup> mice had similar post-transplant mortality (over 85% survival in both groups at 12 months) regardless of the genotype of transplanted marrow. Necropsy of the spinal nerves showed enlargement of dorsal root ganglia in both recipients of *Nf1*<sup>+/-</sup> marrow as well as recipients of *Nf1*<sup>+/-</sup>;*Pak1*<sup>-/-</sup> marrow. Volumetric analysis of these dorsal root ganglia showed no significant changes in the volume of the dorsal root ganglia of the sciatic nerve between recipients of *Nf1*<sup>+/-</sup> marrow versus recipients of *Nf1*<sup>+/-</sup>;*Pak1*<sup>-/-</sup> marrow (Figure 23).

Pathologic analysis demonstrated the presence of plexiform neurofibromas in 100% of *Krox20Cre;Nf1<sup>lox/-</sup>* mice transplanted with *Nf1<sup>+/-</sup>;Pak1<sup>-/-</sup>* bone marrow. Recipients of *Nf1<sup>+/-</sup>;Pak1<sup>-/-</sup>* bone marrow had very similar histological features as recipients of *Nf1<sup>+/-</sup>* bone marrow, including disorganized cellular architecture (Figure 24), increased numbers of blood vessels (Figure 24, red arrows), and large deposits of collagen in the ECM (Figure 25). In contrast to the results shown in Figure 22b which describe a reduction in the number of mast cells present in neurofibromas found in *Krox20Cre;Nf1<sup>lox/lox</sup>* mice transplanted with *Nf1<sup>+/-</sup>;Pak1<sup>-/-</sup>* bone marrow, *Krox20Cre;Nf1<sup>lox/-</sup>* mice transplanted with *Nf1<sup>+/-</sup>;Pak1<sup>-/-</sup>* bone marrow have equal numbers of mast cells as *Krox20Cre;Nf1<sup>lox/-</sup>* mice transplanted with *Nf1<sup>+/-</sup>* bone marrow (Figure 26). These experiments using adoptive transfer of bone marrow into *Krox20Cre;Nf1<sup>lox/-</sup>* mice demonstrate that disruption of *Pak1* in the hematopoietic system is not sufficient to counteract the neurofibroma stimulating phenotype of the *Nf1* haploinsufficient microenvironment.

#### Genetic disruption of *Pak1* in *Krox20Cre;Nf1<sup>lox/-</sup>* mice does not prevent neurofibroma formation

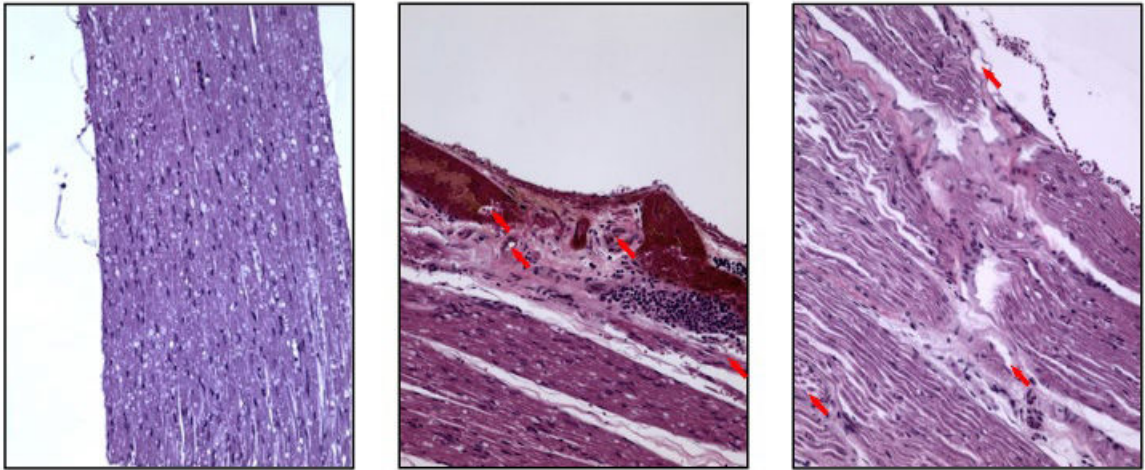
Adoptive transfer of *Nf1<sup>+/-</sup>;Pak1<sup>-/-</sup>* bone marrow into *Krox20Cre;Nf1<sup>lox/lox</sup>* or *Krox20Cre;Nf1<sup>lox/-</sup>* mice resulted in the development of neurofibromas similar to mice transplanted with *Nf1<sup>+/-</sup>* bone marrow. Therefore, we were interested in the tumor forming ability of conditionally disrupted *Nf1* mice that lacked *Pak1* in all lineages, not just the hematopoietic compartment. Genetic intercross of *Krox20Cre;Nf1<sup>lox/-</sup>* mice with

Figure 23



**Figure 23- *Krox20Cre;Nf1<sup>fllox/-</sup>* mice reconstituted with *Nf1<sup>+/-</sup>;Pak1<sup>-/-</sup>* mice develop enlarged sciatic nerve dorsal root ganglia.** *Krox20Cre;Nf1<sup>fllox/-</sup>* mice were sacrificed 12-15 months after transplantation with *Nf1<sup>+/-</sup>* or *Nf1<sup>+/-</sup>;Pak1<sup>-/-</sup>* bone marrow and the spinal cord and nerve roots of each animal were dissected. The dorsal root ganglia dimensions were obtained by measurement with calipers and volume was determined by using the formula  $(0.52 \times (\text{width})^2 \times (\text{length}))$  to approximate spheroidal volume. Values represent the mean of 6 recipients of *Nf1<sup>+/-</sup>* marrow and 4 recipients of *Nf1<sup>+/-</sup>;Pak1<sup>-/-</sup>* marrow, and error bars represent the standard error of the mean. No significant difference between the means of the two genotypes was found using Student's unpaired T test.

Figure 24



Normal

*Nf1*<sup>+/-</sup>

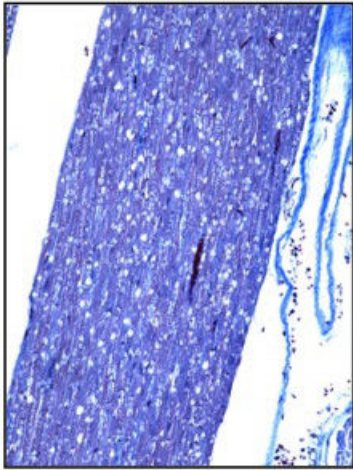
*Nf1*<sup>+/-</sup>;*Pak1*<sup>-/-</sup>

Bone marrow genotype

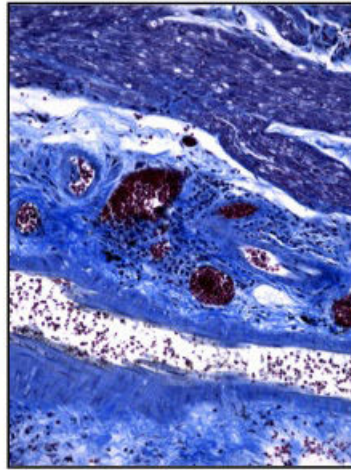


**Figure 24- *Krox20Cre;Nf1<sup>fllox/-</sup>* mice reconstituted with *Nf1<sup>+/-</sup>;Pak1<sup>-/-</sup>* bone marrow develop histologically identifiable plexiform neurofibromas.** Representative hematoxylin and eosin (H&E) stained sections of dorsal root ganglia and proximal peripheral nerves from *Krox20Cre;Nf1<sup>fllox/-</sup>* mice transplanted with either *Nf1<sup>+/-</sup>* marrow or *Nf1<sup>+/-</sup>;Pak1<sup>-/-</sup>* marrow. Blood vessels are identified by red arrows. Genotypes of donor bone marrow are indicated, along with a representative section of normal nerve root. Photos were taken with a light microscope under 200x magnification.

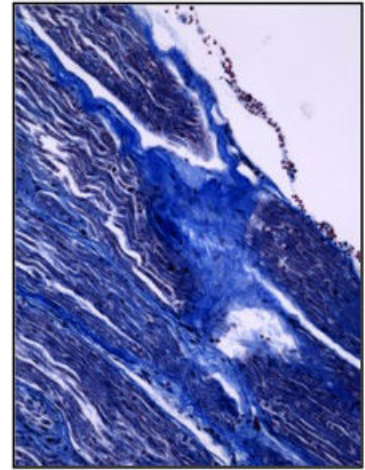
**Figure 25**



**Normal**



*Nf1*<sup>+/-</sup>

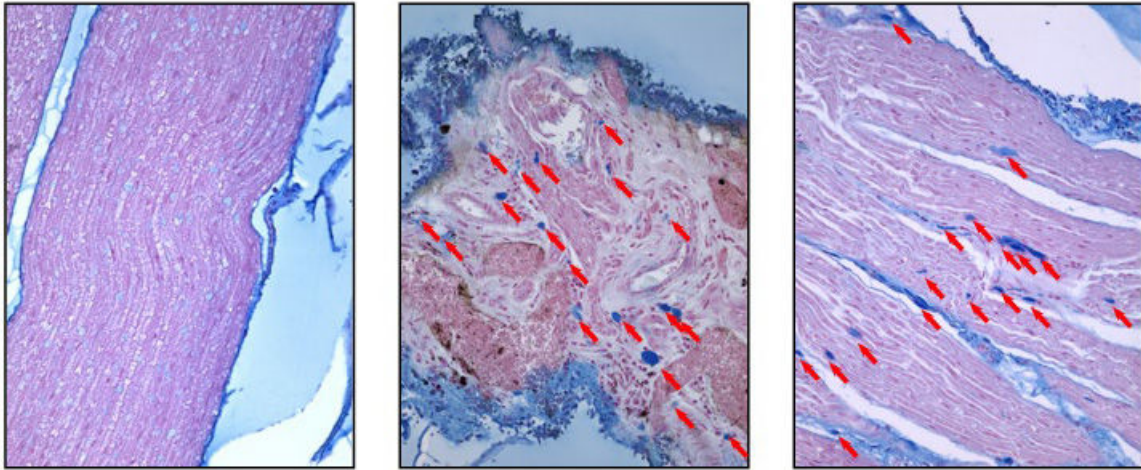


*Nf1*<sup>+/-</sup>;*Pak1*<sup>-/-</sup>

**Bone marrow genotype**

**Figure 25- *Krox20Cre;Nf1<sup>fllox/-</sup>* mice reconstituted with *Nf1<sup>+/-</sup>;Pak1<sup>-/-</sup>* bone marrow have collagen deposition characteristic of plexiform neurofibromas.** Representative sections of dorsal root ganglia and proximal peripheral nerves from *Krox20Cre;Nf1<sup>fllox/-</sup>* mice transplanted with either *Nf1<sup>+/-</sup>* marrow or *Nf1<sup>+/-</sup>;Pak1<sup>-/-</sup>* marrow were stained with Masson's trichrome to identify collagen content. Collagen is identified by bright blue staining. Genotypes of donor bone marrow are indicated, along with a representative section of normal nerve root. Photos were taken with a light microscope under 200x magnification.

Figure 26a



No Tumor

*Nf1*<sup>+/-</sup>

*Nf1*<sup>+/-</sup>;*Pak1*<sup>-/-</sup>

Bone marrow genotype

Figure 26b

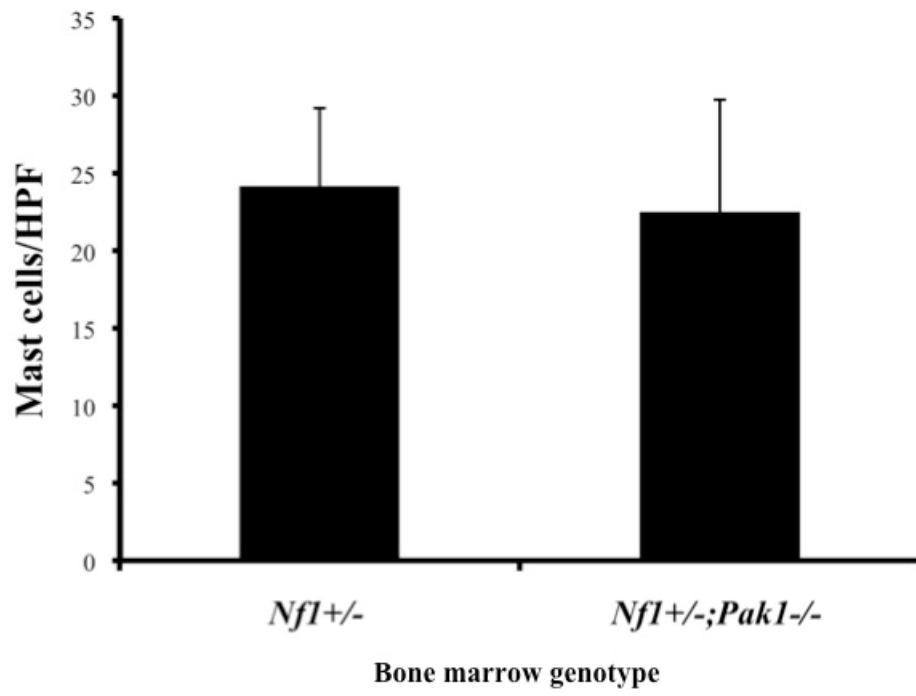


**Figure 26- *Krox20Cre;Nf1<sup>fllox/-</sup>* mice reconstituted with *Nf1<sup>+/-</sup>*; *Pak1<sup>-/-</sup>* bone marrow have plexiform neurofibromas infiltrated with numerous inflammatory mast cells.**

**A)** Representative sections of dorsal root ganglia and proximal peripheral nerves from *Krox20Cre;Nf1<sup>fllox/-</sup>* mice transplanted with either *Nf1<sup>+/-</sup>* marrow or *Nf1<sup>+/-</sup>*; *Pak1<sup>-/-</sup>* marrow were stained with Alcian blue to identify mast cell numbers. Mast cells are identified by red arrows. Genotypes of donor bone marrow are indicated, along with a representative section of normal nerve root. Photos were taken with a light microscope under 200x magnification. **B)** Number of mast cells present in Alcian blue sections from 4 animals per genotype were quantitated by counting mast cells per high power field. Values represent the mean and the error bars represent the standard error of the mean. No significant difference between the means of the two genotypes was found using Student's unpaired T test.

*Nf1*<sup>+/-</sup>; *Pak1*<sup>-/-</sup> mice generated *Krox20Cre;Nf1*<sup>lox/-</sup>; *Pak1*<sup>-/-</sup> progeny in the F2 generation. These *Krox20Cre;Nf1*<sup>lox/-</sup>; *Pak1*<sup>-/-</sup> mice were followed for 12-15 months with *Krox20Cre;Nf1*<sup>lox/-</sup> mice as positive controls to assess plexiform neurofibroma development. After 12 months, the survival of *Krox20Cre;Nf1*<sup>lox/-</sup>; *Pak1*<sup>-/-</sup> mice was equivalent to the *Krox20Cre;Nf1*<sup>lox/-</sup> mice (~50% survival for both genotypes).

Dissection of the spinal cord and proximal spinal nerves revealed enlargement of the dorsal root ganglia and spinal nerve roots in *Krox20Cre;Nf1*<sup>lox/-</sup>; *Pak1*<sup>-/-</sup> mice (Figure 27). Volumetric analysis of these dorsal root ganglia showed no significant changes in the volume of the dorsal root ganglia of the sciatic nerve between *Krox20Cre;Nf1*<sup>lox/-</sup>; *Pak1*<sup>-/-</sup> mice and *Krox20Cre;Nf1*<sup>lox/-</sup> mice (Figure 27).

*Krox20Cre;Nf1*<sup>lox/-</sup>; *Pak1*<sup>-/-</sup> mice displayed histological signs of neurofibroma formation as evidenced by disruptions in nerve root architecture (Figure 28), increased angiogenesis (Figure 28, red arrows), high amounts of collagen deposition (Figure 29), and the infiltration of mast cells (Figure 30a, red arrows). No significant differences in mast cell numbers within the neurofibroma were found (Figure 30b).

Table 1 details the results of plexiform neurofibroma experiments performed by our group and colleagues and lists the genotypes of the relevant cell lineages in each set of trials. The results of the experiments described in detail within this study demonstrate that genetic disruption of *Pak1* in the *Krox20Cre;Nf1*<sup>lox/-</sup> plexiform neurofibroma tumor model is insufficient for preventing tumor formation *in vivo*.

Figure 27

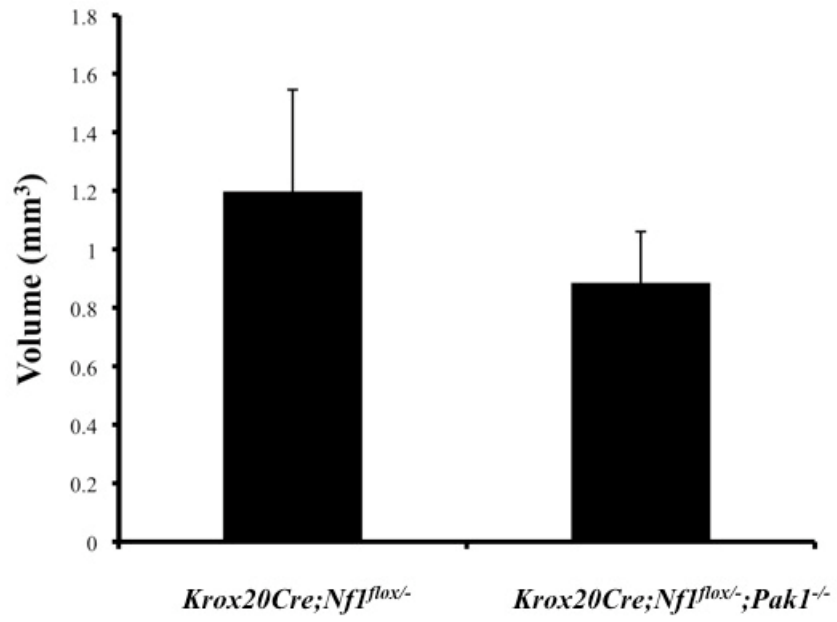
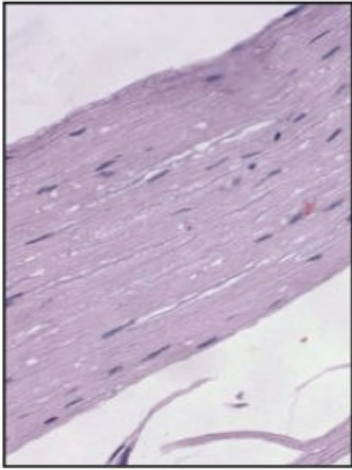


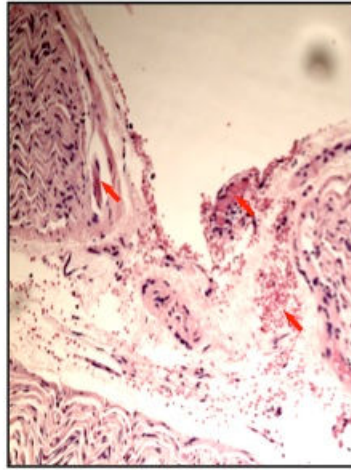


**Figure 27- *Krox20Cre;Nf1<sup>lox/-</sup>;Pak1<sup>-/-</sup>* mice develop enlarged sciatic nerve dorsal root ganglia.** *Krox20Cre;Nf1<sup>lox/-</sup>;Pak1<sup>-/-</sup>* and *Krox20Cre;Nf1<sup>lox/-</sup>* mice were sacrificed after 12-15 months and the spinal cord and nerve roots of each animal were dissected. The dorsal root ganglia dimensions were obtained by measurement with calipers and volume was determined by using the formula  $(0.52 \times (\text{width})^2 \times (\text{length}))$  to approximate spheroidal volume. Values represent the mean of 15 animals per genotype and error bars represent the standard error of the mean. No significant difference between the means of the two genotypes was found using Student's unpaired T test.

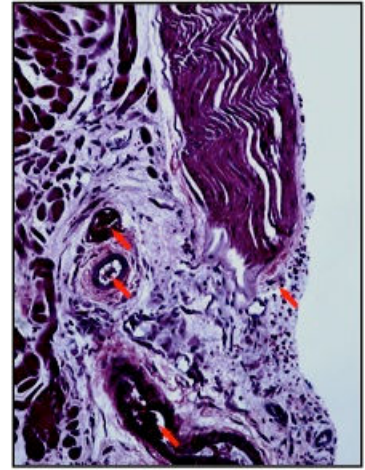
**Figure 28**



**No Tumor**



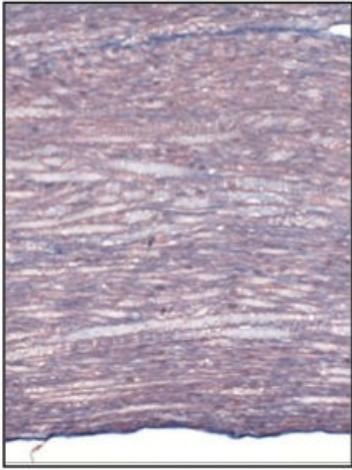
*Krox20Cre;Nf1<sup>fllox/-</sup>*



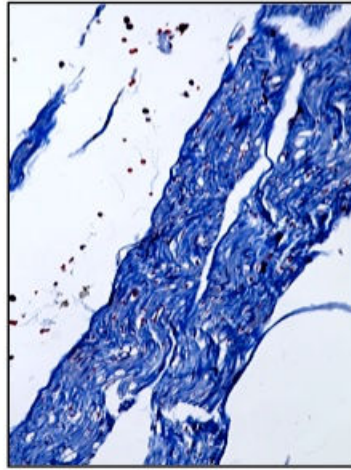
*Krox20Cre;Nf1<sup>fllox/-</sup>;Pak1<sup>-/-</sup>*

**Figure 28- *Krox20Cre;Nf1<sup>lox/-</sup>;Pak1<sup>-/-</sup>* mice develop histologically identifiable plexiform neurofibromas.** Representative hematoxylin and eosin (H&E) stained sections of dorsal root ganglia and proximal peripheral nerves from *Krox20Cre;Nf1<sup>lox/-</sup>;Pak1<sup>-/-</sup>* and *Krox20Cre;Nf1<sup>lox/-</sup>* mice. Blood vessels are identified by red arrows. Genotypes of each group are indicated, along with a representative section of normal nerve root. Photos were taken with a light microscope under 200x magnification.

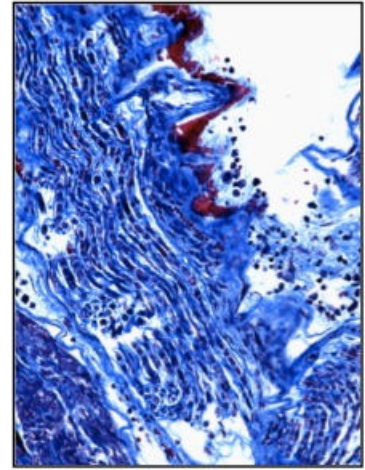
Figure 29



No Tumor



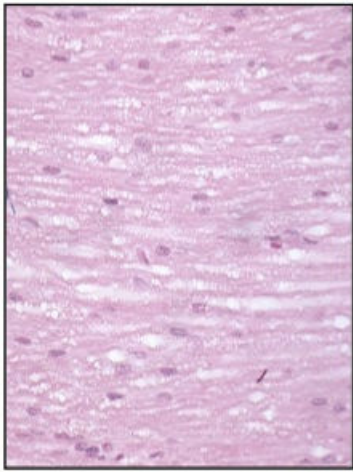
*Krox20Cre;Nf1<sup>lox/-</sup>*



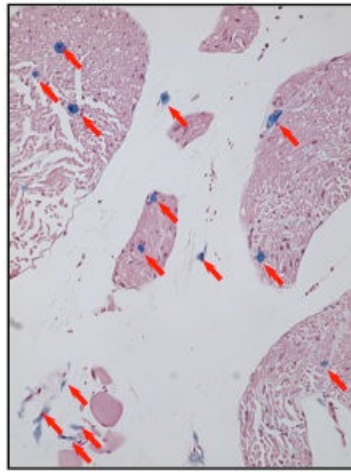
*Krox20Cre;Nf1<sup>lox/-</sup>;Pak1<sup>-/-</sup>*

**Figure 29- *Krox20Cre;Nf1<sup>fllox/-</sup>;Pak1<sup>-/-</sup>* mice have collagen deposition characteristic of plexiform neurofibromas.** Representative sections of dorsal root ganglia and proximal peripheral nerves from *Krox20Cre;Nf1<sup>fllox/-</sup>;Pak1<sup>-/-</sup>* mice and *Krox20Cre;Nf1<sup>fllox/-</sup>* mice were stained with Masson's trichrome to identify collagen content. Collagen is identified by bright blue staining. Genotypes of each group are indicated, along with a representative section of normal nerve root. Photos were taken with a light microscope under 200x magnification.

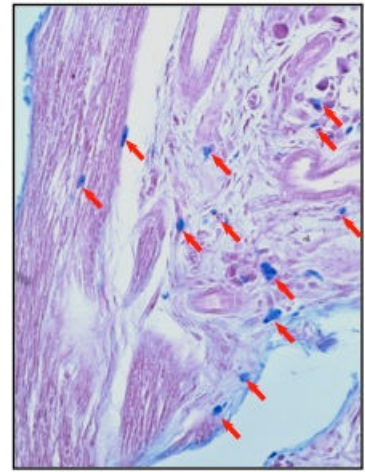
**Figure 30a**



**No Tumor**



*Krox20Cre;Nf1<sup>lox/-</sup>*



*Krox20Cre;Nf1<sup>lox/-</sup>;Pak1<sup>-/-</sup>*

Figure 30b

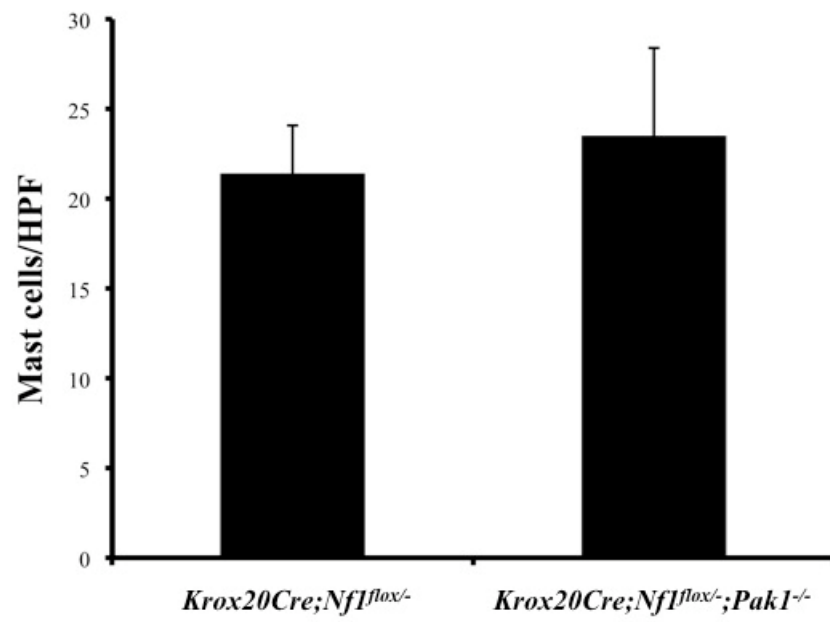


**Figure 30- *Krox20Cre;Nf1<sup>fllox/-</sup>;Pak1<sup>-/-</sup>* mice have plexiform neurofibromas infiltrated with numerous inflammatory mast cells.** **A)** Representative sections of dorsal root ganglia and proximal peripheral nerves from *Krox20Cre;Nf1<sup>fllox/-</sup>;Pak1<sup>-/-</sup>* mice and *Krox20Cre;Nf1<sup>fllox/-</sup>* mice were stained with Alcian blue to identify mast cell numbers. Mast cells are identified by red arrows. Genotypes of each group are indicated, along with a representative section of normal nerve root. Photos were taken with a light microscope under 200x magnification. **B)** Number of mast cells present in Alcian blue sections from 4 animals per genotype were quantitated by counting mast cells per high power field. Values represent the mean and the error bars represent the standard error of the mean. No significant difference between the means of the two genotypes was found using Student's unpaired T test.



**Table 1**

<b>Recipient</b>	<b>Donor</b>	<b>Schwann Cells</b>	<b>Mast/ Hematopoietic cells</b>	<b>Fibroblasts</b>	<b>Neurofibromas</b>
<i>Krox20Cre; Nf1flox/flox</i>	n/a	<i>Nf1-/-</i>	<i>Nf1+ /+</i>	<i>Nf1+ /+</i>	<b>No</b>
<i>Krox20Cre; Nf1flox/-</i>	n/a	<i>Nf1-/-</i>	<i>Nf1+ /-</i>	<i>Nf1+ /-</i>	<b>Yes</b>
<i>Krox20Cre; Nf1flox/flox</i>	<i>Nf1+ /-</i>	<i>Nf1-/-</i>	<i>Nf1+ /-</i>	<i>Nf1+ /+</i>	<b>Yes</b>
<i>Krox20Cre; Nf1flox/-</i>	<i>Nf1+ /+</i>	<i>Nf1-/-</i>	<i>Nf1+ /+</i>	<i>Nf1+ /-</i>	<b>No</b>
<i>Krox20Cre; Nf1flox/flox</i>	<i>Nf1+ /-;Pak1-/-</i>	<i>Nf1-/-</i>	<i>Nf1+ /-;Pak1-/-</i>	<i>Nf1+ /+</i>	<b>Yes</b>
<i>Krox20Cre; Nf1flox/-</i>	<i>Nf1+ /-;Pak1-/-</i>	<i>Nf1-/-</i>	<i>Nf1+ /-;Pak1-/-</i>	<i>Nf1+ /-</i>	<b>Yes</b>
<i>Krox20Cre; Nf1flox/-;Pak1-/-</i>	n/a	<i>Nf1-/-;Pak1-/-</i>	<i>Nf1+ /-;Pak1-/-</i>	<i>Nf1+ /-;Pak1-/-</i>	<b>Yes</b>

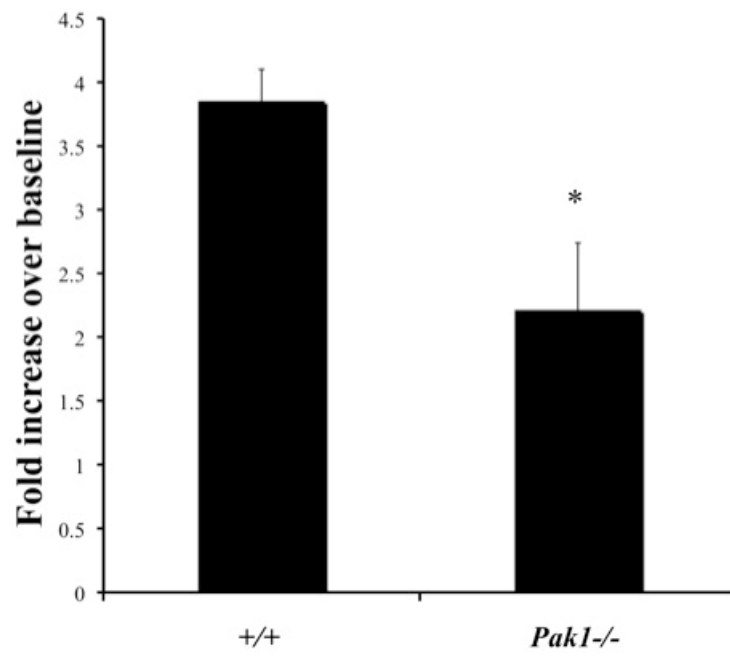
**Table 1- Results of plexiform neurofibroma formation studies using the *Krox20Cre;Nf1<sup>flox</sup>* conditional knockout animal model.**

## **ROLE OF *Pak1* IN MEDIATING PDGF-BB AND TGF- $\beta$ DEPENDENT FUNCTIONS IN FIBROBLASTS**

### PDGF-BB mediated fibroblast proliferation is *Pak1* dependent

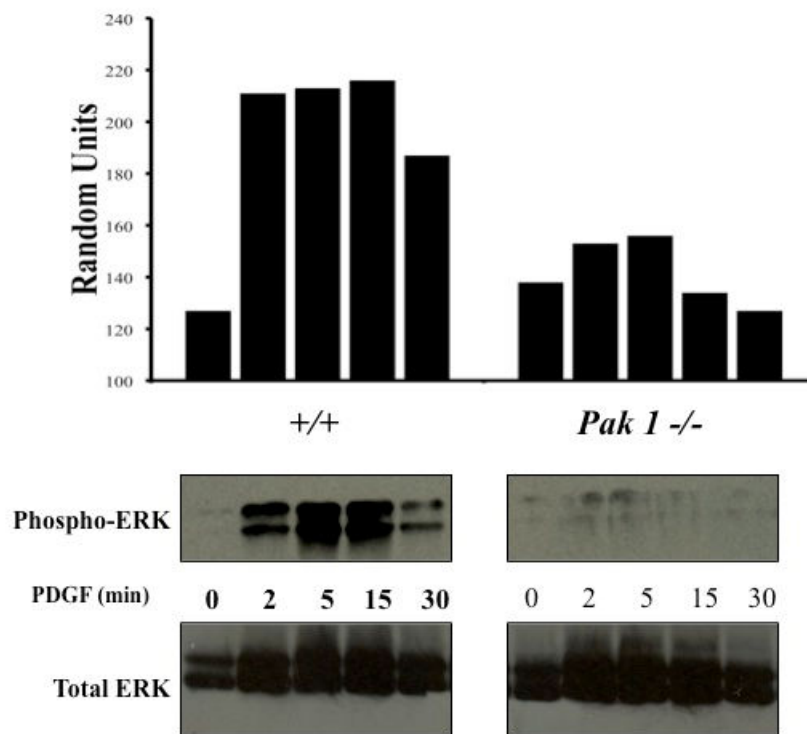
Work by Rhee and Grinnell demonstrated that human fibroblasts treated with siRNA to Pak1 had disruptions in their ability to form cell ruffles and dendritic extensions of the cytoplasm in response to PDGF-BB<sup>186</sup>. Since fibroblast activity and collagen secretion is important to the pathogenesis of plexiform neurofibromas, we examined whether a role for *Pak1* existed in regulating various PDGF-BB dependent functions. First, we stimulated wild type and *Pak1*<sup>-/-</sup> fibroblasts with 50ng/mL of PDGF-BB for 36 hours and carried out [<sup>3</sup>H]thymidine incorporation assays to evaluate proliferation. Figure 31 shows that disruption of *Pak1* causes significant decreases in fibroblast proliferation. PDGF-BB activation of Erk is critical to its role in stimulating proliferation<sup>187</sup>, and we and others have shown that Pak1 is necessary for activation of Erk. Therefore, we stimulated fibroblasts with 50ng/mL of PDGF-BB and assayed for activated Erk1/2 by using phospho-specific antibodies after Western blotting. *Pak1*<sup>-/-</sup> fibroblasts consistently display decreased activation of Erk1/2 (Figure 32) suggesting a molecular mechanism for the findings of Figure 31.

Figure 31



**Figure 31- *Pak1*<sup>-/-</sup> fibroblasts have reduced proliferation following PDGF-BB stimulation.** Approximately  $2 \times 10^4$  fibroblasts were plated and starved for 24 hours before stimulation with 50ng/mL of PDGF-BB. After 24 hours of stimulation at 37°, [<sup>3</sup>H]thymidine was added for 6 hours and its incorporation was measured. Values represent the mean of 3 independent experiments performed with six replicates each and the error bars represent the standard error of the mean. \* indicates  $p < 0.05$  compared to WT control using Student's unpaired T test.

Figure 32



**Figure 32- Loss of *Pak1* reduces Erk activation following PDGF-BB stimulation in fibroblasts.** Fibroblasts were serum starved for 48 hours, stimulated with 50ng/mL of PDGF-BB, and cell lysates isolated at time points indicated following stimulation. 100µg of protein were used for each time point. Levels of active Erk1/2 were determined by immunoblotting using phospho-specific antibodies. Levels of total Erk1/2 are shown as loading controls. Western blot of the results is shown and is a representative of three independent experiments.

### Loss of *Pak1* does not affect TGF- $\beta$ induced fibroblast proliferation

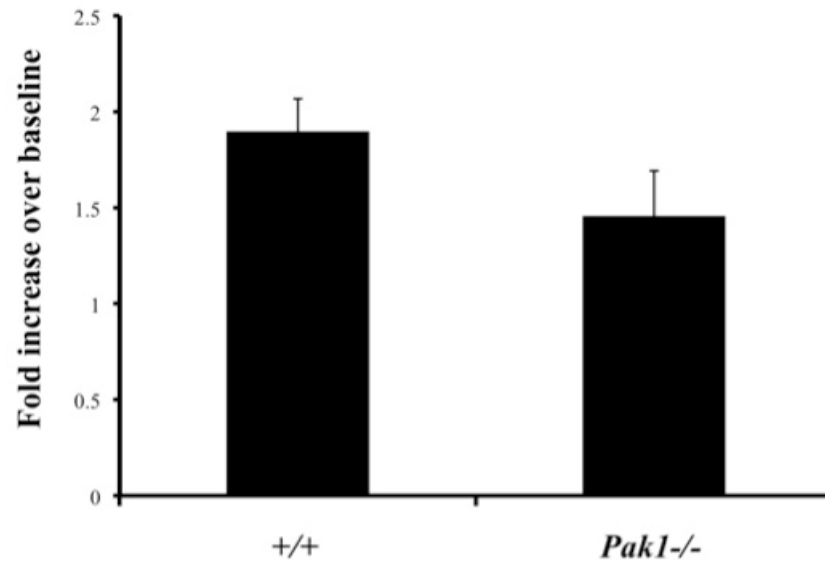
Similar to PDGF-BB, TGF- $\beta$  is a growth factor that stimulates multiple responses from fibroblasts. TGF- $\beta$  is a potent modulator of fibroblast proliferation and is known to be released at high concentrations by mast cells in the neurofibroma microenvironment<sup>71</sup>. Therefore, we examined whether *Pak1* deficient fibroblasts had reduced proliferation after TGF- $\beta$  stimulation. Unlike stimulation with PDGF-BB, *Pak1*<sup>-/-</sup> fibroblasts had no statistically significant changes in [<sup>3</sup>H]thymidine incorporation after 36 hours of incubation with 2ng/mL TGF- $\beta$  (Figure 33). This was accompanied by immunoblots detailing no change in activated Erk levels after TGF- $\beta$  stimulation (Figure 34). Together, these results indicate that Pak1 is important for MAPK activation and proliferation of fibroblast after stimulation with PDGF-BB, but not TGF- $\beta$ .

### *Pak1* deficient fibroblasts have reduced migration following PDGF-BB stimulation

Early work on Pak1 in fibroblast cell lines indicated that Pak1 regulated actin organization and content following PDGF-BB stimulation<sup>124</sup>. More recent work has implied a role for *Pak1* in regulating fibroblast migration in response to PDGF-BB<sup>186</sup>. Based on these reports, we used primary *Pak1*<sup>-/-</sup> fibroblasts to investigate how loss of Pak1 could affect PDGF-BB ability to induce migration and signal to the cytoskeleton. We used a wound-healing assay as an assessment of fibroblast migration following PDGF-BB treatment. These experiments revealed a 2.5 fold increase in the migration of wild type fibroblasts as compared to *Pak1*<sup>-/-</sup> cells (Figure 35). Representative

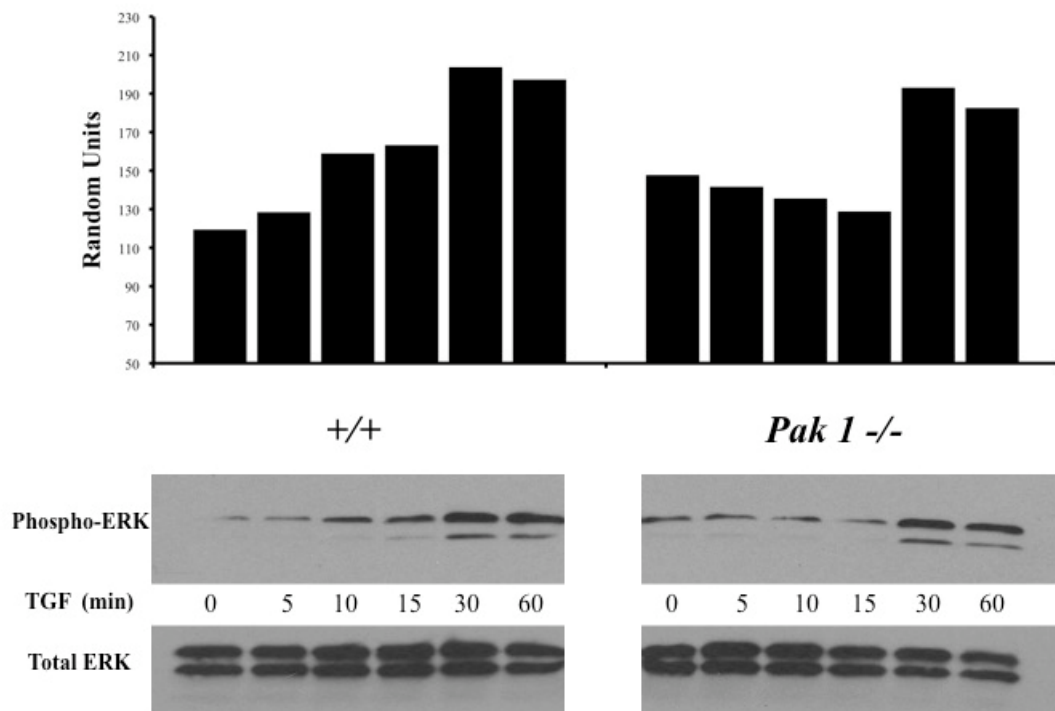


Figure 33



**Figure 33- Loss of *Pak1* does not significantly affect fibroblast proliferation following TGF- $\beta$  stimulation.** Approximately  $2 \times 10^4$  fibroblasts were plated and starved for 24 hours before stimulation with 2ng/mL of TGF- $\beta$ . After 24 hours of stimulation at 37 $^\circ$ , [ $^3\text{H}$ ]thymidine was added for 6 hours and its incorporation was measured. Values represent the mean of 3 independent experiments performed with six replicates each and the error bars represent the standard error of the mean. No significant difference between the means of the two genotypes was found using Student's unpaired T test.

**Figure 34**



**Figure 34- *Pak1*<sup>-/-</sup> fibroblasts have normal Erk activation after stimulation with TGF- $\beta$ .** Fibroblasts were serum starved for 48 hours, stimulated with 2ng/mL of TGF- $\beta$ , and cell lysates isolated at time points indicated following stimulation. 100 $\mu$ g of protein were used for each time point. Levels of active Erk1/2 were determined by immunoblotting using phospho-specific antibodies. Levels of total Erk1/2 are shown as loading controls. Western blot of the results is shown and is a representative of three independent experiments.

photomicrographs of crystal violet stained wild type or *Pak1*<sup>-/-</sup> fibroblasts that migrated into the wound in response to 18 hours of 50ng/mL PDGF-BB stimulation is shown in Figure 35.

Disruptions of PDGF-BB mediated activation of the actin cytoskeleton and associated signaling networks are found in *Pak1*<sup>-/-</sup> fibroblasts

Since we found *Pak1*<sup>-/-</sup> fibroblasts to have reduced migration, and numerous reports describe Pak1 altering migration via the actin cytoskeleton<sup>101</sup>, we investigated the activation of important downstream targets of Pak1 that regulate actin, including filamin A and cofilin. First activation of filamin A was assessed. Phosphorylation of filamin A at Ser2152 increases its ability to bind actin and reorganize the cytoskeleton<sup>126</sup>. We show that *Pak1*<sup>-/-</sup> fibroblasts have decreased Ser2152 phosphorylation of filamin A after PDGF-BB stimulation (Figure 36). Additionally, we examined the phosphorylation status of cofilin, an actin binding protein that, in its dephosphorylated state, leads to depolymerization of actin filaments. Figure 37 shows that fibroblasts that lack *Pak1* have decreased phospho-cofilin, indicating an increase in the actin disrupting ability of cofilin. Taken together, these results implied that the actin cytoskeleton was likely to be deregulated in *Pak1*<sup>-/-</sup> fibroblasts. To visualize the actin networks in PDGF-BB stimulated fibroblasts, cells grown on coverslips were used in wound healing assays and after 5 hours were stained with phalloidin to stain filamentous actin. Representative micrographs taken from confocal analysis of these cells indicates that wild type fibroblasts stimulated with PDGF-BB have increased invasion of the wound compared

Figure 35

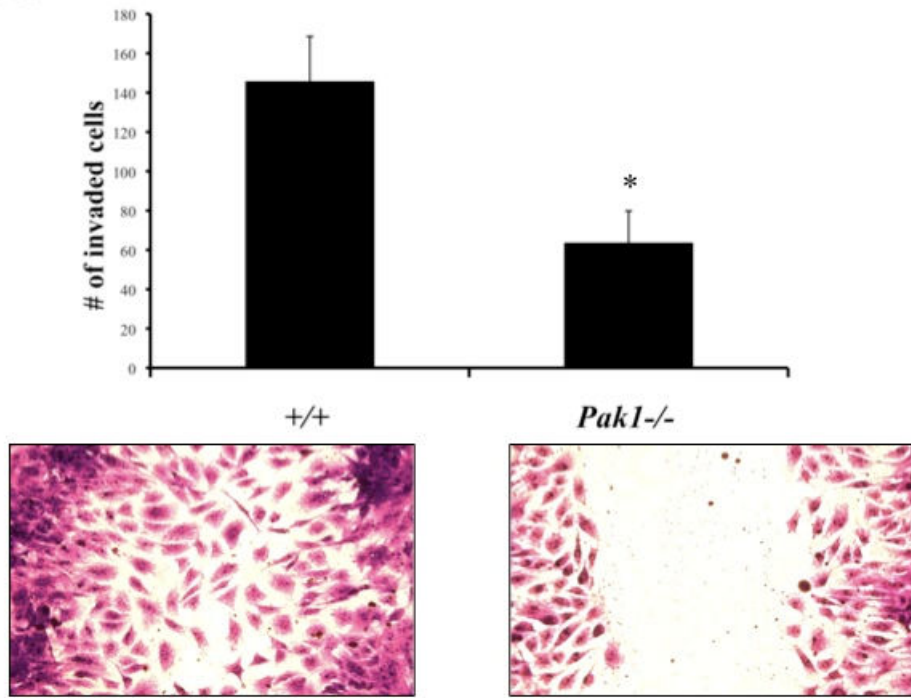


**Figure 35- *Pak1*<sup>-/-</sup> fibroblasts have diminished migration in response to PDGF-BB.**

Quiescent, mitotically inactivated monolayers of fibroblasts were scratched with a pipette tip prior to stimulation with 50ng/mL of PDGF-BB. After 12 hours incubation, the cells were fixed and stained with crystal violet solution and the number of cells that invaded the wound were counted. Photos were taken with a light microscope under 100x magnification. Values represent the mean of 3 independent experiments performed in triplicate and the error bars represent the standard error of the mean. \* indicates  $p < 0.05$  compared to WT control using Student's unpaired T test.

Figure 36

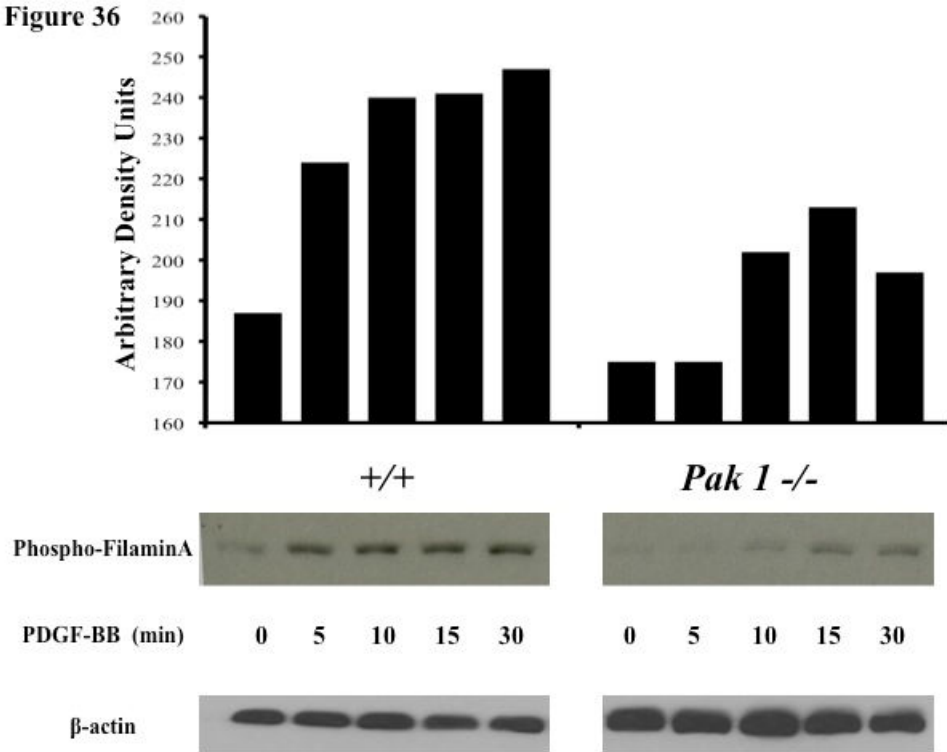
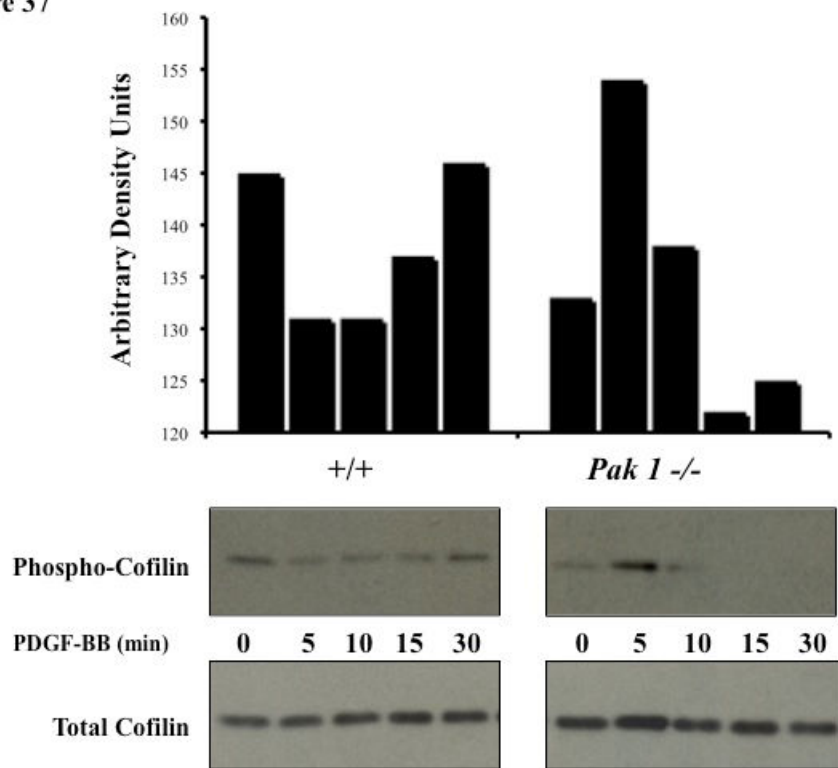




**Figure 36- *Pak1* loss reduces activation of Filamin-A after PDGF-BB stimulation.**

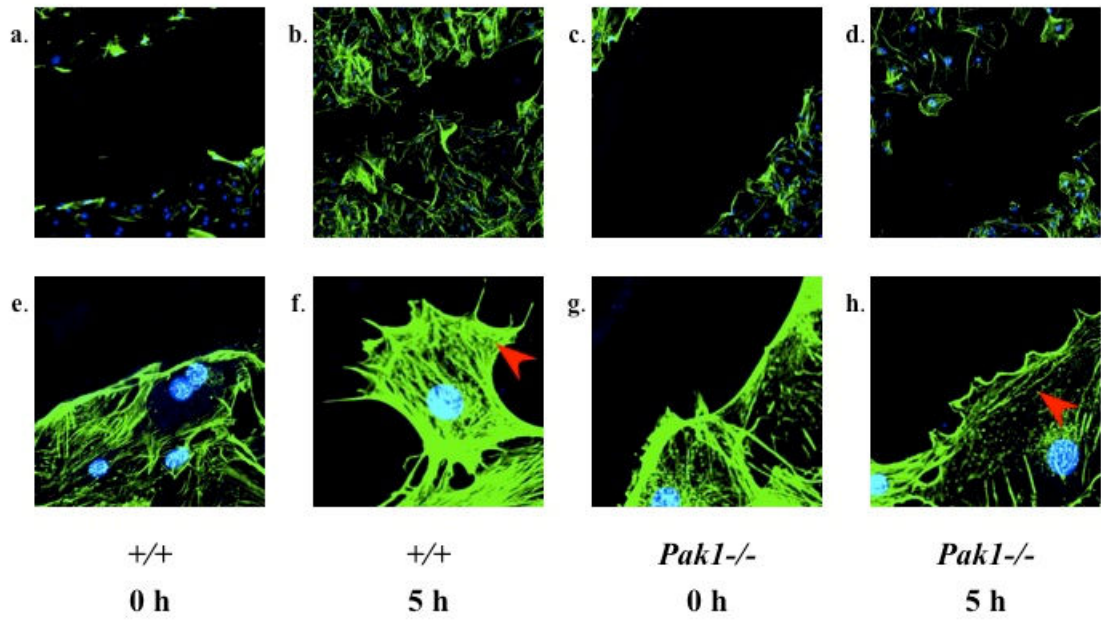
Fibroblasts were serum starved for 48 hours, stimulated with 50ng/mL of PDGF-BB, and cell lysates isolated at time points indicated following stimulation. 100µg of protein were used for each time point. Levels of active Filamin-A were determined by immunoblotting using phospho-specific antibodies. Levels of total  $\beta$ -actin are shown as loading controls. Western blot of the results is shown and is a representative of three independent experiments.

Figure 37



**Figure 37- *Pak1* loss results in reduced inactivation of Cofilin following stimulation by PDGF-BB.** Fibroblasts were serum starved for 48 hours, stimulated with 50ng/mL of PDGF-BB, and cell lysates isolated at time points indicated following stimulation. 100µg of protein were used for each time point. Levels of inactive cofilin were determined by immunoblotting using phospho-specific antibodies. Levels of total cofilin are shown as loading controls. Western blot of the results is shown and is a representative of three independent experiments.

Figure 38



**Figure 38- *Pak1*<sup>-/-</sup> fibroblasts have disruptions in the organization of the F-actin cytoskeleton after PDGF-BB stimulation.** Quiescent, mitotically inactivated monolayers of fibroblasts were scratched with a pipette tip prior to stimulation with 50ng/mL of PDGF-BB. After 5 hours incubation, the cells were fixed and stained with phalloidin and DAPI to visualize F-actin and nuclei, respectively. Low power micrographs in **A-D)** were taken with the Zeiss UV LSM-510 confocal microscope system. Green=phalloidin stain, blue=DAPI nuclear stain. Original magnification x100. **E-F)** are high power views of similar fields of cells. Original magnification x400.

to *Pak1*<sup>-/-</sup> cells (Figure 38b and 38d). Furthermore, wild type fibroblasts have qualitatively more F-actin in the cytoplasm of cells invading the wound than the *Pak*<sup>-/-</sup> cells, as evidenced by the high power micrographs shown in Figure 38 f and h, respectively. As a group, the results of these experiments indicate that loss of *Pak1* results in decreased phosphorylation of filamin A and cofilin, leading to disruptions of the actin cytoskeleton that impair normal migration in response to PDGF-BB.

#### Loss of *Pak1* decreases TGF- $\beta$ dependent fibroblast migration

TGF- $\beta$  mediated wound invasion is an important step in many pathological processes, including tumor formation<sup>69</sup>. To determine if Pak1 signaling downstream of TGF- $\beta$  was involved in the regulation of fibroblast migration, wound healing assays using 2ng/mL of TGF- $\beta$  for stimulation were performed. After 24 hours of stimulation, the *Pak1*<sup>-/-</sup> fibroblasts displayed a significant reduction in wound invasion compared to wild type (Figure 39). Similar to the results found with PDGF-BB, *Pak1*<sup>-/-</sup> fibroblasts have impaired migration ability.

#### TGF- $\beta$ stimulated fibroblasts have decreased activation of filamin A and disrupted actin cytoskeletal networks

Since *Pak1*<sup>-/-</sup> fibroblasts had comparable deficits in migration in response to both PDGF-BB and TGF- $\beta$  stimulation, we were interested if TGF- $\beta$  induced similar disruption of actin signaling networks found in PDGF-BB stimulated *Pak1* null cells

(Figures 36-38). Analogous to PDGF-BB stimulated fibroblasts, loss of *Pak1* results in impaired phosphorylation of filamin A at Ser 2152 (Figure 40). Interestingly, in response to TGF- $\beta$ , cofilin phosphorylation remained intact in *Pak1*<sup>-/-</sup> cells (Figure 41). However, confocal analysis of phalloidin stained fibroblasts stimulated with 2ng/mL of TGF- $\beta$  for 5 hours showed decreased amounts of higher level actin bundle organization in wound invading *Pak1*<sup>-/-</sup> cells (Figure 42 h, red arrow) compared to wild type cells. These experiments point toward a potential Pak1 mediated signaling pathway where Filamin A, but not cofilin, is an important regulator of TGF- $\beta$  mediated actin organization and fibroblast migration.

*Pak1*<sup>-/-</sup> fibroblasts have reduced collagen synthesis *in vitro* in response to TGF- $\beta$

Interstitial collagen secretion is one of the primary functions of fibroblasts and is associated with numerous disease processes, including plexiform neurofibroma formation<sup>71,188</sup>. Since both PDGF-BB and TGF- $\beta$  are known profibrotic cytokines and are released in large amounts by mast cells at the site of plexiform neurofibroma formation, we investigated if loss of *Pak1*<sup>-/-</sup> would alter the ability of fibroblasts to secrete collagen following stimulation with either growth factor. Using the Sircol™ collagen assay system, we evaluated the supernatants from confluent cultures of fibroblasts stimulated for 48 hours with either 50ng/mL PDGF-BB or 2ng/mL TGF- $\beta$  for collagen production. Although PDGF-BB stimulated *Pak1*<sup>-/-</sup> fibroblasts had statistically similar amounts of collagen secretion as wild type cells; TGF- $\beta$  stimulation led to decreased collagen production in *Pak1* null cells (Figure 43). This experiment supports a

Figure 39

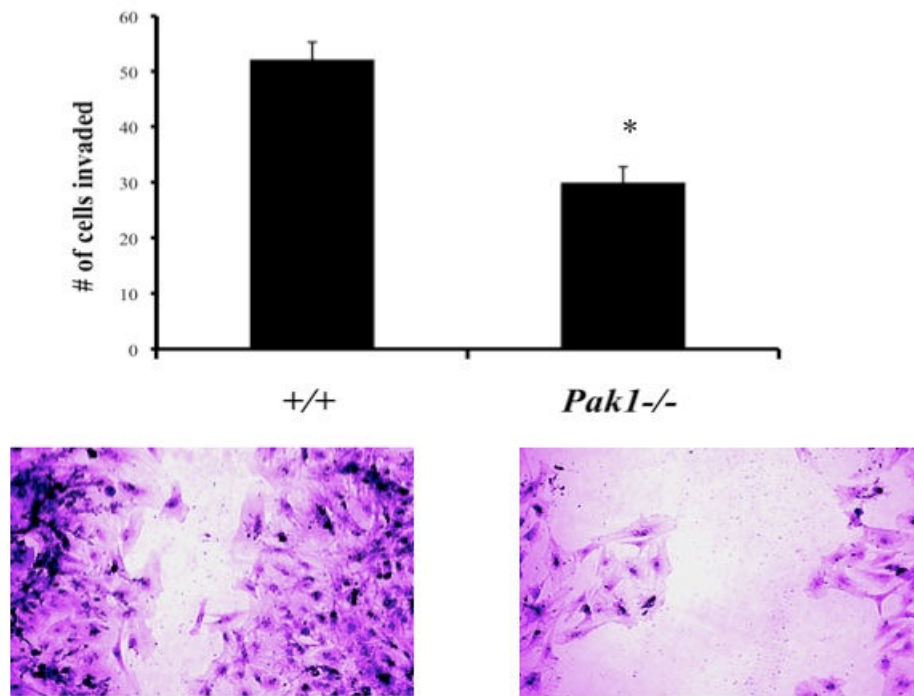
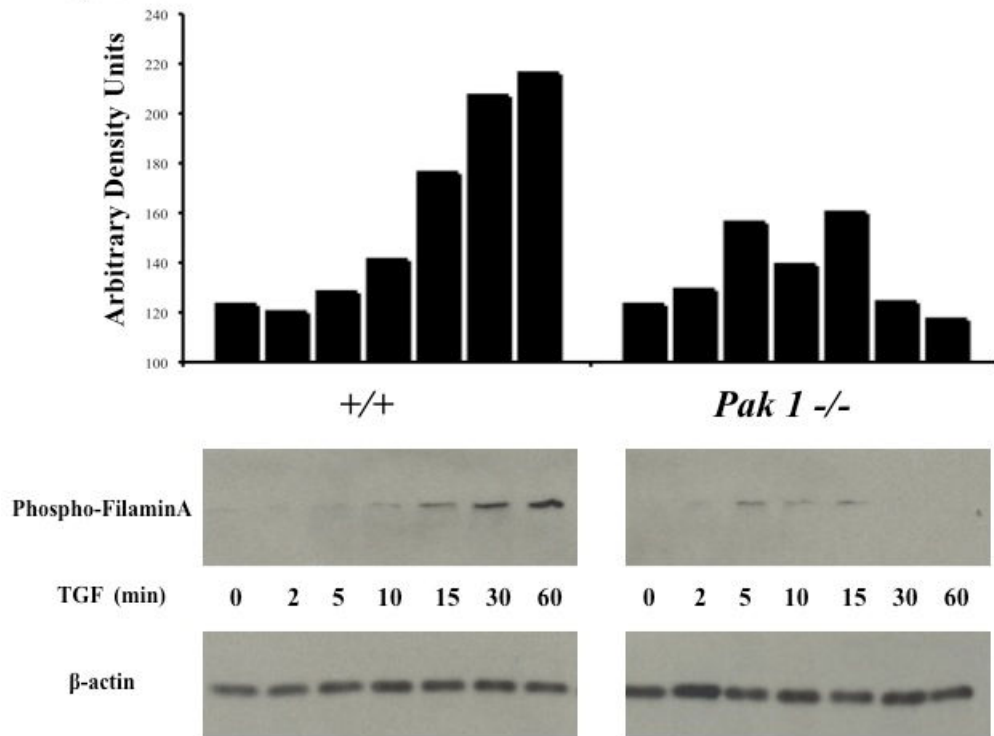




**Figure 39- *Pak1*<sup>-/-</sup> fibroblasts have diminished migration in response to TGF- $\beta$ .**

Quiescent, mitotically inactivated monolayers of fibroblasts were scratched with a pipette tip prior to stimulation with 2ng/mL of TGF- $\beta$ . After 24 hours incubation, the cells were fixed and stained with crystal violet solution and the number of cells that invaded the wound were counted. Photos were taken with a light microscope under 100x magnification. Values represent the mean of 3 independent experiments performed in triplicate and the error bars represent the standard error of the mean. \* indicates  $p < 0.05$  compared to WT control using Student's unpaired T test.

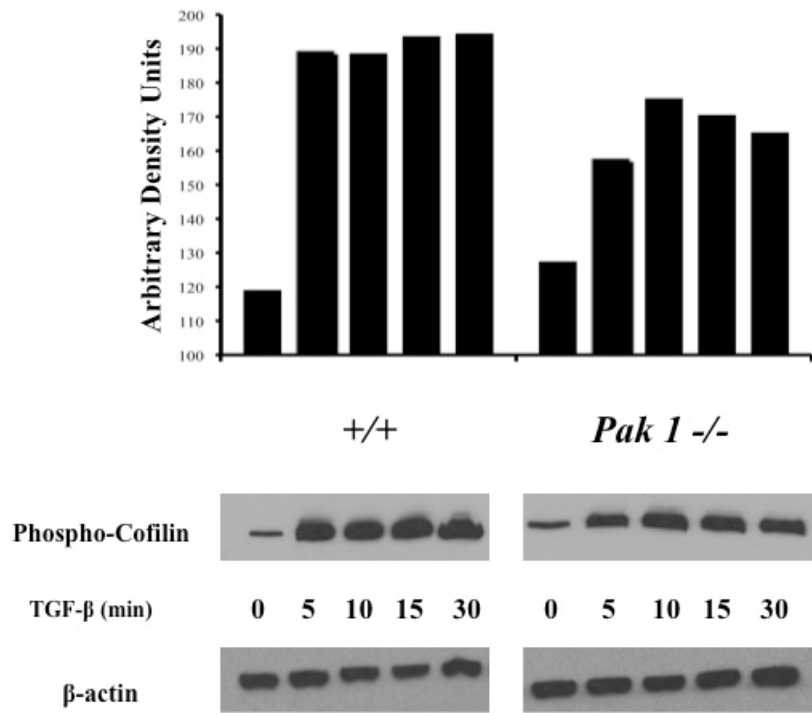
**Figure 40**



**Figure 40- *Pak1* loss reduces activation of Filamin-A after TGF- $\beta$  stimulation.**

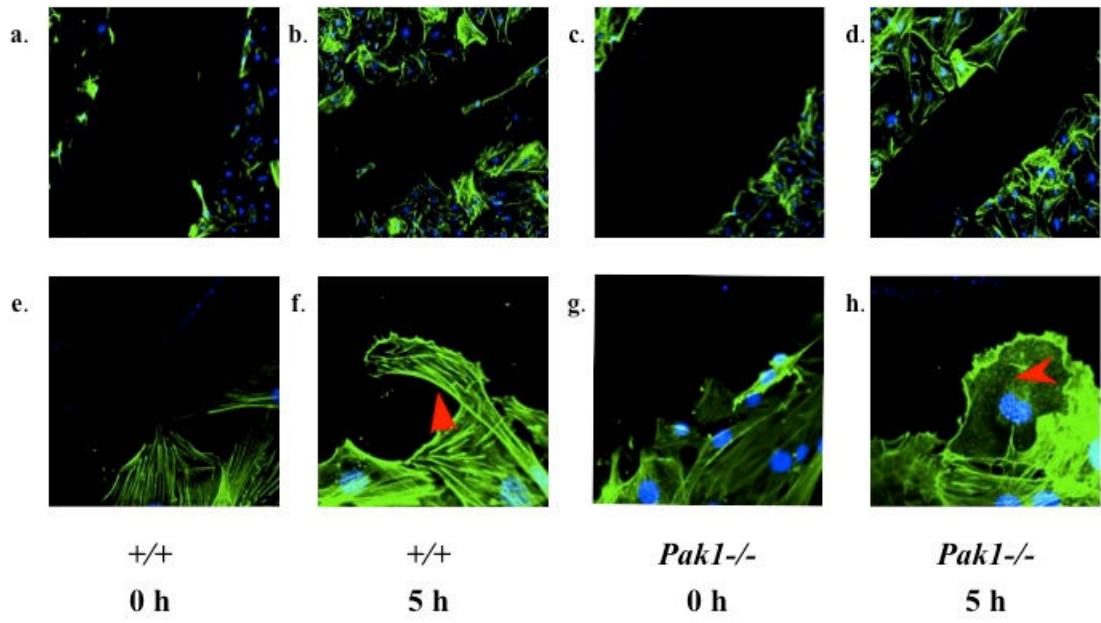
Fibroblasts were serum starved for 48 hours, stimulated with 2ng/mL of TGF- $\beta$ , and cell lysates isolated at time points indicated following stimulation. 100 $\mu$ g of protein were used for each time point. Levels of active Filamin-A were determined by immunoblotting using phospho-specific antibodies. Levels of total  $\beta$ -actin are shown as loading controls. Western blot of the results is shown and is a representative of three independent experiments.

Figure 41



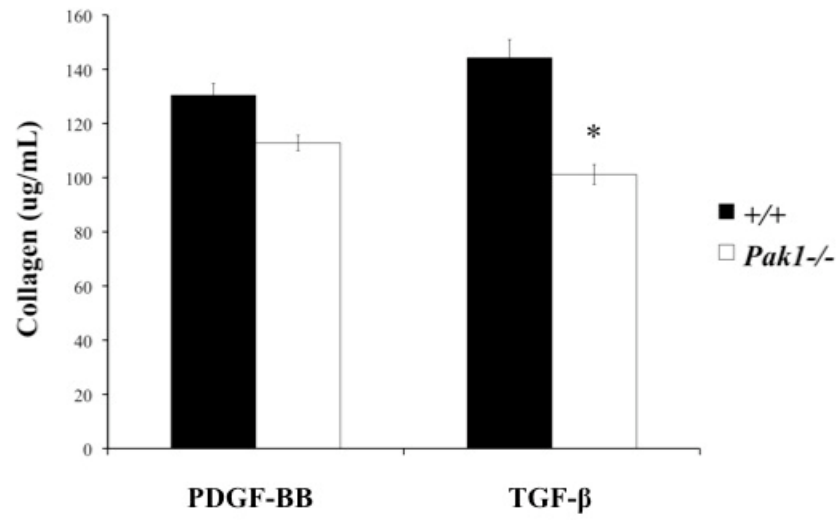
**Figure 41- *Pak1* loss does not significantly affect phosphorylation of Cofilin following stimulation by TGF- $\beta$ .** Fibroblasts were serum starved for 48 hours, stimulated with 50ng/mL of TGF- $\beta$ , and cell lysates isolated at time points indicated following stimulation. 100 $\mu$ g of protein were used for each time point. Levels of inactive cofilin were determined by immunoblotting using phospho-specific antibodies. Levels of  $\beta$ -actin are shown as loading controls. Western blot of the results is shown and is a representative of three independent experiments.

Figure 42



**Figure 42- *Pak1*<sup>-/-</sup> fibroblasts have disruptions in the organization of the F-actin cytoskeleton after TGF- $\beta$  stimulation.** Quiescent, mitotically inactivated monolayers of fibroblasts were scratched with a pipette tip prior to stimulation with 2ng/mL of TGF- $\beta$ . After 5 hours incubation, the cells were fixed and stained with phalloidin and DAPI to visualize F-actin and nuclei, respectively. Low power micrographs in **A-D)** were taken with the Zeiss UV LSM-510 confocal microscope system. Green=phalloidin stain, blue=DAPI nuclear stain. Original magnification x100. **E-F)** are high power views of similar fields of cells. Original magnification x400.

Figure 43





**Figure 43- Loss of *Pak1* reduces collagen production after TGF- $\beta$  stimulation.**

Confluent monolayers of fibroblasts were stimulated with 50ng/mL of PDGF-BB or 2ng/mL of TGF- $\beta$  for 48 hours at 37°. Collagen levels in the supernatant were measured using the Sircol™ dye reagent and OD levels assessed using a microplate reader. Values represent the mean of 3 independent experiments performed in triplicate and the error bars represent the standard error of the mean. \* indicates  $p < 0.05$  compared to WT using Student's unpaired T test.

role for *Pak1* in regulating collagen production from fibroblasts in response to TGF- $\beta$ .

#### Reduced survival of *Pak1* null fibroblasts in response to TGF- $\beta$ and PDGF-BB

Due to the fact that Pak1 is associated with anti-apoptotic actions in other cell types<sup>143,184,185</sup>, we were interested to see if genetic disruption of *Pak1* in fibroblasts would affect their survival in response to PDGF-BB or TGF- $\beta$ . Confluent fibroblasts were serum starved for 24 hours before being treated with 10% fetal calf serum, 50ng/mL PDGF-BB, or 2ng/mL TGF- $\beta$ . Cells were fixed and subjected to a TUNEL assay and analyzed for survival using fluorescence cytometry. Cells that were left in 10% fetal calf serum showed no difference in apoptosis (as determined by TUNEL positivity) between the genotypes (Figure 44a). However, *Pak1*<sup>-/-</sup> cells have small but significant increases in apoptosis compared to wild type when exposed to both PDGF-BB and TGF- $\beta$  (Figure 44 c and d). This finding is in contrast to the results of Figure 16, which show that mast cell survival in response to SCF is not affected by loss of *Pak1*. Taken together, these studies demonstrate that *Pak1* anti-apoptotic effects are cell type and stimulus dependent.

#### Loss of *Pak1* inhibits fibroblast recruitment *in vivo*

In order to determine whether *Pak1* regulates the migration of fibroblasts in response to growth factors *in vivo*, we performed ECM matrix invasion assays with wild type and *Pak1*<sup>-/-</sup> mice. Our lab has previously established that implantation of Cultrex™

**Figure 44**

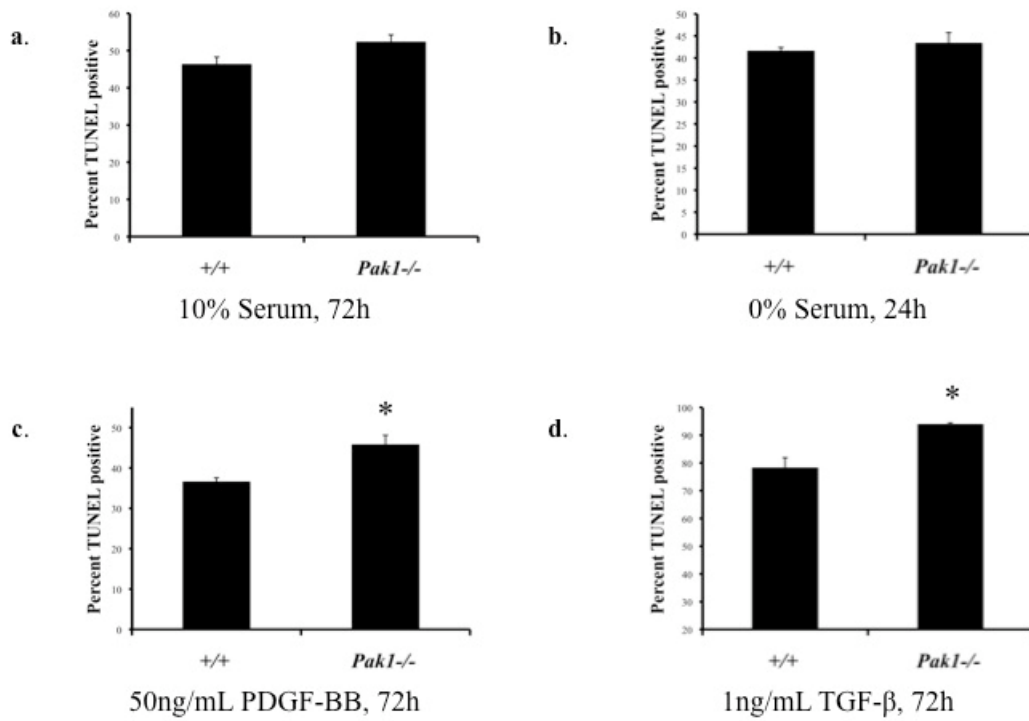


**Figure 44- Pak1<sup>-/-</sup> fibroblasts have decreased survival after PDGF-BB and TGF- $\beta$  exposure.** Confluent monolayers of fibroblasts were starved for 24 hour prior to stimulation with 50ng/mL of PDGF-BB or 2ng/mL of TGF- $\beta$  in media lacking serum. After 72 hours, survival was assessed by TUNEL assay according to the manufacturers instructions. Values represent the mean of 6 independent experiments performed in triplicate and the error bars represent the standard error of the mean. \* indicates  $p < 0.05$  compared to WT using Student's unpaired T test.

basement membrane extract with PDGF-BB or TGF- $\beta$  into the groin of mice induces fibroblast invasion from the surrounding tissue<sup>71</sup>. Seven days after Cultrex™ implantation, the plugs were removed, sectioned, and stained with hematoxylin and eosin (H&E) to visualize the extent of fibroblast migration. Figure 45a displays the results taken from mice implanted with PDGF-BB or vehicle, showing a significant reduction in fibroblast recruitment in *Pak1*<sup>-/-</sup> mice. Representative sections that display the invading fibroblasts are also shown (Figure 45b-d). In parallel experiments using plugs containing TGF- $\beta$ , we found similar results, with a significant decrease in invading fibroblasts from *Pak1*<sup>-/-</sup> mice (Figure 46a). The amount of fibroblast infiltration can be observed in the representative plug sections shown in Figure 46b-d.

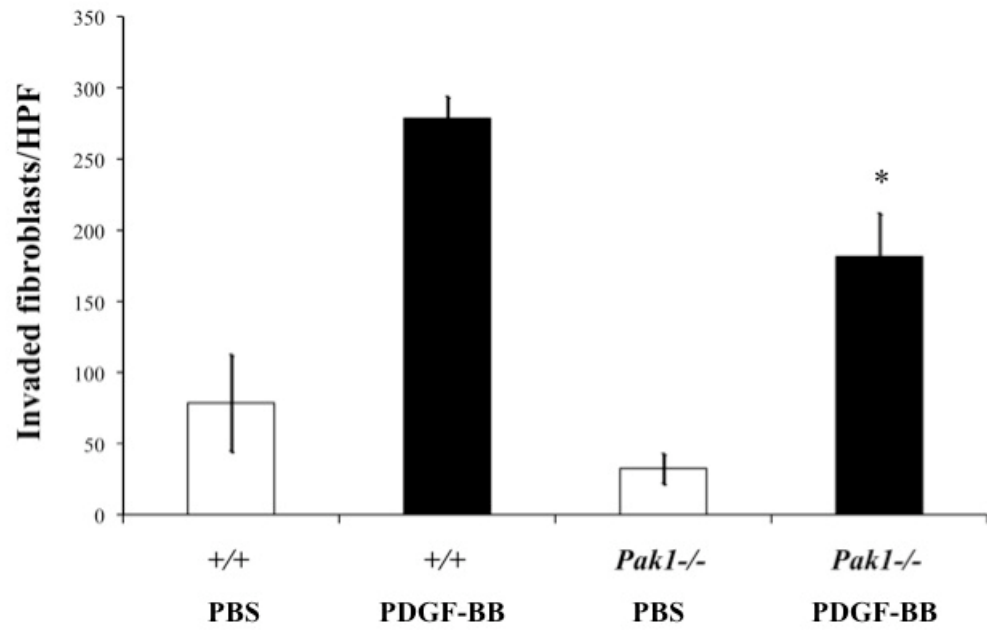
#### Genetic disruption of *Pak1* reduces the severity of bleomycin induced lung fibrosis

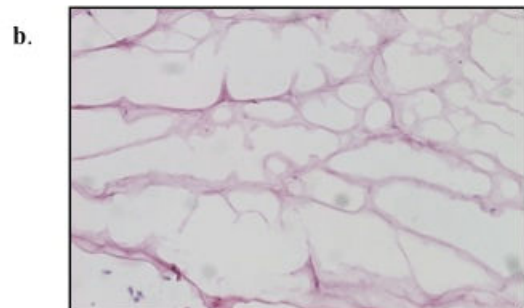
Harrison and Lezo have described an *in vivo* experimental murine model to stimulate pathologic fibrosis in lungs using bleomycin sulfate delivered from subcutaneously implanted micro-osmotic pumps<sup>172</sup>. Bleomycin induces lung fibrosis by activating both the TGF- $\beta$ <sup>189-191</sup> as well as PDGF-BB<sup>192-194</sup> pathways to stimulate fibroblast proliferation and collagen deposition. Inhibition of the PDGF-BB and TGF- $\beta$  pathways via imatinib prevents bleomycin induced lung fibrosis in mice<sup>193</sup>.

Based on these previous reports and on our *in vitro* findings implicating Pak1 as an important downstream mediator of PDGF-BB and TGF- $\beta$  signals in fibroblasts, we used bleomycin to induce lung fibrosis in wild type and *Pak1*<sup>-/-</sup> mice. After 28 days of bleomycin or PBS exposure, lungs were harvested and either fixed for histological

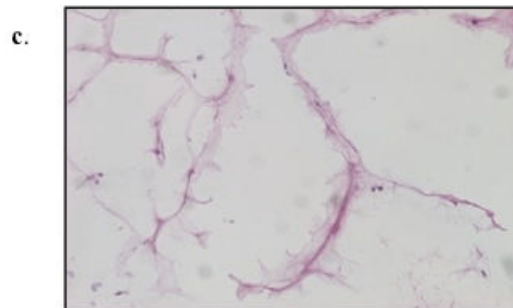
sections or used for collagen content assays. Figure 47a-d displays representative hematoxylin and eosin (H&E) stained slides taken from each genotype, revealing that

Figure 45a

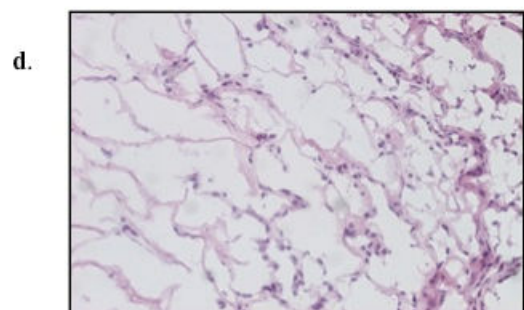




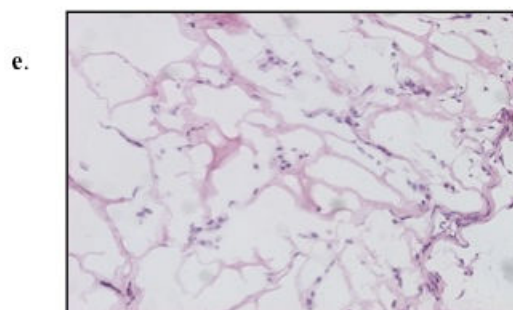
+/+  
PBS



*Pak1*<sup>-/-</sup>  
PBS



+/+  
PDGF-BB

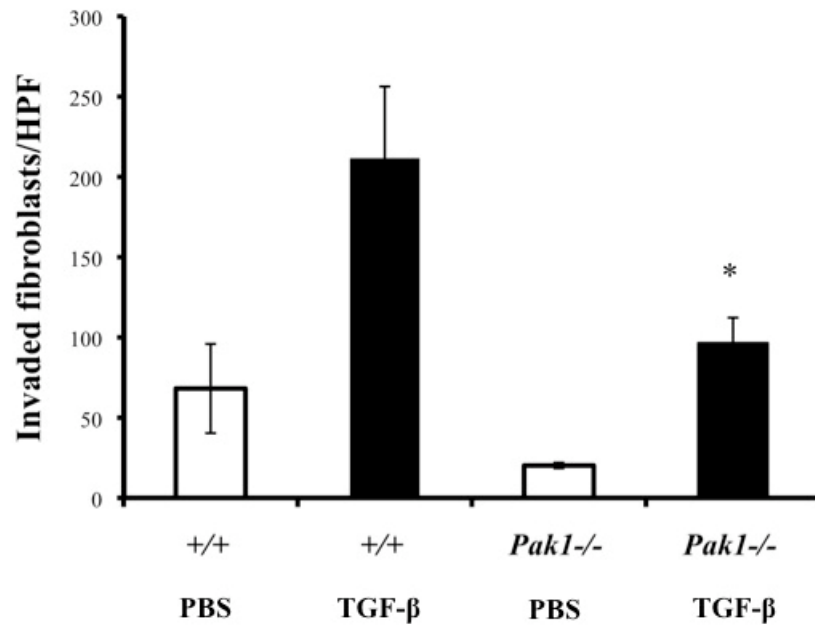


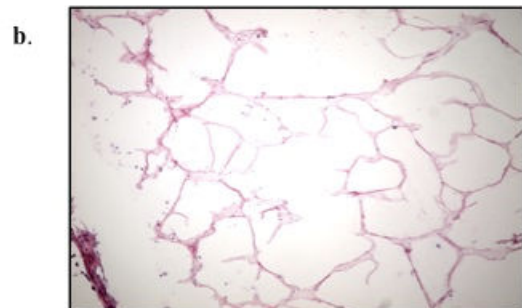
*Pak1*<sup>-/-</sup>  
PDGF-BB



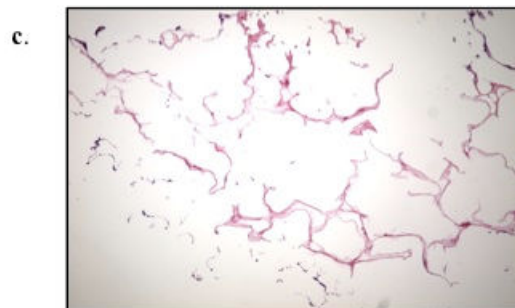
**Figure 45- *Pak1*<sup>-/-</sup> mice have decreased PDGF-BB mediated fibroblast invasion into Cultrex™ plugs.** A) Quantitative scoring of fibroblast invasion into Cultrex™ plugs containing PBS or 200ng/mL of PDGF-BB. Values represent the mean of five individual sections from 4 mice per genotype and error bars represent the standard error of the mean. \* indicates p<0.05 compared to WT using Student's unpaired T test. Also shown (B-E) are representative hematoxylin and eosin (H&E) stained sections from Cultrex plugs containing PDGF-BB or PBS.

Figure 46a

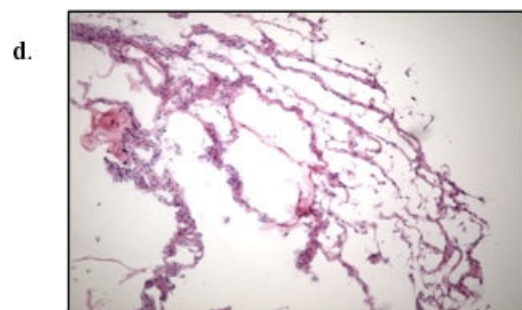




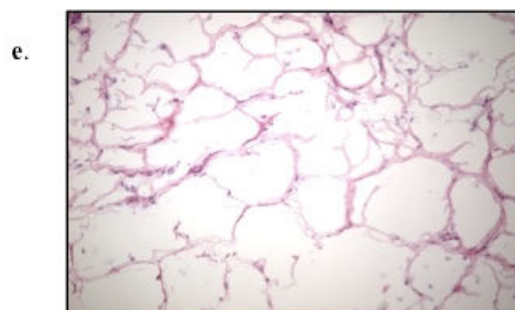
**+/+**  
**PBS**



***Pak1*<sup>-/-</sup>**  
**PBS**



**+/+**  
**TGF- $\beta$**



***Pak1*<sup>-/-</sup>**  
**TGF- $\beta$**

**Figure 46- *Pak1*<sup>-/-</sup> mice have decreased TGF- $\beta$  mediated fibroblast invasion into Cultrex™ plugs.** A) Quantitative scoring of fibroblast invasion into Cultrex™ plugs containing PBS or 10ng/mL of TGF- $\beta$ . Values represent the mean of five individual sections from 4 mice per genotype and error bars represent the standard error of the mean. \* indicates  $p < 0.05$  compared to WT using Student's unpaired T test. Also shown (B-E) are representative hematoxylin and eosin (H&E) stained sections from Cultrex plugs containing TGF- $\beta$ .

exposure to bleomycin induces dramatic fibrosis compared to PBS treated animals.

Using a quantitative measurement of lung fibrosis developed by Ashcroft, we determined that *Pak1*<sup>-/-</sup> mice had a modest (~20%), but significant (p<.0001) reduction in fibrosis severity compared to wild type animals (Figure 47e). Correspondingly, using the Sircol™ assay system, we found that lungs from *Pak1*<sup>-/-</sup> mice had a significant decrease in collagen content (Figure 47f), similar in degree to the change in fibrosis severity.

Collectively, the results of Figure 47 indicate a role for Pak1 in the pathophysiology of bleomycin mediated lung fibrosis disease model.

Figure 47

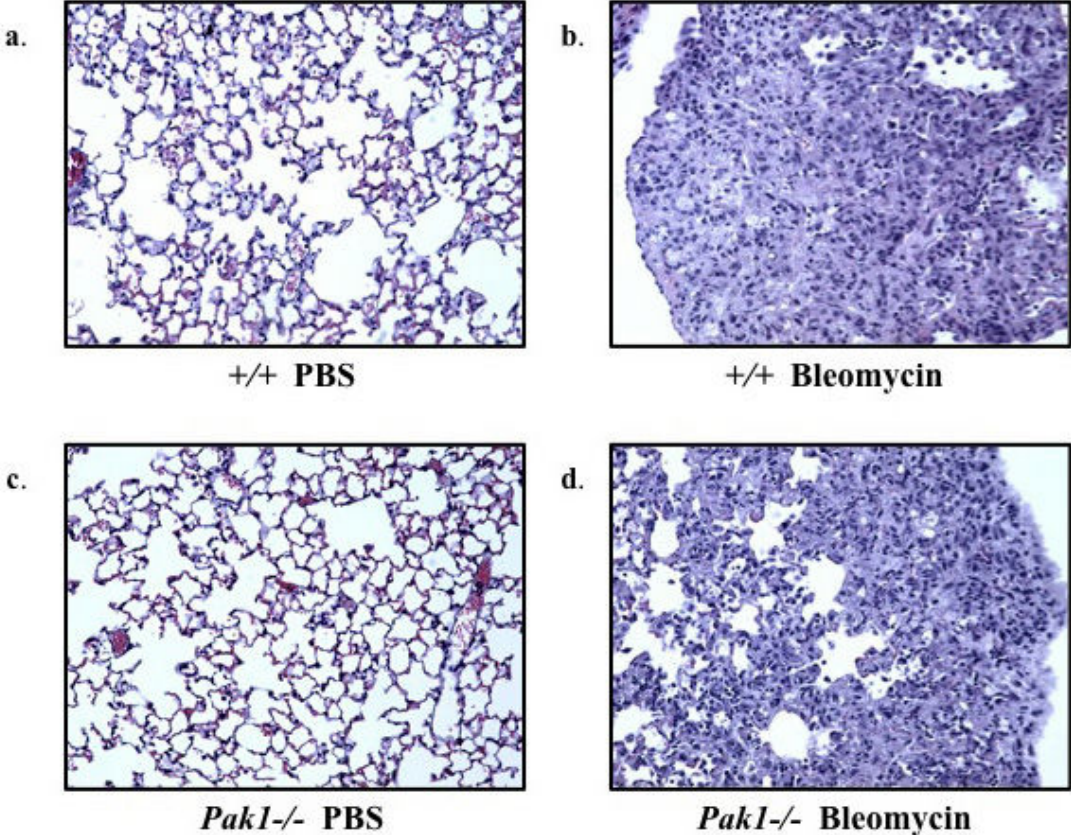


Figure 47e

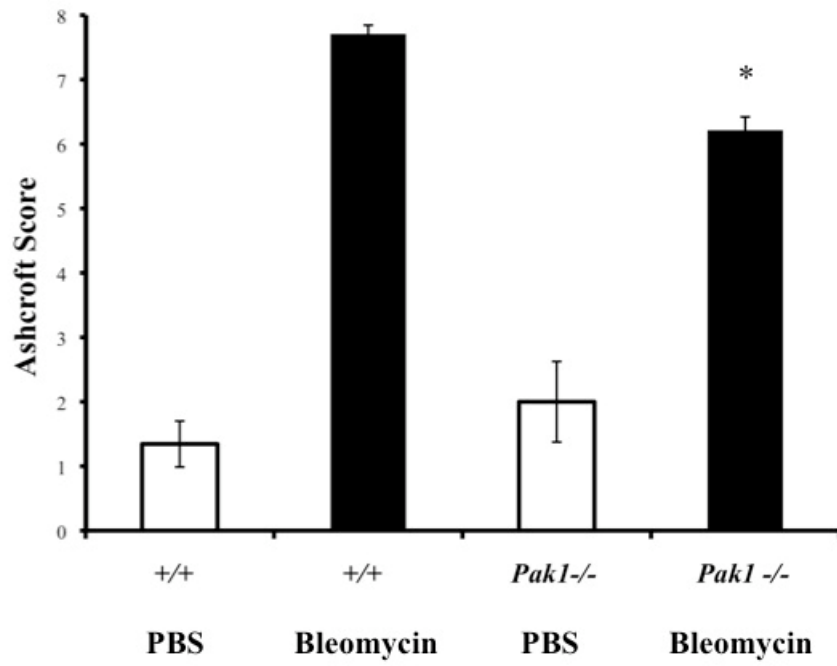
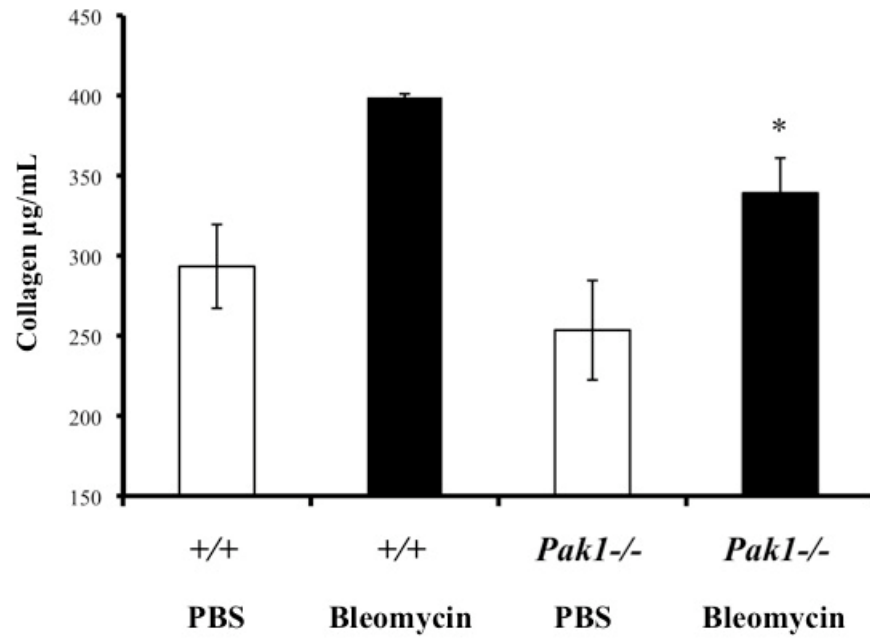


Figure 47f





**Figure 47- Loss of *Pak1* reduces bleomycin induced lung fibrosis.**

**A-D)** Representative hematoxylin and eosin (H&E) stained sections from lungs treated with either PBS or 125mg/kg/day of bleomycin sulfate for 28 days. **E)** Extent of lung fibrosis as measured by the Ashcroft scoring system. Fields from 8 mice per genotype that received either PBS or bleomycin sulfate were scored in a blinded fashion by 4 independent researchers. Values represent the mean score of 8 animals per condition and error bars represent the standard error of the mean. \* indicates  $p < 0.05$  compared to WT using Student's unpaired T test. **F)** After 28 days of drug exposure, lungs were removed, minced and collagen extracted with pepsin and acetic acid. The amount of collagen present in each lung was assessed by Sircol™ dye assay. Values represent the mean amount of collagen from lungs of 4 animals per condition performed in triplicate and error bars represent the standard error of the mean. \* indicates  $p < 0.05$  compared to WT using Student's unpaired T test.

## DISCUSSION

In the history of neurofibromatosis type I, identification of the *NF1* gene and the GTPase activating ability of its gene product neurofibromin<sup>24</sup> provided the keystone for future research into the molecular alterations responsible for the pathophysiology of this disease. Based on the autosomal dominant mode of disease inheritance and the genetic background of tissue samples taken from patient tumors<sup>195</sup>, neurofibromin has been commonly classified as a tumor suppressor protein. However, work from our lab<sup>59,62,75</sup> and others<sup>30,196,197</sup> has demonstrated that in mouse models, single copy loss of *Nf1* leads to tumor promoting gains-in-function, in opposition to Knudson's "two-hit" hypothesis<sup>198</sup>. Clinical observations from NF1 patients such as patient-to-patient variability in tumor number and the overall low risk of malignant transformation in neurofibromas support these findings of gene dosage effects. Therefore, it is critical for researchers in the neurofibromatosis field to uncover the molecular nature of *Nf1* haploinsufficient phenotypes in order to completely understand the disease's progression.

Thus, a primary objective of this thesis was to examine whether a candidate protein, Pak1, functioned in regulating intracellular signal transduction in NF1 relevant pathways and if so, whether Pak1 played a role in neurofibroma tumorigenesis. To this end, a genetically engineered *Pak1* knockout mouse was employed in various intercrosses to assess molecular, cellular, and disease phenotypes. Loss of *Pak1* corrected multiple *Nf1* haploinsufficient gain-in-function phenotypes in mast cells and Pak1 was demonstrated to be an important regulator of fibroblast function in response to two significant growth factors. However, using genetic intercrosses as well as

hematopoietic cell transplantation in an *in vivo* animal model that closely recapitulates human disease, we established that *Pak1* loss is insufficient for prevention of neurofibroma formation.

### Role of *Pak1* in regulating c-kit mediated *Nf1*<sup>+/-</sup> mast cell function

Mast cells carry out their functions by migrating toward signals emanating from local microenvironments, followed by local proliferation, and subsequently releasing inflammatory mediators (including proteases). The NF1 disease model has well known associations between Ras related gains-in-function in mast cells and the pathologic complications this disorder<sup>59,63,199,200</sup>. These cellular phenotypes and increased Ras activity have also been observed in NF1 patient samples (S. Chen, F.C. Yang, D.W. Clapp, unpublished results).

Bone marrow mononuclear cells from *Pak1*<sup>-/-</sup> animals develop *in vitro* into mature mast cells normally, as measured by the expression of c-kit and FcεRI surface markers (Figure 6). Additionally, haploinsufficiency at *Nf1* also did not affect c-kit or FcεRI expression levels. Therefore the results shown in experiments utilizing mast cells were not the consequence of alterations in the number of ligand binding sites for SCF and instead due to changes in intracellular signaling.

Here we use pharmacologic, genetic, and biochemical approaches to demonstrate that the hyperproliferation of *Nf1*<sup>+/-</sup> mast cells in response to SCF is the result of Pak1 signaling to the MEK/Erk pathway. Although multiple studies link Pak1 to MAPK signaling in overexpression systems<sup>131-133,160,201,202</sup>, in this report we establish for the first

time in primary cells using a knockout model that *Pak1* loss leads to decreased activation of MEK and Erk. Importantly, subcutaneous insertion of microosmotic pumps continuously releasing SCF in *Nfl<sup>+/-</sup>;Pak1<sup>-/-</sup>* mice corrected the increased accumulation of mast cells in the dermis seen in *Nfl<sup>+/-</sup>* mice to wild type levels, correlating our *in vivo* results in a physiologically relevant system (Figure 17a) the mechanisms identified *in vitro* (Figure 7).

Furthermore, we also demonstrate that the increased release of preformed mediators associated with *Nfl* haploinsufficiency seen *in vitro* is corrected when *Pak1* is genetically disrupted. Interestingly, *Pak1<sup>-/-</sup>* mast cells do not have significant decreases in degranulation compared to wild type cells in response to SCF and IgE stimulation combined (Figure 14), but do have impaired degranulation in response to IgE stimulation alone (Figure 15). SCF stimulation could preferentially activate the Mek/Erk pathway, which we show to independent of Pak1 with regards to degranulation (Figure 15), to compensate for the decreased IgE dependent signals (J.D. Allen, D.W. Clapp, unpublished results) seen in *Pak1<sup>-/-</sup>* cells. Importantly, the amount of mast cell degranulation found in *Nfl<sup>+/-</sup>;Pak1<sup>-/-</sup>* mice *in vivo* is significantly reduced compared to *Nfl<sup>+/-</sup>* mice (Figure 17b).

Interestingly, although *Nfl<sup>+/-</sup>* mast cells have prolonged, Akt-mediated survival in response to SCF stimulation<sup>60</sup>, and Pak1 has been implicated as a potential anti-apoptotic mediator in some cell types, we found that loss of *Pak1* had no significant effect on apoptosis or survival in mast cells (Figure 16). A potential explanation for this finding lies in the fact that Pak1's anti-apoptotic actions have been reported to be the result of activation of Bad-1<sup>143-145</sup>. However, recent reports indicate that phosphorylation of Bad-

1 is not essential to hematopoietic cell survival responses resulting from PI-3K/Akt activation<sup>203</sup>. Therefore our findings demonstrating the inconsequential role of Pak1 with regards to mast cell apoptosis correlate well with data disassociating Bad-1 from hematopoietic cell survival.

A basic tenet of mast cell biology is that the mast cell progenitors circulate in the peripheral blood after development in the bone marrow and must migrate from the bloodstream to peripheral tissues. *Nfl* null Schwann cells (the tumorigenic cell of the neurofibroma) secrete a 6-7 fold higher concentration of SCF compared to wild type cells<sup>62</sup>, which stimulates a pathologic gain in migration and proliferation of *Nfl*<sup>+/-</sup> but not WT mast cells *in vitro*. Hyperactive *Nfl*<sup>+/-</sup> mast cells at the site of developing tumors could enhance the tumor forming ability of Schwann cells by means of their described role as potential “inducers” of neurofibroma pathogenesis via effects on the microenvironment<sup>63</sup>. Work submitted from our group confirms this hypothesis after we observed that adoptive transfer of *Nfl*<sup>+/-</sup> mast cells, but not WT mast cells, into mice that have *Nfl* conditionally deleted in the Schwann cell compartment (*Krox20Cre;Nfl<sup>lox/lox</sup>*) is necessary and sufficient to allow plexiform neurofibromas to develop *in vivo* (F.C. Yang, D.A. Ingram and D.W. Clapp, manuscript submitted April 2008).

In figure 11 we demonstrate that loss of *Pak1* reduces *Nfl*<sup>+/-</sup> mast cell migration by ~40% in response to SCF and that this reduction is p38 dependent. Additionally, we present experimental evidence that SCF mediated increases in the F-actin cytoskeleton in *Nfl*<sup>+/-</sup> BMDCs are dependent on a Pak1-p38 pathway. *Pak1*<sup>-/-</sup> mast cells also have a significant decrease in mast cell migration compared to wild type cells, but to a lesser degree than seen between *Nfl*<sup>+/-</sup> and *Nfl*<sup>+/-</sup>;*Pak1*<sup>-/-</sup> cells. This result is similar to the

characteristics of *p85 $\alpha$ <sup>-/-</sup>* and *Rac2<sup>-/-</sup>* mast cells, as they are only modestly impaired in their SCF mediated migration but cause large decreases in haptotaxis in the context of *Nfl* heterozygosity<sup>60</sup>. These findings indicate that the PI-3K/Rac2/Pak1 signaling axis, and by extension p38, are preferentially activated to stimulate the actin cytoskeleton and cell migration in the context of hyperactive Ras, and that under conditions of normal neurofibromin activity, other accessory pathways are also used to coordinate cell movement.

In *Nfl<sup>+/-</sup>* BMMCs, after stimulation by SCF, Ras becomes hyperactivated due to the lack of neurofibromin GAP activity. This leads to increased PI-3K/Rac activation<sup>59,61,204</sup>, and subsequent increases in Pak1 activity<sup>60</sup>. Hyperactivated Pak1 transmits mitogenic signals through selective activation of MEK and Erk and migratory signals through selective activation of p38 and the actin cytoskeleton. Therefore we propose that *Pak1* acts as a significant “hub” of c-kit mediated hyperactive Ras signaling and that disruption of *Pak1* can reduce the pathologic increases in proliferation and migration in *Nfl* haploinsufficient BMMCs.

#### *Pak1* and plexiform neurofibroma formation

Greater than 25% of NF1 patients have plexiform neurofibromas surrounding spinal nerve roots<sup>15</sup>, which can cause significant morbidity and premature death<sup>12</sup>. These tumors present major challenges to surgical treatment and no effective medical therapies for these tumors are available<sup>63</sup>. Further, plexiform neurofibromas have a propensity to transform into malignant peripheral nerve sheath tumors. Lack of existing

medical therapies has encouraged investigations into the cellular interactions in the neurofibroma microenvironment and molecular pathways regulating them in an attempt to identify potential pharmacologic targets for clinical use. Emerging evidence designating the mast cell as a key moderator of the pathophysiology at the site of neurofibroma development provides an attractive target for pharmacologic interventions.

If molecular therapeutics designed for correcting hyperactive pathways in *Nf1*<sup>+/-</sup> mast cells is developed, plexiform neurofibroma formation may be delayed or even prevented. For example, in recently submitted studies using the *Krox20Cre;Nf1*<sup>fllox/-</sup> murine tumor model, we have effectively used the small molecule imatinib (which inhibits c-kit and other RTKs) to reduce plexiform neurofibroma mass and significantly extend survival<sup>64</sup>. Currently, we are using this agent in a phase II clinical trial in pediatric NF1 patients with plexiform neurofibromas. Therefore, based on the *in vitro* data that implicated Pak1 as an important signaling molecule in disease related mast cell functions, we were eager to investigate whether loss of *Pak1* would alter tumorigenesis using the *Krox20Cre* mouse model of NF1.

However, using both an adoptive transfer and genetic intercross approach, we were not able to prevent neurofibroma formation by targeted disruption of *Pak1*. This could be due to the influence of many factors. The findings described above that show corrections in gains of function in *Nf1*<sup>+/-</sup>;*Pak1*<sup>-/-</sup> mast cells were generated from experiments that used soluble SCF as the stimulus. However, in the actual tumor microenvironment, in addition to the soluble form, membrane bound forms of SCF exist, which has been described as a more potent activator of c-kit responses<sup>205</sup>. In neurofibromatosis type 1 in general, and plexiform neurofibroma pathophysiology

specifically, the relative contribution of membrane bound SCF vis-à-vis soluble SCF is unknown.

The *Sl<sup>d</sup>* mutation deletes the transmembrane and cytoplasmic domains of SCF, and *Sl/Sl<sup>d</sup>* mice produce soluble but not membrane bound SCF<sup>45,206,207</sup>. *Sl/Sl<sup>d</sup>* mice have macrocytic anemia and melanocyte deficits, and importantly, markedly reduced tissue mast cells. Since soluble and membrane bound SCF have similar affinity for c-kit<sup>206</sup>, the reduced mast cell numbers found in *Sl/Sl<sup>d</sup>* mice imply that membrane bound SCF activates molecular signals downstream of c-kit that are essential for mast cell development and growth and are different than those activated by soluble SCF. The idea that soluble SCF cannot fully compensate for membrane bound SCF has been shown for other processes such as spermatogenesis<sup>208</sup>, erythropoiesis<sup>209</sup>, and *in vivo* melanocyte survival<sup>210</sup> as well. Therefore, it is possible that membrane bound SCF at the site of developing neurofibromas might stimulate c-Kit to activate non-Pak1 dependent pathways to trigger mast cell tumor inducing phenotypes in *Krox20Cre;NfI<sup>fllox/fllox</sup>* or *Krox20Cre;NfI<sup>fllox/-</sup>* mice that were reconstituted with *NfI<sup>+/-</sup>;Pak1<sup>-/-</sup>* bone marrow.

One notable finding from the adoptive transfer experiments was that although both *Krox20Cre;NfI<sup>fllox/fllox</sup>* and *Krox20Cre;NfI<sup>fllox/-</sup>* mice reconstituted with *NfI<sup>+/-</sup>;Pak1<sup>-/-</sup>* bone marrow developed tumors, only *Krox20Cre;NfI<sup>fllox/fllox</sup>* recipients of *NfI<sup>+/-</sup>;Pak1<sup>-/-</sup>* bone marrow showed a decrease in mast cell numbers in the tumor compared to recipients of *NfI<sup>+/-</sup>* bone marrow (Figure 22b). *Krox20Cre;NfI<sup>fllox/-</sup>* mice had similar numbers of invaded mast cells, regardless of marrow genotype (Figure 26b). One conclusion that could be drawn from this finding is that haploinsufficiency of the non-mast cell lineages of the tumor microenvironment produces more mast cell activating



factors compared to a wild type background. Given that fibroblasts are obligate producers of membrane bound SCF<sup>211,212</sup>, and that *Nfl*<sup>+/-</sup> fibroblasts activate *Nfl*<sup>+/-</sup> mast cells more intensely than wild type fibroblasts<sup>71</sup>; the findings of Figure 22b and 26b may be explained by increased production of membrane bound SCF in fibroblasts of *Krox20Cre;Nfl<sup>flox/-</sup>* mice, stimulating *Nfl*<sup>+/-</sup>; *Pak1*<sup>-/-</sup> mast cells to proliferate and release their granules in a *Pak1* independent fashion.

Another explanation for the results of the adoptive transfer neurofibroma experiments may lie in the unknown role of *Pak2* in *Nfl*<sup>+/-</sup> cells. *Pak2* carries out critical functions in cells, as homozygous disruption of the gene is embryonically lethal at a very early stage, and attempts to make a conditionally disrupted *Pak2* knockout mouse have been unsuccessful at generating *Pak2<sup>flox/flox</sup>* progeny so far (data not shown). *Pak2* shares high sequence homology with *Pak1* (~77%)<sup>103</sup>, and is highly expressed in mast cells (data not shown). It is possible that after adoptive transfer of *Nfl*<sup>+/-</sup>; *Pak1*<sup>-/-</sup> bone marrow, *Pak2* expression or *Pak2* kinase activity is increased to compensate for the loss of *Pak1*. An analogous result was found in murine MPD studies, where after adoptive transfer of *Nfl*<sup>-/-</sup>; *Rac2*<sup>-/-</sup> bone marrow, the levels of Rac1-GTP increased steadily *in vivo* and leukemias developed in these mice (D.W. Clapp, unpublished data). The relative, non-redundant contributions of *Pak1* and *Pak2* to cellular functions are still unclear for all cell types, and will need to be examined carefully in order to determine if the Pak kinases are important to neurofibroma pathogenesis.

Other reports indicated that overexpression of dominant negative *Pak1* in *Nfl*<sup>-/-</sup> Schwann cell lines prevented malignant transformation *in vitro*, leading us to hypothesize that mice with genetic disruption of *Pak1* in tumorigenic, *Nfl* null Schwann cells would

disrupt neurofibroma formation <sup>161</sup>. Nonetheless, the results of the genetic intercross of *Pak1*<sup>-/-</sup> mice with *Krox20Cre;Nf1<sup>lox/-</sup>* also indicated that *Pak1* loss in each lineage of the neurofibroma was inadequate for preventing tumor development. In addition, preliminary work in our laboratory using Schwann cells cultured from murine dorsal root ganglia has shown that *Nf1*<sup>-/-</sup>;*Pak1*<sup>-/-</sup> Schwann cells have increased invasion and proliferation compared to both wild type and *Nf1*<sup>-/-</sup> cells, in opposition to the findings of Tang et al. (F.C. Yang and D.W. Clapp, unpublished results). Further investigations of *Pak1* and its effects on Schwann cell functions are warranted, as these early findings hint toward a fundamentally different role for *Pak1* in regulating Ras signals in the tumorigenic lineage in comparison to the cells of the microenvironment.

As discussed above, the non-hematopoietic portion of the tumor microenvironment provides mast cell growth promoting factors. Since *Krox20Cre;Nf1<sup>lox/-</sup>;Pak1*<sup>-/-</sup> mice have similar numbers of mast cells within plexiform neurofibromas as *Krox20Cre;Nf1<sup>lox/-</sup>* mice, it appears that the signaling pathways that control the production of these factors are intact in *Krox20Cre;Nf1<sup>lox/-</sup>;Pak1*<sup>-/-</sup> mice to fully induce mast cell activation and therefore do not involve *Pak1*.

As a whole, the experiments utilizing the *Krox20Cre;Nf1<sup>lox</sup>* model clearly indicate that loss of *Pak1* alone cannot prevent the formation of plexiform neurofibromas. Although loss of *Pak1* clearly affects *Nf1*<sup>+/-</sup> mast cell responses to SCF *in vitro*, we show that the rather specific conditions of those experiments are not duplicated in the complex milieu of differing cellular lineages and various growth factors found in the regions surrounding *Nf1* null Schwann cells where neurofibromas originate. Consequently, attempts at using recently published small molecule inhibitors of *Pak1* <sup>213</sup> as a single

agent to treat *Krox20Cre;Nf1<sup>fllox/-</sup>* mice with tumors as we have done with imatinib would not be recommended. It is more plausible that successful pharmacologic approaches to the treatment of this disease will have to target multiple signaling molecules simultaneously, as the inhibition of a single component of a pathway can likely be compensated for by other molecules activated by one of the other cytokines present in the tumor. Indeed, part of imatinib's success at ameliorating neurofibroma progression is due to the fact that it inhibits RTKs other than c-Kit, such as c-Abl and PDGFR- $\beta$ . Therefore, the future of *Pak1* as a pharmacologic target in the therapy of neurofibromatosis type I may be relegated to that as an adjuvant therapy as part of a cocktail of rationally designed small molecules.

#### The role of *Pak1* in PDGF-BB and TGF- $\beta$ mediated signaling in fibroblasts

Under normal conditions, fibroblasts provide structural integrity and synthesize growth factors and extracellular matrix in nearly every tissue system. In addition, fibroblasts are intimately linked with numerous pathological conditions, including arthritis<sup>214</sup>, asthma<sup>215</sup>, and neoplasia<sup>216</sup>, including plexiform neurofibromas<sup>67,68,71</sup>. Invading fibroblasts carry out crucial tasks in cancer progression by altering the local extracellular matrix and by providing mitogenic signals to neoplastic cells<sup>217-219</sup>. The involvement of *Pak1* in fibroblasts has been investigated in numerous publications using transformed fibroblast cell lines and overexpression systems<sup>101</sup>. Here, we present for the first time, evidence in a genetic knockout system using primary cells outlining an

important role for *Pak1* in mediating PDGF-BB and TGF- $\beta$  mediated responses *in vitro* and *in vivo*.

Our results show that Pak1 activity is critical for the coordinated activation of the cytoskeleton necessary for fibroblast migration. In cells stimulated with either PDGF-BB or TGF- $\beta$ , *Pak1*<sup>-/-</sup> cells had decreased levels of activated filamin A (Figures 36 and 40), disruptions in F-actin organization (Figures 38h and 42h), and reduced wound healing responses *in vitro* (Figures 35 and 39). Additionally, using an animal model assay system known to induce fibroblast invasion, we demonstrate that the infiltration of fibroblasts *in vivo* is significantly reduced in *Pak1*<sup>-/-</sup> mice (Figure 45a and 46a). Fibroblast migration and invasion into the provisional matrix of the fibrin clot is an initiating event of wound healing that precedes reproduction and contraction of the extracellular matrix. This invasion step has been linked to PDGF-BB and TGF- $\beta$  release by activated platelets at the site of the wound<sup>220</sup>. Our results indicate that Pak1 activation mediates the molecular responses necessary for this important physiologic process.

Further experiments with *Pak1*<sup>-/-</sup> fibroblasts revealed the involvement of *Pak1* in multiple cellular functions. We identified modest but significant increases in apoptosis for *Pak1*<sup>-/-</sup> cells stimulated with PDGF-BB or TGF- $\beta$  (Figure 44 c and d). This finding is in contrast to the results of Figure 16, which show that mast cell survival in response to SCF is not affected by loss of *Pak1*. Taken together, these studies demonstrate that *Pak1* anti-apoptotic effects are cell type and stimulus dependent. Interestingly, *Pak1*<sup>-/-</sup> fibroblasts showed selective functional deficits depending on whether PDGF-BB or TGF- $\beta$  was used as the stimulus. Loss of *Pak1* resulted in reduced Erk activation and decreased proliferation in fibroblasts stimulated with PDGF-BB (Figure 31 and 32), but

not cells stimulated with TGF- $\beta$  (Figure 32 and 33). Other reports have utilized RNAi approaches to identify Pak2 as an important non-Smad pathway effector of TGF- $\beta$  mitogenic signaling in fibroblasts<sup>221</sup>. Our findings indicate that this growth promoting function in response to TGF- $\beta$  is specific to *Pak2*. Furthermore, we find that *Pak1* null cells have reduced collagen production in response to TGF- $\beta$  stimulation, but not PDGF-BB (Figure 43). While both growth factors are able stimulate collagen production, *Pak1* involvement seems to be unique to TGF- $\beta$  stimulation.

Idiopathic pulmonary fibrosis (IPF) is a disease that kills 40,000 patients per year and is associated with progressive dyspnea, decreased pulmonary function, and radiographically identifiable pulmonary infiltrates<sup>222</sup>. Based upon the supposed inflammatory etiology of the disease, IPF was traditionally treated with systemic corticosteroids. However, clinical studies have revealed that corticosteroid treatments are ineffective and do not improve survival<sup>223,224</sup>. Currently, IPF is believed to be the result of overactive fibroblast activation in response to fibrogenic factors released by alveolar epithelial cells following repeated pulmonary microinjury<sup>225</sup>. Two of the most prominently increased cytokines in the lungs of IPF patients include PDGF-BB and TGF- $\beta$ <sup>225</sup>. Using an established animal model of bleomycin induced lung fibrosis<sup>172</sup>, we found that *Pak1*<sup>-/-</sup> mice developed a significantly less severe fibrosis and had decreased amounts of newly synthesized collagen after exposure to bleomycin (Figure 47e and f). However, the magnitude of difference of fibrosis severity between wild type and *Pak1*<sup>-/-</sup> mice was not dramatic (~20%), despite the high amount of statistical significance (p<0.0001). This could be due to the fact that following exposure to bleomycin, fibroblasts in the lung proliferate in response to PDGF-BB and TGF- $\beta$ <sup>226</sup>. However, our

*in vitro* data indicates that *Pak1*<sup>-/-</sup> fibroblasts are deficient in only PDGF-BB mediated proliferation. TGF-β mediated mitogenic responses are intact in these animals and this could account for the only modest improvement in fibrosis in *Pak1*<sup>-/-</sup> mice.

In summary, these studies recognize a function for *Pak1* in mediating PDGF-BB and TGF-β signaling in fibroblasts. In addition, we demonstrate that Pak1 activates of the actin cytoskeleton leading to cell migration and invasion, an early and critical process of the wound healing response. Finally, we show that loss of *Pak1* improves the lung pathology in an animal model of a serious human disease.

#### Conclusions and future directions

In the studies described here, we identify a role for *Pak1* in coordinating molecular signaling in multiple cell types. We report for the first time in a primary cell model that *Pak1* activates the MAPK signaling pathway. We establish that *Pak1* regulates the characteristic hyperactivation of the MAPK pathway and several associated gain-in-function phenotypes found in *Nfl*<sup>+/-</sup> mast cells stimulated with SCF, including proliferation, migration, and degranulation. Surprisingly, we found that the corrections in *Nfl* haploinsufficient mast cell functions caused by loss of *Pak1* *in vitro* did not affect the development of plexiform neurofibromas in *Krox20Cre;Nfl*<sup>lox/-</sup> mice. The unexpected results of the plexiform neurofibroma studies underscore the unique insight provided by animal models into the complex cell-to-cell interactions underlying tumorigenesis in a manner that *in vitro* studies cannot replicate. Further experiments utilizing the

*Krox20Cre;Nf1<sup>fllox/-</sup>* mouse model are critical for validating the proposed biochemical schema generated from our cellular data.

One set of studies with particular relevance to the role of *Pak1* and neurofibroma formation involves the adoptive transfer of *Nf1<sup>+/-</sup>;Rac1<sup>-/-</sup>* bone marrow into *Krox20Cre;Nf1<sup>fllox/-</sup>* mice. If these mice have interrupted tumor formation, it would provide more evidence that Rac-GTPase signaling in hematopoietic cells during tumor formation employs other downstream mediators in addition to *Pak1*, and that signaling cues from the microenvironment preferentially activate these alternate pathways. In addition, the successful development of a *Pak2* conditional knockout mouse would prove very useful for the study of neurofibroma pathophysiology. The mast cell assays described here be repeated with *Nf1<sup>+/-</sup>;Pak2<sup>fllox/fllox</sup>* mice, and compared to the results described here using *Pak1<sup>-/-</sup>* cells to determine if non-redundant functions of the Pak isoforms exist. In particular, it would be of interest to see if *Pak2* null mast cells had changes in survival or maturation, two functions where *Pak1* appears to be non-essential. The generation of *Nf1<sup>+/-</sup>;Pak1<sup>-/-</sup>;Pak2<sup>fllox/fllox</sup>* mutant bone marrow would be particularly valuable for adoptive transfer into *Krox20Cre;Nf1<sup>fllox/-</sup>* mice for tumor studies similar to those performed here. We hypothesize that transplantation of *Nf1* haploinsufficient hematopoietic cells lacking both Pak1 and Pak2 will delay neurofibroma formation. An additional line of experimentation to follow up on these studies involves the role of membrane bound SCF to neurofibroma formation. Intercrossing the *Krox20Cre;Nf1<sup>fllox/-</sup>* mouse with *Sl/Sl<sup>d</sup>* mouse and following plexiform neurofibroma formation in the progeny would provide an easily interpretable method for assessing the contribution of the membrane bound form of SCF to tumor pathology.

In addition, this report demonstrates that *Pak1* is necessary for activating various fibroblast functions in response to PDGF-BB and TGF- $\beta$ . These fibroblast studies point out a potential responsibility for *Pak1* in regulating physiologic functions such as wound healing. Keloids are pathologic scars formed by overactive wound healing responses. Experiments utilizing recently developed *Pak1* inhibitors<sup>213</sup> could be used in murine models of keloid development<sup>227</sup>, to investigate whether the putative role for *Pak1* in wound healing outlined in this work is involved in this disease process. Lastly, we also establish a role for *Pak1* in a significant respiratory disease, idiopathic pulmonary fibrosis. Although the decreases in bleomycin induced lung fibrosis are not drastic in *Pak1*<sup>-/-</sup> mice, it is unknown what a 20% change in fibrosis severity and collagen content means in relation to overall pulmonary function. Therefore, it would be of interest to compare airway morphometry, resistance, and ventilation/perfusion ratios of lungs harvested from bleomycin treated wild type and *Pak1*<sup>-/-</sup> mice.

These studies demonstrate that *Pak1* is a key regulator of various cellular functions in both mast cells and fibroblasts by activating multiple pathways, including Ras/Raf/Mek/Erk, p38 MAPK, and actin regulating proteins, in the context of both normal and hyperactivated Ras. We provide novel data that identifies Pak1 as a potential target for therapeutic interventions in fibrotic diseases. Our findings have enhanced the understanding of the molecular underpinnings of neurofibromatosis type 1, providing knowledge into the pathogenesis of this common and debilitating disease. Due to its critical location at the intersection of numerous signaling networks responsible for important biological outcomes, further investigation into *Pak1* and related isoforms holds great potential for future researchers and clinicians.



## REFERENCES

1. Reynolds RM, Browning GG, Nawroz I, Campbell IW. Von Recklinghausen's neurofibromatosis: neurofibromatosis type 1. *Lancet*. 2003;361:1552-1554.
2. Hirsch NP, Murphy A, Radcliffe JJ. Neurofibromatosis: clinical presentations and anaesthetic implications. *Br J Anaesth*. 2001;86:555-564.
3. Brodeur GM. The NF1 gene in myelopoiesis and childhood myelodysplastic syndromes. *N Engl J Med*. 1994;330:637-638.
4. Friedman JM, Birch PH. Type 1 neurofibromatosis: a descriptive analysis of the disorder in 1,728 patients. *Am J Med Genet*. 1997;70:138-143.
5. Side L, Taylor B, Cayouette M, et al. Homozygous inactivation of the *NF1* gene in bone marrow cells from children with neurofibromatosis type 1 and malignant myeloid disorders. *N Engl J Med*. 1997;336:1713-1720.
6. Shannon KM, O'Connell P, Martin GA, et al. Loss of the normal *NF1* allele from the bone marrow of children with type 1 neurofibromatosis and malignant myeloid disorders. *N Engl J Med*. 1994;330:597-601.
7. Bader JL. Neurofibromatosis and cancer. *Ann N Y Acad Sci*. 1986;486:57-65.
8. Peltonen J, Jaakkola S, Lebwohl M, et al. Cellular differentiation and expression of matrix genes in type 1 neurofibromatosis. *Lab Invest*. 1988;59:760-771.
9. Hirota S, Nomura S, Asada H, Ito A, Morii E, Kitamura Y. Possible involvement of c-kit Receptor and its ligand in increase of mast cells in neurofibroma tissues. *Arch Pathol Lab Med*. 1993;117:996-999.
10. Le LQ, Parada LF. Tumor microenvironment and neurofibromatosis type I: connecting the GAPs. *Oncogene*. 2007;26:4609-4616.
11. Ferner RE, Huson SM, Thomas N, et al. Guidelines for the diagnosis and management of individuals with neurofibromatosis 1. *J Med Genet*. 2007;44:81-88.
12. Korf BR. Plexiform neurofibromas. *Am J Med Genet*. 1999;89:31-37.
13. Korf BR. Diagnostic outcome in children with multiple cafe au lait spots. *Pediatrics*. 1992;90:924-927.
14. Dugoff L, Sujansky E. Neurofibromatosis type 1 and pregnancy. *Am J Med Genet*. 1996;66:7-10.
15. Huson SM, Harper PS, Compston DA. Von Recklinghausen neurofibromatosis. A clinical and population study in south-east Wales. *Brain*. 1988;111 ( Pt 6):1355-1381.
16. Ferner RE. Neurofibromatosis 1. *Eur J Hum Genet*. 2007;15:131-138.
17. Lakkis MM, Tennekoon GI. Neurofibromatosis type 1. I. General overview. *J Neurosci Res*. 2000;62:755-763.
18. Goldgar DE, Green P, Parry DM, Mulvihill JJ. Multipoint linkage analysis in neurofibromatosis type I: an international collaboration. *Am J Hum Genet*. 1989;44:6-12.
19. Gutmann DH, Wood DL, Collins FS. Identification of the neurofibromatosis type 1 gene product. *Proc Natl Acad Sci U S A*. 1991;88:9658-9662.
20. Ballester R, Marchuk D, Boguski M, et al. The NF1 locus encodes a protein functionally related to mammalian GAP and yeast IRA proteins. *Cell*. 1990;63:851-859.

21. Cawthon RM, O'Connell P, Buchberg AM, et al. Identification and characterization of transcripts from the neurofibromatosis 1 region: the sequence and genomic structure of EVI2 and mapping of other transcripts. *Genomics*. 1990;7:555-565.
22. Wallace MR, Marchuk DA, Andersen LB, et al. Type 1 neurofibromatosis gene: identification of a large transcript disrupted in three NF1 patients. *Science*. 1990;249:181-186.
23. Gutmann DH, Collins FS. The Neurofibromatosis Type 1 Gene and Its Protein Product, Neurofibromin. *Neuron*. 1993;10:335-343.
24. Xu GF, O'Connell P, Viskochil D, et al. The neurofibromatosis type 1 gene encodes a protein related to GAP. *Cell*. 1990;62:599-608.
25. Daston MM, Scrabble H, Nordlund M, Sturbaum AK, Nissen LM, Ratner N. The protein product of the neurofibromatosis type 1 gene is expressed at highest abundance in neurons, Schwann cells, and oligodendrocytes. *Neuron*. 1992;8:415-428.
26. Yohay KH. The genetic and molecular pathogenesis of NF1 and NF2. *Semin Pediatr Neurol*. 2006;13:21-26.
27. Castle B, Baser ME, Huson SM, Cooper DN, Upadhyaya M. Evaluation of genotype-phenotype correlations in neurofibromatosis type 1. *J Med Genet*. 2003;40:e109.
28. Jacks T, Shih TS, Schmitt EM, Bronson RT, Bernards A, Weinberg RA. Tumour predisposition in mice heterozygous for a targeted mutation in *NF1*. *Nature Genet*. 1994;7:353-361.
29. Largaespada DA, Brannan CI, Jenkins NA, Copeland NG. *Nf1* deficiency causes Ras-mediated granulocyte/macrophage colony stimulating factor hypersensitivity and chronic myeloid leukaemia. *Nat Genet*. 1996;12:137-143.
30. Zhu Y, Ghosh P, Charnay P, Burns DK, Parada LF. Neurofibromas in NF1: Schwann cell origin and role of tumor environment. *Science*. 2002;296:920-922.
31. Serra E, Rosenbaum T, Winner U, et al. Schwann cells harbor the somatic NF1 mutation in neurofibromas: evidence of two different Schwann cell subpopulations. *Hum Mol Genet*. 2000;9:3055-3064.
32. Balkwill F, Mantovani A. Inflammation and cancer: back to Virchow? *Lancet*. 2001;357:539-545.
33. Scholl SM, Pallud C, Beuvon F, et al. Anti-colony-stimulating factor-1 antibody staining in primary breast adenocarcinomas correlates with marked inflammatory cell infiltrates and prognosis. *J Natl Cancer Inst*. 1994;86:120-126.
34. Kuper H, Adami HO, Trichopoulos D. Infections as a major preventable cause of human cancer. *J Intern Med*. 2000;248:171-183.
35. Brocker EB, Zwadlo G, Holzmann B, Macher E, Sorg C. Inflammatory cell infiltrates in human melanoma at different stages of tumor progression. *Int J Cancer*. 1988;41:562-567.
36. Ness RB, Cottreau C. Possible role of ovarian epithelial inflammation in ovarian cancer. *J Natl Cancer Inst*. 1999;91:1459-1467.
37. DeMarzo AM, Nelson WG, Isaacs WB, Epstein JI. Pathological and molecular aspects of prostate cancer. *Lancet*. 2003;361:955-964.
38. Coussens LM, Werb Z. Inflammation and cancer. *Nature*. 2002;420:860-867.

39. Garcia-Rodriguez LA, Huerta-Alvarez C. Reduced risk of colorectal cancer among long-term users of aspirin and nonaspirin nonsteroidal antiinflammatory drugs. *Epidemiology*. 2001;12:88-93.
40. Crivellato E, Beltrami C, Mallardi F, Ribatti D. Paul Ehrlich's doctoral thesis: a milestone in the study of mast cells. *Br J Haematol*. 2003;123:19-21.
41. Coussens LM, Raymond W, Bergers G, et al. Inflammatory mast cells up-regulate angiogenesis during squamous epithelial carcinogenesis. *Genes Dev*. 1999;13:1382-1397.
42. Huang E, Nocka K, Beier DR, et al. The hematopoietic growth factor KL is encoded by the *Sl* locus and is the ligand of the *c-kit* receptor, the gene product of the *W* locus. *Cell*. 1990;63:225-233.
43. Reber L, Da Silva CA, Frossard N. Stem cell factor and its receptor c-Kit as targets for inflammatory diseases. *Eur J Pharmacol*. 2006;533:327-340.
44. Anderson DM, Williams DE, Tushinski R, et al. Alternate splicing of mRNAs encoding human mast cell growth factor and localization of the gene to chromosome 12q22-q24. *Cell Growth Differ*. 1991;2:373-378.
45. Broudy VC. Stem cell factor and hematopoiesis. *Blood*. 1997;90:1345-1364.
46. Sette C, Dolci S, Geremia R, Rossi P. The role of stem cell factor and of alternative c-kit gene products in the establishment, maintenance and function of germ cells. *Int J Dev Biol*. 2000;44:599-608.
47. Yoshida H, Kunisada T, Grimm T, Nishimura EK, Nishioka E, Nishikawa SI. Review: melanocyte migration and survival controlled by SCF/c-kit expression. *J Investig Dermatol Symp Proc*. 2001;6:1-5.
48. Kirshenbaum AS, Goff JP, Kessler SW, Mican JM, Zsebo KM, Metcalfe DD. Effect of IL-3 and stem cell factor on the appearance of human basophils and mast cells from CD34+ pluripotent progenitor cells. *J Immunol*. 1992;148:772-777.
49. Saito H, Ebisawa M, Tachimoto H, et al. Selective growth of human mast cells induced by Steel factor, IL-6, and prostaglandin E2 from cord blood mononuclear cells. *J Immunol*. 1996;157:343-350.
50. Kinoshita T, Sawai N, Hidaka E, Yamashita T, Koike K. Interleukin-6 directly modulates stem cell factor-dependent development of human mast cells derived from CD34(+) cord blood cells. *Blood*. 1999;94:496-508.
51. Meininger C, Yano H, Rottapel R, Bernstein A, Zsebo K, Zetter B. The c-kit receptor ligand functions as a mast cell chemoattractant. *Blood*. 1992;79:958-963.
52. Kiener HP, Hofbauer R, Tohidast-Akrad M, et al. Tumor necrosis factor alpha promotes the expression of stem cell factor in synovial fibroblasts and their capacity to induce mast cell chemotaxis. *Arthritis Rheum*. 2000;43:164-174.
53. Yee NS, Paek I, Besmer P. Role of kit-ligand in proliferation and suppression of apoptosis in mast cells: basis for radiosensitivity of white spotting and steel mutant mice. *J Exp Med*. 1994;179:1777-1787.
54. Iemura A, Tsai M, Ando A, Wershil B, Galli S. The c-kit ligand, stem cell factor, promotes mast cell survival by suppressing apoptosis. *Am J Pathol*. 1994;144:321-328.
55. Columbo M, Horowitz EM, Botana LM, et al. The human recombinant c-kit receptor ligand, rhSCF, induces mediator release from human cutaneous mast cells and enhances IgE-dependent mediator release from both skin mast cells and peripheral blood basophils. *J Immunol*. 1992;149:599-608.

56. Galli SJ, Tsai M, Wershil BK. The c-kit receptor, stem cell factor, and mast cells. *Am J Pathol.* 1993;142:965-974.
57. Sondell M, Lundborg G, Kanje M. Vascular endothelial growth factor has neurotrophic activity and stimulates axonal outgrowth, enhancing cell survival and Schwann cell proliferation in the peripheral nervous system. *J Neurosci.* 1999;19:5731-5740.
58. Kendall JC, Li XH, Galli SJ, Gordon JR. Promotion of mouse fibroblast proliferation by IgE-dependent activation of mouse mast cells: role for mast cell tumor necrosis factor-alpha and transforming growth factor-beta 1. *J Allergy Clin Immunol.* 1997;99:113-123.
59. Ingram DA, Yang FC, Travers JB, et al. Genetic and biochemical evidence that haploinsufficiency of the *Nf1* tumor suppressor gene modulates melanocyte and mast cell fates in vivo. *J Exp Med.* 2000;191:181-188.
60. Ingram DA, Hiatt K, King AJ, et al. Hyperactivation of p21(ras) and the hematopoietic-specific Rho GTPase, Rac2, cooperate to alter the proliferation of neurofibromin deficient mast cells *in vivo* and *in vitro*. *J Exp Med.* 2001;194:57-69.
61. Khalaf WF, Yang FC, Chen S, et al. K-ras is critical for modulating multiple c-kit-mediated cellular functions in wild-type and *Nf1*+/- mast cells. *J Immunol.* 2007;178:2527-2534.
62. Yang FC, Ingram DA, Chen S, et al. Neurofibromin-deficient Schwann cells secrete a potent migratory stimulus for *Nf1* +/- mast cells. *Journal of Clin Invest.* 2003;112:1851-1861.
63. Viskochil DH. It takes two to tango: mast cell and Schwann cell interactions in neurofibromas. *J Clin Invest.* 2003;112:1791-1793.
64. Yang FC, Ingram DA, Chen S, et al. NF1 tumor suppressor haploinsufficient bone marrow complements nullizygous Schwann cells to form plexiform neurofibromas. *Cell.* 2008.
65. Nocka K, Buck J, Levi E, Besmer P. Candidate ligand for the c-kit transmembrane kinase receptor: KL, a fibroblast derived growth factor stimulates mast cells and erythroid progenitors. *Embo.* 1990;9:3287-3294.
66. Puxeddu I, Levi-Schaffer F. Mast cells and tissue remodeling. *Revue française d'allergologie et d'immunologie clinique* 2002;42:16-18.
67. Jaakkola S, Peltonen J, Riccardi V, Chu ML, Uitto J. Type 1 neurofibromatosis: selective expression of extracellular matrix genes by Schwann cells, perineurial cells, and fibroblasts in mixed cultures. *J Clin Invest.* 1989;84:253-261.
68. Peltonen J, Penttinen R, Larjava H, Aho HJ. Collagens in neurofibromas and neurofibroma cell cultures. *Ann N Y Acad Sci.* 1986;486:260-270.
69. Bhowmick NA, Neilson EG, Moses HL. Stromal fibroblasts in cancer initiation and progression. *Nature.* 2004;432:332-337.
70. Rosenbaum T, Boissy YL, Kombrinck K, et al. Neurofibromin-deficient fibroblasts fail to form perineurium in vitro. *Development.* 1995;121:3583-3592.
71. Yang FC, Chen S, Clegg T, et al. *Nf1*+/- mast cells induce neurofibroma like phenotypes through secreted TGF-beta signaling. *Hum Mol Genet.* 2006;15:2421-2437.
72. Xu G, O'Connell P, Viskochil D, et al. The Neurofibromatosis type 1 gene encodes a protein related to GAP. *Cell.* 1990;62:599-608.

73. Eerola I, Boon LM, Mulliken JB, et al. Capillary malformation-arteriovenous malformation, a new clinical and genetic disorder caused by RASA1 mutations. *Am J Hum Genet.* 2003;73:1240-1249.
74. Hiatt K, Ingram DA, Huddleston H, Spandau DF, Kapur R, Clapp DW. Loss of the *Nf1* tumor suppressor gene decreases Fas antigen expression in myeloid cells. *Am J Pathol.* 2004;164:1471-1479.
75. Hiatt K, Ingram DA, Zhang Y, Bollag G, Clapp DW. Neurofibromin GTPase-activating Protein-related Domains Restore Normal Growth in *Nf1* *-/-* Cells. *J Biol Chem.* 2001;276:7240-7245.
76. Tong J, Hannan F, Zhu Y, Bernardis A, Zhong Y. Neurofibromin regulates G protein-stimulated adenylyl cyclase activity. *Nat Neurosci.* 2002;5:95-96.
77. Gregory PE, Gutmann DH, Mitchell A, et al. Neurofibromatosis type 1 gene product (neurofibromin) associates with microtubules. *Somat Cell Mol Genet.* 1993;19:265-274.
78. Bourne HR, Sanders DA, McCormick F. The GTPase superfamily: a conserved switch for diverse cell functions. *Nature.* 1990;348:125-132.
79. DeClue JE, Papageorge AG, Fletcher JA, et al. Abnormal regulation of mammalian p21 ras contributes to malignant tumor growth in von Recklinghausen (Type 1) neurofibromatosis. *Cell.* 1992;69:265-273.
80. Le DT, Kong N, Zhu Y, et al. Somatic inactivation of *Nf1* in hematopoietic cells results in a progressive myeloproliferative disorder. *Blood.* 2004;103:4243-4250.
81. Dasgupta B, Yi Y, Chen DY, Weber JD, Gutmann DH. Proteomic analysis reveals hyperactivation of the mammalian target of rapamycin pathway in neurofibromatosis 1-associated human and mouse brain tumors. *Cancer Res.* 2005;65:2755-2760.
82. Zhu Y, Harada T, Liu L, et al. Inactivation of *NF1* in CNS causes increased glial progenitor proliferation and optic glioma formation. *Development.* 2005;132:5577-5588.
83. Costa RM, Federov NB, Kogan JH, et al. Mechanism for the learning deficits in a mouse model of neurofibromatosis type 1. *Nature.* 2002;415:526-530.
84. Dasgupta B, Gutmann DH. Neurofibromatosis 1: closing the GAP between mice and men. *Curr Opin Genet Dev.* 2003;13:20-27.
85. Stokoe D, Macdonald SG, Cadwallader K, Symons M, Hancock JF. Activation of Raf as a result of recruitment to the plasma membrane. *Science.* 1994;264:1463-1467.
86. Kyriakis JM, App H, Zhang XF, et al. Raf-1 activates MAP kinase-kinase. *Nature.* 1992;358:417-421.
87. Crews CM, Erikson RL. Purification of a murine protein-tyrosine/threonine kinase that phosphorylates and activates the Erk-1 gene product: relationship to the fission yeast *byr1* gene product. *Proc Natl Acad Sci U S A.* 1992;89:8205-8209.
88. Itoh T, Kaibuchi K, Masuda T, et al. A protein factor for ras p21-dependent activation of mitogen-activated protein (MAP) kinase through MAP kinase kinase. *Proc Natl Acad Sci U S A.* 1993;90:975-979.
89. Satoh T, Uehara Y, Kaziro Y. Inhibition of interleukin 3 and granulocyte-macrophage colony-stimulating factor stimulated increase of active ras.GTP by herbimycin A, a specific inhibitor of tyrosine kinases. *J Biol Chem.* 1992;267:2537-2541.
90. Marshall CJ. Tumor suppressor genes. *Cell.* 1991;64:313-326.

91. Campbell SL, Khosravi-Far R, Rossman KL, Clark GJ, Der CJ. Increasing complexity of Ras signaling. *Oncogene*. 1998;17:1395-1413.
92. Kim HA, Rosenbaum T, Marchionni MA, Ratner N, DeClue JE. Schwann cells from neurofibromin deficient mice exhibit activation of p21ras, inhibition of cell proliferation and morphological changes. *Oncogene*. 1995;11:325-335.
93. Munchhof AM, Li F, White HA, et al. Neurofibroma-associated growth factors activate a distinct signaling network to alter the function of neurofibromin-deficient endothelial cells. *Hum Mol Genet*. 2006;15:1858-1869.
94. Li F, Munchhof AM, White HA, et al. Neurofibromin is a novel regulator of RAS-induced signals in primary vascular smooth muscle cells. *Hum Mol Genet*. 2006;15:1921-1930.
95. Kodaki T, Woscholski R, Hallberg B, Rodriguez-Viciano P, Downward J, Parker PJ. The activation of phosphatidylinositol 3-kinase by Ras. *Curr Biol*. 1994;4:798-806.
96. Lau N, Feldkamp MM, Roncari L, et al. Loss of neurofibromin is associated with activation of RAS/MAPK and PI3-K/AKT signaling in a neurofibromatosis 1 astrocytoma. *J Neuropathol Exp Neurol*. 2000;59:759-767.
97. Johannessen CM, Reczek EE, James MF, Brems H, Legius E, Cichowski K. The NF1 tumor suppressor critically regulates TSC2 and mTOR. *Proc Natl Acad Sci U S A*. 2005;102:8573-8578.
98. Grammer TC, Blenis J. Evidence for MEK-independent pathways regulating the prolonged activation of the ERK-MAP kinases. *Oncogene*. 1997;14:1635-1642.
99. Bishop AL, Hall A. Rho GTPases and their effector proteins. *Biochem J*. 2000;348 Pt 2:241-255.
100. Zhao ZS, Manser E. PAK and other Rho-associated kinases--effectors with surprisingly diverse mechanisms of regulation. *Biochem J*. 2005;386:201-214.
101. Bokoch GM. Biology of the p21-Activated Kinases. *Annu Rev Biochem*. 2003.
102. Manser E, Leung T, Salihuddin H, Zhao ZS, Lim L. A brain serine/threonine protein kinase activated by Cdc42 and Rac1. *Nature*. 1994;367:40-46.
103. Mayhew MW, Jeffery ED, Sherman NE, et al. Identification of phosphorylation sites in betaPIX and PAK1. *J Cell Sci*. 2007;120:3911-3918.
104. Knaus UG, Morris S, Dong HJ, Chernoff J, Bokoch GM. Regulation of human leukocyte p21-activated kinases through G protein--coupled receptors. *Science*. 1995;269:221-223.
105. Sells MA, Knaus UG, Bagrodia S, Ambrose DM, Bokoch GM, Chernoff J. Human p21-activated kinase (Pak1) regulates actin organization in mammalian cells. *Curr Biol*. 1997;7:202-210.
106. Dan C, Kelly A, Bernard O, Minden A. Cytoskeletal changes regulated by the PAK4 serine/threonine kinase are mediated by LIM kinase 1 and cofilin. *J Biol Chem*. 2001;276:32115-32121.
107. Lei M, Lu W, Meng W, et al. Structure of PAK1 in an autoinhibited conformation reveals a multistage activation switch. *Cell*. 2000;102:387-397.
108. Bokoch GM, Wang Y, Bohl BP, Sells MA, Quilliam LA, Knaus UG. Interaction of the Nck adapter protein with p21-activated kinase (PAK1). *J Biol Chem*. 1996;271:25746-25749.

109. Puto LA, Pestonjamas K, King CC, Bokoch GM. p21-activated kinase 1 (PAK1) interacts with the Grb2 adapter protein to couple to growth factor signaling. *J Biol Chem.* 2003;278:9388-9393.
110. Manser E, Loo TH, Koh CG, et al. PAK kinases are directly coupled to the PIX family of nucleotide exchange factors. *Mol Cell.* 1998;1:183-192.
111. Parrini MC, Lei M, Harrison SC, Mayer BJ. Pak1 kinase homodimers are autoinhibited in trans and dissociated upon activation by Cdc42 and Rac1. *Mol Cell.* 2002;9:73-83.
112. Gatti A, Huang Z, Tuazon PT, Traugh JA. Multisite autophosphorylation of p21-activated protein kinase gamma-PAK as a function of activation. *J Biol Chem.* 1999;274:8022-8028.
113. Zenke FT, King CC, Bohl BP, Bokoch GM. Identification of a central phosphorylation site in p21-activated kinase regulating autoinhibition and kinase activity. *J Biol Chem.* 1999;274:32565-32573.
114. Yu JS, Chen WJ, Ni MH, Chan WH, Yang SD. Identification of the regulatory autophosphorylation site of autophosphorylation-dependent protein kinase (auto-kinase). Evidence that auto-kinase belongs to a member of the p21-activated kinase family. *Biochem J.* 1998;334 ( Pt 1):121-131.
115. Chong C, Tan L, Lim L, Manser E. The mechanism of PAK activation. Autophosphorylation events in both regulatory and kinase domains control activity. *J Biol Chem.* 2001;276:17347-17353.
116. King CC, Gardiner EM, Zenke FT, et al. p21-activated kinase (PAK1) is phosphorylated and activated by 3-phosphoinositide-dependent kinase-1 (PDK1). *J Biol Chem.* 2000;275:41201-41209.
117. Galisteo ML, Chernoff J, Su YC, Skolnik EY, Schlessinger J. The adaptor protein Nck links receptor tyrosine kinases with the serine-threonine kinase Pak1. *J Biol Chem.* 1996;271:20997-21000.
118. Lu W, Katz S, Gupta R, Mayer BJ. Activation of Pak by membrane localization mediated by an SH3 domain from the adaptor protein Nck. *Curr Biol.* 1997;7:85-94.
119. Bubeck Wardenburg J, Pappu R, Bu JY, et al. Regulation of PAK activation and the T cell cytoskeleton by the linker protein SLP-76. *Immunity.* 1998;9:607-616.
120. Benner GE, Dennis PB, Masaracchia RA. Activation of an S6/H4 kinase (PAK 65) from human placenta by intramolecular and intermolecular autophosphorylation. *J Biol Chem.* 1995;270:21121-21128.
121. Rudel T, Bokoch GM. Membrane and morphological changes in apoptotic cells regulated by caspase-mediated activation of PAK2. *Science.* 1997;276:1571-1574.
122. Bokoch GM, Reilly AM, Daniels RH, et al. A GTPase-independent mechanism of p21-activated kinase activation. Regulation by sphingosine and other biologically active lipids. *J Biol Chem.* 1998;273:8137-8144.
123. Tuazon PT, Chinwah M, Traugh JA. Autophosphorylation and protein kinase activity of p21-activated protein kinase gamma-PAK are differentially affected by magnesium and manganese. *Biochemistry.* 1998;37:17024-17029.
124. Dharmawardhane S, Sanders LC, Martin SS, Daniels RH, Bokoch GM. Localization of p21-activated kinase 1 (PAK1) to pinocytic vesicles and cortical actin structures in stimulated cells. *J Cell Biol.* 1997;138:1265-1278.

125. Sells MA, Boyd JT, Chernoff J. p21-activated kinase 1 (Pak1) regulates cell motility in mammalian fibroblasts. *J Cell Biol.* 1999;145:837-849.
126. Vadlamudi RK, Li F, Adam L, et al. Filamin is essential in actin cytoskeletal assembly mediated by p21-activated kinase 1. *Nat Cell Biol.* 2002;4:681-690.
127. Edwards DC, Sanders LC, Bokoch GM, Gill GN. Activation of LIM-kinase by Pak1 couples Rac/Cdc42 GTPase signalling to actin cytoskeletal dynamics. *Nat Cell Biol.* 1999;1:253-259.
128. Daub H, Gevaert K, Vandekerckhove J, Sobel A, Hall A. Rac/Cdc42 and p65PAK regulate the microtubule-destabilizing protein stathmin through phosphorylation at serine 16. *J Biol Chem.* 2001;276:1677-1680.
129. King AJ, Sun H, Diaz B, et al. The protein kinase Pak3 positively regulates Raf-1 activity through phosphorylation of serine 338. *Nature.* 1998;396:180-183.
130. Zang M, Hayne C, Luo Z. Interaction between active Pak1 and Raf-1 is necessary for phosphorylation and activation of Raf-1. *J Biol Chem.* 2002;277:4395-4405.
131. Frost JA, Steen H, Shapiro P, et al. Cross-cascade activation of ERKs and ternary complex factors by Rho family proteins. *Embo J.* 1997;16:6426-6438.
132. Coles LC, Shaw PE. PAK1 primes MEK1 for phosphorylation by Raf-1 kinase during cross-cascade activation of the ERK pathway. *Oncogene.* 2002;21:2236-2244.
133. Beeser A, Jaffer ZM, Hofmann C, Chernoff J. Role of group A p21-activated kinases in activation of extracellular-regulated kinase by growth factors. *J Biol Chem.* 2005;280:36609-36615.
134. Park ER, Eblen ST, Catling AD. MEK1 activation by PAK: a novel mechanism. *Cell Signal.* 2007;19:1488-1496.
135. Frost JA, Xu S, Hutchison MR, Marcus S, Cobb MH. Actions of Rho family small G proteins and p21-activated protein kinases on mitogen-activated protein kinase family members. *Mol Cell Biol.* 1996;16:3707-3713.
136. Zhang S, Han J, Sells MA, et al. Rho family GTPases regulate p38 mitogen-activated protein kinase through the downstream mediator Pak1. *J Biol Chem.* 1995;270:23934-23936.
137. Dechert MA, Holder JM, Gerthoffer WT. p21-activated kinase 1 participates in tracheal smooth muscle cell migration by signaling to p38 Mapk. *Am J Physiol Cell Physiol.* 2001;281:C123-132.
138. Rousseau S, Dolado I, Beardmore V, et al. CXCL12 and C5a trigger cell migration via a PAK1/2-p38alpha MAPK-MAPKAP-K2-HSP27 pathway. *Cell Signal.* 2006;18:1897-1905.
139. Bagrodia S, Taylor SJ, Creasy CL, Chernoff J, Cerione RA. Identification of a mouse p21Cdc42/Rac activated kinase. *J Biol Chem.* 1995;270:22731-22737.
140. Brown JL, Stowers L, Baer M, Trejo J, Coughlin S, Chant J. Human Ste20 homologue hPAK1 links GTPases to the JNK MAP kinase pathway. *Curr Biol.* 1996;6:598-605.
141. Westwick JK, Lambert QT, Clark GJ, et al. Rac regulation of transformation, gene expression, and actin organization by multiple, PAK-independent pathways. *Mol Cell Biol.* 1997;17:1324-1335.
142. Teramoto H, Crespo P, Coso OA, Igishi T, Xu N, Gutkind JS. The small GTP-binding protein rho activates c-Jun N-terminal kinases/stress-activated protein kinases in



- human kidney 293T cells. Evidence for a Pak-independent signaling pathway. *J Biol Chem.* 1996;271:25731-25734.
143. Schurmann A, Mooney AF, Sanders LC, et al. p21-activated kinase 1 phosphorylates the death agonist bad and protects cells from apoptosis. *Mol Cell Biol.* 2000;20:453-461.
144. Sastry KS, Smith AJ, Karpova Y, Datta SR, Kulik G. Diverse antiapoptotic signaling pathways activated by vasoactive intestinal polypeptide, epidermal growth factor, and phosphatidylinositol 3-kinase in prostate cancer cells converge on BAD. *J Biol Chem.* 2006;281:20891-20901.
145. Wang SE, Shin I, Wu FY, Friedman DB, Arteaga CL. HER2/Neu (ErbB2) signaling to Rac1-Pak1 is temporally and spatially modulated by transforming growth factor beta. *Cancer Res.* 2006;66:9591-9600.
146. Gajewski TF, Thompson CB. Apoptosis meets signal transduction: elimination of a BAD influence. *Cell.* 1996;87:589-592.
147. Li Q, Mullins SR, Sloane BF, Mattingly RR. p21-Activated kinase 1 coordinates aberrant cell survival and pericellular proteolysis in a three-dimensional culture model for premalignant progression of human breast cancer. *Neoplasia.* 2008;10:314-329.
148. Wang RA, Zhang H, Balasenthil S, Medina D, Kumar R. PAK1 hyperactivation is sufficient for mammary gland tumor formation. *Oncogene.* 2006;25:2931-2936.
149. Balasenthil S, Sahin AA, Barnes CJ, et al. p21-activated kinase-1 signaling mediates cyclin D1 expression in mammary epithelial and cancer cells. *J Biol Chem.* 2004;279:1422-1428.
150. Jung ID, Lee J, Lee KB, et al. Activation of p21-activated kinase 1 is required for lysophosphatidic acid-induced focal adhesion kinase phosphorylation and cell motility in human melanoma A2058 cells. *Eur J Biochem.* 2004;271:1557-1565.
151. Aoki H, Yokoyama T, Fujiwara K, et al. Phosphorylated Pak1 level in the cytoplasm correlates with shorter survival time in patients with glioblastoma. *Clin Cancer Res.* 2007;13:6603-6609.
152. Ito M, Nishiyama H, Kawanishi H, et al. P21-activated kinase 1: a new molecular marker for intravesical recurrence after transurethral resection of bladder cancer. *J Urol.* 2007;178:1073-1079.
153. O'Sullivan GC, Tangney M, Casey G, Ambrose M, Houston A, Barry OP. Modulation of p21-activated kinase 1 alters the behavior of renal cell carcinoma. *Int J Cancer.* 2007;121:1930-1940.
154. Bourguignon LY, Gilad E, Peyrollier K. Heregulin-mediated ErbB2-ERK signaling activates hyaluronan synthases leading to CD44-dependent ovarian tumor cell growth and migration. *J Biol Chem.* 2007;282:19426-19441.
155. Ching YP, Leong VY, Lee MF, Xu HT, Jin DY, Ng IO. P21-activated protein kinase is overexpressed in hepatocellular carcinoma and enhances cancer metastasis involving c-Jun NH2-terminal kinase activation and paxillin phosphorylation. *Cancer Res.* 2007;67:3601-3608.
156. Shekarabi M, Moore SW, Tritsch NX, Morris SJ, Bouchard JF, Kennedy TE. Deleted in colorectal cancer binding netrin-1 mediates cell substrate adhesion and recruits Cdc42, Rac1, Pak1, and N-WASP into an intracellular signaling complex that promotes growth cone expansion. *J Neurosci.* 2005;25:3132-3141.

157. Hirokawa Y, Levitzki A, Lessene G, et al. Signal therapy of human pancreatic cancer and NF1-deficient breast cancer xenograft in mice by a combination of PP1 and GL-2003, anti-PAK1 drugs (Tyr-kinase inhibitors). *Cancer Lett.* 2007;245:242-251.
158. Adam L, Vadlamudi R, Kondapaka SB, Chernoff J, Mendelsohn J, Kumar R. Heregulin regulates cytoskeletal reorganization and cell migration through the p21-activated kinase-1 via phosphatidylinositol-3 kinase. *J Biol Chem.* 1998;273:28238-28246.
159. Rayala SK, Molli PR, Kumar R. Nuclear p21-activated kinase 1 in breast cancer packs off tamoxifen sensitivity. *Cancer Res.* 2006;66:5985-5988.
160. Tang Y, Chen Z, Ambrose D, et al. Kinase-deficient Pak1 mutants inhibit Ras transformation of Rat-1 fibroblasts. *Mol Cell Biol.* 1997;17:4454-4464.
161. Tang Y, Marwaha S, Rutkowski JL, Tennekoon GI, Phillips PC, Field J. A role for Pak protein kinases in Schwann cell transformation. *Proc Natl Acad Sci U S A.* 1998;95:5139-5144.
162. Hirokawa Y, Nakajima H, Hanemann CO, et al. Signal therapy of NF1-deficient tumor xenograft in mice by the anti-PAK1 drug FK228. *Cancer Biol Ther.* 2005;4:379-381.
163. Zhang Y, Vik TA, Ryder JW, et al. *Nfl* regulates hematopoietic progenitor cell growth and ras signaling in response to multiple cytokines. *J Exp Med.* 1998;187:1893-1902.
164. Yang FC, Kapur R, King AJ, et al. Rac2 stimulates Akt activation affecting BAD/Bcl-XL expression while mediating survival and actin function in primary mast cells. *Immunity.* 2000;12:557-568.
165. Dastyk J, Costa JJ, Thompson HL, Metcalfe DD. Mast cell adhesion to fibronectin. *Immunology.* 1991;73:478-484.
166. Kim DK, Morii E, Ogihara H, et al. Impaired expression of integrin alpha-4 subunit in cultured mast cells derived from mutant mice of mi/mi genotype. *Blood.* 1998;92:1973-1980.
167. Manetz TS, Gonzalez-Espinosa C, Arudchandran R, Xirasagar S, Tybulewicz V, Rivera J. Vav1 regulates phospholipase cgamma activation and calcium responses in mast cells. *Mol Cell Biol.* 2001;21:3763-3774.
168. Nishizumi H, Yamamoto T. Impaired tyrosine phosphorylation and Ca<sup>2+</sup> mobilization, but not degranulation, in lyn-deficient bone marrow-derived mast cells. *J Immunol.* 1997;158:2350-2355.
169. Tsai M, Shih L, Newlands G, et al. Rat c-kit ligand, stem cell factor, induces the development of connective tissue-type and mucosal mast cells in vivo. Analysis by anatomical distribution, histochemistry, and protease phenotype. *J Exp Med.* 1991;174:125-131.
170. Levy D, Burstein R, Kainz V, Jakubowski M, Strassman AM. Mast cell degranulation activates a pain pathway underlying migraine headache. *Pain.* 2007;130:166-176.
171. Gyorffy S, Palmer K, Gauldie J. Adenoviral vector expressing murine angiostatin inhibits a model of breast cancer metastatic growth in the lungs of mice. *Am J Pathol.* 2001;159:1137-1147.

172. Harrison JH, Jr., Lazo JS. High dose continuous infusion of bleomycin in mice: a new model for drug-induced pulmonary fibrosis. *J Pharmacol Exp Ther.* 1987;243:1185-1194.
173. Chaudhary A, King WG, Mattaliano MD, et al. Phosphatidylinositol 3-kinase regulates Raf1 through Pak phosphorylation of serine 338. *Curr Biol.* 2000;10:551-554.
174. Ling BC, Wu J, Miller SJ, et al. Role for the epidermal growth factor receptor in neurofibromatosis-related peripheral nerve tumorigenesis. *Cancer Cell.* 2005;7:65-75.
175. Sundstrom M, Alfredsson J, Olsson N, Nilsson G. Stem cell factor-induced migration of mast cells requires p38 mitogen-activated protein kinase activity. *Exp Cell Res.* 2001;267:144-151.
176. Ishizuka T, Okajima F, Ishiwara M, et al. Sensitized mast cells migrate toward the antigen: a response regulated by p38 mitogen-activated protein kinase and Rho-associated coiled-coil-forming protein kinase. *J Immunol.* 2001;167:2298-2304.
177. Jeong HJ, Na HJ, Hong SH, Kim HM. Inhibition of the stem cell factor-induced migration of mast cells by dexamethasone. *Endocrinology.* 2003;144:4080-4086.
178. Webb DJ, Parsons JT, Horwitz AF. Adhesion assembly, disassembly and turnover in migrating cells -- over and over and over again. *Nat Cell Biol.* 2002;4:E97-100.
179. Sawada J, Itakura A, Tanaka A, Furusaka T, Matsuda H. Nerve growth factor functions as a chemoattractant for mast cells through both mitogen-activated protein kinase and phosphatidylinositol 3-kinase signaling pathways. *Blood.* 2000;95:2052-2058.
180. Vosseller K, Stella G, Yee NS, Besmer P. c-kit receptor signaling through its phosphatidylinositide-3'-kinase-binding site and protein kinase C: role in mast cell enhancement of degranulation, adhesion, and membrane ruffling. *Mol Biol Cell.* 1997;8:909-922.
181. Yang L, Wang L, Zheng Y. Gene targeting of Cdc42 and Cdc42GAP affirms the critical involvement of Cdc42 in filopodia induction, directed migration, and proliferation in primary mouse embryonic fibroblasts. *Mol Biol Cell.* 2006;17:4675-4685.
182. Tam SY, Tsai M, Snouwaert JN, et al. RabGEF1 is a negative regulator of mast cell activation and skin inflammation. *Nat Immunol.* 2004;5:844-852.
183. Koranteng RD, Swindle EJ, Davis BJ, et al. Differential regulation of mast cell cytokines by both dexamethasone and the p38 mitogen-activated protein kinase (MAPK) inhibitor SB203580. *Clin Exp Immunol.* 2004;137:81-87.
184. Johnson K, D'Mello SR. p21-Activated kinase-1 is necessary for depolarization-mediated neuronal survival. *J Neurosci Res.* 2005;79:809-815.
185. Jin S, Zhuo Y, Guo W, Field J. p21-activated Kinase 1 (Pak1)-dependent phosphorylation of Raf-1 regulates its mitochondrial localization, phosphorylation of BAD, and Bcl-2 association. *J Biol Chem.* 2005;280:24698-24705.
186. Rhee S, Grinnell F. P21-activated kinase 1: convergence point in PDGF- and LPA-stimulated collagen matrix contraction by human fibroblasts. *J Cell Biol.* 2006;172:423-432.
187. Bornfeldt KE, Raines EW, Graves LM, Skinner MP, Krebs EG, Ross R. Platelet-derived growth factor. Distinct signal transduction pathways associated with migration versus proliferation. *Ann N Y Acad Sci.* 1995;766:416-430.
188. Sherman LS, Atit R, Rosenbaum T, Cox AD, Ratner N. Single cell Ras-GTP analysis reveals altered Ras activity in a subpopulation of neurofibroma Schwann cells but not fibroblasts. *J Biol Chem.* 2000;275:30740-30745.

189. Santana A, Saxena B, Noble NA, Gold LI, Marshall BC. Increased expression of transforming growth factor beta isoforms (beta 1, beta 2, beta 3) in bleomycin-induced pulmonary fibrosis. *Am J Respir Cell Mol Biol.* 1995;13:34-44.
190. Giri SN, Hyde DM, Hollinger MA. Effect of antibody to transforming growth factor beta on bleomycin induced accumulation of lung collagen in mice. *Thorax.* 1993;48:959-966.
191. Cutroneo KR, White SL, Phan SH, Ehrlich HP. Therapies for bleomycin induced lung fibrosis through regulation of TGF-beta1 induced collagen gene expression. *J Cell Physiol.* 2007;211:585-589.
192. Antoniadis HN, Bravo MA, Avila RE, et al. Platelet-derived growth factor in idiopathic pulmonary fibrosis. *J Clin Invest.* 1990;86:1055-1064.
193. Aono Y, Nishioka Y, Inayama M, et al. Imatinib as a novel antifibrotic agent in bleomycin-induced pulmonary fibrosis in mice. *Am J Respir Crit Care Med.* 2005;171:1279-1285.
194. Maeda A, Hiyama K, Yamakido H, Ishioka S, Yamakido M. Increased expression of platelet-derived growth factor A and insulin-like growth factor-I in BAL cells during the development of bleomycin-induced pulmonary fibrosis in mice. *Chest.* 1996;109:780-786.
195. Kluwe L, Friedrich RE, Mautner VF. Allelic loss of the NF1 gene in NF1-associated plexiform neurofibromas. *Cancer Genet Cytogenet.* 1999;113:65-69.
196. Bajenaru ML, Hernandez MR, Perry A, et al. Optic nerve glioma in mice requires astrocyte Nf1 gene inactivation and Nf1 brain heterozygosity. *Cancer Res.* 2003;63:8573-8577.
197. Gutmann DH, Loehr A, Zhang Y, Kim J, Henkemeyer M, Cashen A. Haploinsufficiency for the neurofibromatosis 1 (NF1) tumor suppressor results in increased astrocyte proliferation. *Oncogene.* 1999;18:4450-4459.
198. Knudson AG, Jr. Mutation and cancer: statistical study of retinoblastoma. *Proc Natl Acad Sci U S A.* 1971;68:820-823.
199. Isaacson P. Mast cells in benign nerve sheath tumours. *The Journal of Pathology.* 1976;119:193-196.
200. Riccardi VM. Cutaneous manifestation of neurofibromatosis: cellular interaction, pigmentation, and mast cells. *Birth Defects Orig Artic Ser.* 1981;17:129-145.
201. Slack-Davis JK, Eblen ST, Zecevic M, et al. PAK1 phosphorylation of MEK1 regulates fibronectin-stimulated MAPK activation. *J Cell Biol.* 2003;162:281-291.
202. Vadlamudi RK, Adam L, Wang RA, et al. Regulatable expression of p21-activated kinase-1 promotes anchorage-independent growth and abnormal organization of mitotic spindles in human epithelial breast cancer cells. *J Biol Chem.* 2000;275:36238-36244.
203. Wang SW, Denny TA, Steinbrecher UP, Duronio V. Phosphorylation of Bad is not essential for PKB-mediated survival signaling in hemopoietic cells. *Apoptosis.* 2005;10:341-348.
204. Kalesnikoff J, Rios EJ, Chen CC, et al. RabGEF1 regulates stem cell factor/c-Kit-mediated signaling events and biological responses in mast cells. *Proc Natl Acad Sci U S A.* 2006;103:2659-2664.

205. Allard EK, Blanchard KT, Boekelheide K. Exogenous stem cell factor (SCF) compensates for altered endogenous SCF expression in 2,5-hexanedione-induced testicular atrophy in rats. *Biol Reprod.* 1996;55:185-193.
206. Flanagan JG, Chan DC, Leder P. Transmembrane form of the kit ligand growth factor is determined by alternative splicing and is missing in the Sld mutant. *Cell.* 1991;64:1025-1035.
207. Brannan CI, Lyman SD, Williams DE, et al. Steel-Dickie mutation encodes a c-kit ligand lacking transmembrane and cytoplasmic domains. *Proc Natl Acad Sci U S A.* 1991;88:4671-4674.
208. Tajima Y, Onoue H, Kitamura Y, Nishimune Y. Biologically active kit ligand growth factor is produced by mouse Sertoli cells and is defective in Sld mutant mice. *Development.* 1991;113:1031-1035.
209. Kapur R, Majumdar M, Xiao X, McAndrews-Hill M, Schindler K, Williams DA. Signaling through the interaction of membrane-restricted stem cell factor and c-kit receptor tyrosine kinase: genetic evidence for a differential role in erythropoiesis. *Blood.* 1998;91:879-889.
210. Wehrle-Haller B, Weston JA. Soluble and cell-bound forms of steel factor activity play distinct roles in melanocyte precursor dispersal and survival on the lateral neural crest migration pathway. *Development.* 1995;121:731-742.
211. Heinrich MC, Dooley DC, Freed AC, et al. Constitutive expression of steel factor gene by human stromal cells. *Blood.* 1993;82:771-783.
212. Linenberger ML, Jacobson FW, Bennett LG, Broudy VC, Martin FH, Abkowitz JL. Stem cell factor production by human marrow stromal fibroblasts. *Exp Hematol.* 1995;23:1104-1114.
213. Deacon SW, Beeser A, Fukui JA, et al. An isoform-selective, small-molecule inhibitor targets the autoregulatory mechanism of p21-activated kinase. *Chem Biol.* 2008;15:322-331.
214. Kontoyiannis D, Kollias G. Fibroblast biology. Synovial fibroblasts in rheumatoid arthritis: leading role or chorus line? *Arthritis Res.* 2000;2:342-343.
215. Roche WR. Fibroblasts and asthma. *Clin Exp Allergy.* 1991;21:545-548.
216. Kalluri R, Zeisberg M. Fibroblasts in cancer. *Nat Rev Cancer.* 2006;6:392-401.
217. De Wever O, Mareel M. Role of myofibroblasts at the invasion front. *Biol Chem.* 2002;383:55-67.
218. Desmouliere A, Guyot C, Gabbiani G. The stroma reaction myofibroblast: a key player in the control of tumor cell behavior. *Int J Dev Biol.* 2004;48:509-517.
219. Kataoka H, Tanaka H, Nagaike K, Uchiyama S, Itoh H. Role of cancer cell-stroma interaction in invasive growth of cancer cells. *Hum Cell.* 2003;16:1-14.
220. Haugh JM. Deterministic model of dermal wound invasion incorporating receptor-mediated signal transduction and spatial gradient sensing. *Biophys J.* 2006;90:2297-2308.
221. Wilkes MC, Mitchell H, Penheiter SG, et al. Transforming growth factor-beta activation of phosphatidylinositol 3-kinase is independent of Smad2 and Smad3 and regulates fibroblast responses via p21-activated kinase-2. *Cancer Res.* 2005;65:10431-10440.
222. Dempsey OJ, Kerr KM, Gomersall L, Remmen H, Currie GP. Idiopathic pulmonary fibrosis: an update. *QJM.* 2006;99:643-654.

223. Collard HR, King TE, Jr. Treatment of idiopathic pulmonary fibrosis: the rise and fall of corticosteroids. *Am J Med.* 2001;110:326-328.
224. Mapel DW, Samet JM, Coultas DB. Corticosteroids and the treatment of idiopathic pulmonary fibrosis. Past, present, and future. *Chest.* 1996;110:1058-1067.
225. Selman M, King TE, Pardo A. Idiopathic pulmonary fibrosis: prevailing and evolving hypotheses about its pathogenesis and implications for therapy. *Ann Intern Med.* 2001;134:136-151.
226. Lasky JA, Brody AR. Interstitial fibrosis and growth factors. *Environ Health Perspect.* 2000;108 Suppl 4:751-762.
227. Ramos ML, Gragnani A, Ferreira LM. Is there an ideal animal model to study hypertrophic scarring? *J Burn Care Res.* 2008;29:363-36

## Curriculum Vitae

**Name:** Andrew S. McDaniel

### **Current Position:**

2002-present: Student, M.D./Ph.D. program  
Indiana University School of Medicine  
Department of Microbiology/Immunology  
Advisor- D. Wade Clapp, M.D.

### **Education**

2002: B.S.-Biology, Indiana University, Bloomington IN  
2008: Ph.D.- Microbiology/Immunology, Indiana University, Indianapolis, IN

### **Honors/Awards**

Academic Honors Scholarship, Anderson University, 1998-2000  
Dean's List, Anderson University, 1998-2000  
Dean's List, Indiana University, 2000-2002  
Winner, Wells Center Summer Student Intern Poster Competition, Indiana University School of Medicine, 2001  
Indiana Genomic Initiative Scholar Award, Indiana University, 2002  
Winner, Sigma Xi Graduate Student Research Competition, Indiana University, 2006  
Best Overall Student Presentation, Department of Microbiology/Immunology Research in Progress, Indiana University, 2006  
ASH Merit Award, American Society of Hematology, 2007  
Best Overall Student Presentation, Department of Microbiology/Immunology Research in Progress, Indiana University, 2006  
SPR Student Research Award, Society for Pediatric Research, 2008

### **Grants/Fellowships**

Indiana Medical Scientist Training Program Fellowship, Indiana University 2002-2004  
Predoctoral Fellow- "Regulation of Hematopoietic Cell Production" Institutional NRSA T32 DK07519, National Institute of Diabetes and Digestive and Kidney Diseases, National Institutes of Health, 2004-2007

Principal Investigator- “The role of Pak1 in regulating plexiform neurofibroma formation” Individual NRSA F30 NS060322-01 National Institute of Neurological Diseases and Stroke, National Institutes of Health, 2007-2010

## Publications

1. McDaniel AS, Allen JD, Park SJ, Jaffer ZM, Michels EG, Burgin SJ, Chen S, Bessler WK, Hoffmann C, Ingram DA, Chernoff J, Clapp DW. “*Pak1* regulates multiple c-Kit mediated Ras-MAPK gain-in-function phenotypes in *Nfl*<sup>+/-</sup> mast cells.” *Blood*. *Accepted/In press*.
2. Allen JD, Jaffer ZM, Park SJ, Burgin SJ, Hoffmann C, Sells MA, Chen S, Derr-Yellin E, Michels EG, McDaniel AS, Bessler WK, Ingram DA, Atkinson SJ, Travers JB, Chernoff J, Clapp DW. “p21 activated kinase regulates mast cell degranulation via effects on calcium mobilization and cytoskeletal dynamics.” Submitted 5/2008.
3. Mantel CR, Gelfano VM, Kim YJ, McDaniel A, Lee Y, Boswell HS, Broxmeyer HE. “p21waf1-Chk1-pathway monitors G1 phase microtubule integrity and is crucial for restriction point transition” *Cell Cycle*. 1(5):327-36, 2002.

## Abstracts

1. McDaniel AS, Allen JD, Chernoff J, Clapp DW. “Loss of *Pak1* corrects multiple gain of function phenotypes in *Nfl*<sup>+/-</sup> mast cells.” Pediatric Academic Societies Annual Meeting, May 2008, Honolulu, HI.
2. McDaniel AS, Allen JD, Chernoff J, Clapp, DW. “Loss of *Pak1* corrects multiple gain of function phenotypes in *Nfl*<sup>+/-</sup> mast cells.” 49th Annual American Society for Hematology Annual Meeting, December 2007, Atlanta, GA.
3. McDaniel AS, Allen JD, Chernoff J, Clapp DW. “Loss of *Pak1* corrects multiple gain of function phenotypes in *Nfl* haploinsufficient mast cells via activation of specific MAPK pathways.” 22<sup>th</sup> Annual National M.D./Ph.D. Student Conference, July 2007, Keystone, CO.
4. McDaniel AS, Allen JD, Chernoff J, Clapp DW. “Loss of *Pak1* corrects multiple gain of function phenotypes in *Nfl* haploinsufficient mast cells via activation of specific MAPK pathways.” Indiana University Cancer Center Cancer Research Day, May 2007, Indianapolis, IN.



5. McDaniel AS, Allen JD, Chernoff J, Clapp DW. “p21-activated kinase 1 regulates hyperproliferation of *Nf1* haploinsufficient mast cells *in vitro* and *in vivo* via activation of the MAPK pathway.” 47th Annual American Society for Hematology Annual Meeting, December 2005, Atlanta, GA.
6. McDaniel AS, Allen JD, Chernoff J, Clapp DW. “p21-activated kinase 1 (PAK1) regulates mast cell proliferation via the Ras/Raf/Erk pathway.” 20<sup>th</sup> Annual National M.D./Ph.D. Student Conference, July 2005, Keystone, CO.
7. McDaniel AS, Allen JD, Chernoff J, Clapp DW. “p21-activated kinase 1 (PAK1) regulates mast cell proliferation via the Ras/Raf/Erk pathway.” 2005 NF Consortium Meeting, June 2005, Aspen, CO.